Investigating projections from the ventral hippocampus (vHC) to the prelimbic (PL) and infralimbic (IL) cortices in the mouse

Polina Ash

Integrated Program in Neuroscience
McGill University, Montreal

May 2018

A thesis submitted to McGill University in partial fulfillment of the requirements of the degree of Master of Science in Neuroscience

Table of Contents

Abstract

The ventral hippocampus (vHC) to medial prefrontal cortex (mPFC) circuit is composed of monosynaptic long range projections originating in the vHC and terminating in the mPFC. This pathway plays a vital role in functions such as emotional processing and contextual memory, with vHC-mPFC circuit dysfunction associated with a large variety of neuropsychiatric disorders such as anxiety and schizophrenia. The identity and extent of long range projections from different subregions of the vHC (vCA1 and vSub) to the mPFC (infralimbic, IL and prelimbic, PL) and their functional role in a richer repertoire of behaviors has not been investigated in the mouse. The present study presents an attempt to characterize these features of the circuit in mice with injections of the retrograde tracer CTB into the PL and IL or anterograde AAV into the vHC. Our results indicate greater vHC innervation of the IL rather than PL, with a small population of neurons projecting to both. Moreover, we observed that the mPFC receives more numerous projections from the vCA1 than the vSub. In addition, we found a lack of GABAergic vHC projections to the mPFC. Lastly, we were able to use the molecular marker Neurotensin (Nts) to target a subpopulation of cells topographically restricted to distal vCA1 and proximal vSub with a unique pattern of PFC innervation. Optogenetic inhibition of this $Nts^{vHC\text{-}IL}$ circuit with NpHR did not alter anxiety-like behavior or social memory and had unclear effects on extinction learning and renewal. Taken together, our anatomical data from the mouse are largely aligned with the results of previous studies in rats and support translation of findings between both rodent species. The lack of changes with optogenetic inhibition are suggestive of the $Nts^{vHC\text{-}IL}$ circuit not having a functional role in the behaviors of emotional processing and memory tested and reveals previously unknown complexity within the vHC-mPFC pathway. Future studies should further delineate the pattern of anatomical connectivity and the functional

role of this pathway in more nuanced behaviors, as well as assessing the significance of Neurotensin signaling and excitation/inhibition (E/I) balance within the circuit. Greater understanding of this pathway in rodent models could shed light on anatomical substrates of complex behaviors and how the functional roles of circuits are disrupted in diverse neuropsychiatric disorders.

Résumé

Le circuit de l'hippocampe ventral (vHC) vers le cortex préfrontal médian (mPFC) est composé de projections monosynaptiques de longue distance provenant du vHC et se terminant dans le mPFC. Cette voie joue un rôle essentiel dans des fonctions telles que le traitement émotionnel ainsi que la mémoire contextuelle, avec un dysfonctionnement du circuit vHC-mPFC associé à une grande variété de troubles neuropsychiatriques tels que l'anxiété et la schizophrénie. L'identité et l'étendue des projections à longue distance de différentes sous-régions du vHC (vCA1 et vSub) au mPFC (infra-limbique, IL et pré-limbique, PL) et leur rôle fonctionnel dans un répertoire plus riche de comportements n'ont pas été étudiés chez la souris. La présente étude tente de caractériser ce circuit chez des souris avec des injections du traceur rétrograde CTB dans le PL et IL ou antérograde AAV dans le vHC. Nos résultats indiquent une plus grande innervation vHC de l'IL plutôt que PL, avec une petite population de neurones projetant à la fois. De plus, nous avons observé que le mPFC reçoit plus de projections du vCA1 que du vSub. En outre, nous avons trouvé un manque de projections GABA vHC pour le mPFC. Enfin, nous avons pu utiliser le marqueur moléculaire Neurotensin (Nts) pour cibler une sous-population de cellules topographiquement restreinte à vCA1 distale et vSub proximale avec un modèle unique d'innervation PFC. L'inhibition optogénétique de ce circuit $Nts^{vHC\text{-}IL}$ avec NpHR n'a pas altéré le comportement anxieux ou la mémoire sociale. Pris ensemble, nos données anatomiques de la souris sont en grande partie alignés avec les résultats d'études antérieures chez les rats et soutiennent la translation des résultats entre les deux espèces de rongeurs. L'absence de changements avec l'inhibition optogénétique suggère que le circuit $Nts^{vHC\text{-}IL}$ ne joue pas un rôle fonctionnel dans les comportements de traitement émotionnel et de mémoire testée et révèle une complexité jusqu'alors inconnue dans la voie vHC-mPFC. Des études futures devraient préciser

davantage le modèle de connectivité anatomique et le rôle fonctionnel de cette voie dans des comportements plus nuancés, ainsi que l'évaluation de la signification de la signalisation Neurotensin et de l'équilibre excitation/inhibition (E/I) dans le circuit. Une meilleure compréhension de cette voie dans les modèles de rongeurs pourrait éclairer les substrats anatomiques des comportements complexes et comment les rôles fonctionnels des circuits sont perturbés dans divers troubles neuropsychiatriques.

Acknowledgements

My time at McGill University and the Douglas Mental Health University Mental Health Institute has been instrumental in my growth as a scientist, but more importantly as an individual. I have been presented with numerous opportunities to push my limits and cultivate resilience. What I have learned through this experience will serve me well in my future pursuits.

I would like to acknowledge Dr. Sylvain Williams and Dr. Lalit Srivastava for funding and supervising my thesis work. I am grateful for the opportunity they provided to conduct meaningful and innovative research. Their input honed my scientific thinking and formulation of research questions. Thank you to Dr. Williams for demonstrating pursuit of methodological novelty and cultivating independence. And to Dr. Srivastava for your patience and putting findings into perspective.

I would also like to recognize Dr. Mark Brandon and Dr. Naguib Mechawar for making time to serve on my committee and providing valuable guidance to improve my project. Additionally, I want to thank Dr. Tak Pan Wong, my IPN mentor, for being a source of wisdom and encouragement. Furthermore, I am grateful to the PIs and members of the labs I spent time in during my first year graduate rotations. The opportunities provided by Dr. Cecilia Flores, Dr. Chawki Benkelfat, and Dr. Michael Meaney were vital for expanding my perspectives as well as expertise. Likewise, I'd like to thank the directors of the IPN rotation program, Dr. Ed Ruthazer, Dr. Carl Ernst, Dr. Joe Rochford, and Dr. Josephine Nalbantoglu, for providing this worthwhile experience and lending your insight along the way.

I want to extend my appreciation to the many other individuals at McGill and Douglas who supported the project through ensuring facilities and resources were accessible. Including to Étienne Labrie-Dion, Molecular and Cellular Microscopy Platform (MCMP) coordinator at the

Douglas, for your expertise and optimism regarding the possibilities of fluorescence imaging. Also to Erika Vigneault for assistance in the project through performing the FISH experiments for this project as well as sharing your knowledge. And to Eve-Marie Charbonneau and the other members of the animal facility for providing their expertise in animal care.

I am grateful for the privilege of meeting diverse scientists who served as inspirational colleagues and mentors. The many members of the Williams lab were a pleasure to work with and alongside of. I would like to highlight Dr Fred Manseau, Dr. Béné Amilhon, and Dr. Guillaume Etter for lending their expertise in training and answering questions, particularly at the beginning of the project. Likewise, Dr. Amy Chee for extensive training and manuscript editing and Ingrid Inema for project assistance and editing. Otherwise, I am thankful for the scientific and moral support provided by (now Dr.) Jennifer Robinson, (now Dr.) Richard Boyce, Dr. Guillaume Ducharme, Dr. Lorène Penazzi, Dr. Jean-Bastien Bott, Dr. Jun-Il Kang, Eva Vico, Aurelie Ky, Bruno Rivard, Jisoo Choi, and Suzanne van der Veldt. Big thanks to our research assistant Ke Cui for animal colony support, lab orders, and aiding experiments. Similarly, I also want to thank Teresa Joseph and Dr. Sanjeev Bhardwaj in the Srivastava lab for valuable conversations and experimental assistance. Moreover, I want to thank Dr. Rob Rozeske for constructive discussions about brain regions and behavioral experiments.

There were numerous passionate graduate students at McGill with whom I formed friendships with and I want to mention my thanks to several who made the experience particularly worthwhile. First, to my fellow rotation students who made the transition to graduate school so much more bearable. Next to members of GSAN, many of them now friends, for helping provide an outlet for organizing and participating in cool academic and social events for Neurdz. To Daniel Almeida, my extremely dynamic BrainReach partner, who demonstrated that

sharing science wasn't only about sharing objective knowledge but required enthusiasm, transforming the way I thought about teaching. To Nastia Glushko for all the yoga classes, vegan cooking, and utilitarian and emotional support. As well as many other novel friends within and without McGill who made my time in Montreal extremely memorable.

Finally, I want to express immense gratitude to my family for their perpetual love and support. To my partner Misha for encouragement, patience, academic discussions, and maintaining my sanity. To my sister Kat for being a constant friend and reminding me where I came from. And to my mother and grandparents for believing in me and providing the opportunities that allowed me to pursue my passions.

Preface & Contribution of Authors

Polina Ash served as lead investigator for all aspects of study design under the guidance of Dr. Sylvain Williams and Dr. Lalit Srivastava. The majority of the anatomical and behavioral experiments were performed by the author. Ingrid Inema acquired and analyzed in-vitro patch clamp electrophysiology data in Neurotensin mice previously injected by the author. Erika Vigneault created custom probes and conducted FISH experiments on Neurotensin mice. Data analyses, figure construction, and thesis writing was completed by Polina Ash.

Introduction

Approximately 1 in 5 people are affected by mental disorders that psychiatry currently classifies and characterizes as distinct conditions (Steel et al. 2014). Yet substantial comorbidity and symptom overlap exist among these disorders. For example, emotional dysregulation is a core symptom of depression, anxiety, ADHD, and schizophrenia (Braga et al. 2005; Godsil et al. 2013; Shaw et al. 2014). The neural circuits that, when disrupted, underlie such symptoms have become the focus of novel research efforts (Insel 2014; Perusini and Fanselow 2015). Dysfunctions in the hippocampus-medial prefrontal cortex (HC-mPFC) circuit have been associated with several neuropsychiatric disorders such as anxiety, addiction, and schizophrenia (Li, Long, and Yang 2015; Godsil et al. 2013; Tost, Bilek, and Meyer-Lindenberg 2012). Research in animal models promises to yield more specific characterization of the anatomy and physiology of this circuit in its relation to these behavioural symptoms, with findings thus far in line with those in humans (Sigurdsson and Duvarci 2015).

Although data gathered from human subjects are too limited to provide sufficiently fine-grained characterizations of the anatomical, physiological, and functional profile of the HC-mPFC circuit, evidence from the best available diffusion tensor imaging (DTI) studies demonstrates a pathway connecting the anterior hippocampus to the ventromedial PFC by way of the fornix, similar to that seen in rodents (Croxson et al. 2005). Data from electrophysiology and fMRI studies suggests that communication between the HC and mPFC is essential for cognitive processes like working and episodic memory (Kalisch et al. 2006; Simons and Spiers 2003). Furthermore, aberrant functional coupling in the HC-mPFC pathway has been linked to deficits in emotional regulation and associative memory, as seen in PTSD and schizophrenia (Liberzon

and Sripada 2008; Meyer-Lindenberg et al. 2005). In rodents, the vHC to mPFC circuit is composed of monosynaptic long range projections originating in the ventral portion of the hippocampus and terminating in the mPFC (Cenquizca and Swanson 2007; Verwer et al. 1997). Yet much remains unknown about the vHC-mPFC circuit, particularly in the mouse, the model organism of choice in neuroscience today. The unknown properties of this pathway include its precise anatomical connectivity across spatial axes, which can be assessed with novel tools, as well as its functional role in a richer repertoire of behaviors. This proposed project aims to characterize the anatomy and functional contributions of the vHC-mPFC circuit in greater detail in the mouse. Such circuit based research will illuminate how information integration is disrupted in psychiatric disease and contribute to improving mental health. Accordingly, before we can address our questions of interest, it is important to understand the details of the anatomy, interactions, and functional roles of the components individually as well within the vHC-mPFC circuit.

Anatomical Organization of the vHC-mPFC Circuit

The hippocampus is an allocortical, primitive three-layered, subcortical structure found in all mammals. It is one of the most studied parts of the brain, particularly in terms of its role in memory, and extends long range projections to participate in the vHC-mPFC circuit (Gall 1990; Lopes da Silva et al. 1990; M. B. Moser and Moser 1998). In rodents, the hippocampus can be subdivided longitudinally into a functionally distinct dorsal (septal) and ventral (temporal) component based on a variety of properties, such as chemoarchitecture, molecular profiles, distribution of cells, and inputs and outputs (Fanselow and Dong 2010; Igarashi et al. 2014; Malik et al. 2016; Strange et al. 2014; Thompson et al. 2008). Distal and proximal coordinates are established relative to the dentate gyrus (Nakazawa et al. 2016). The relatively simple

structure, laminar organization, and unidirectional connections (e.g., the trisynaptic loop) of the hippocampus lend themselves to studies that rely on defined routes of information flow originating in specific subregions (Naber, Witter, and Lopes da Silva 2000).

Morphological and functional diversity of hippocampal cells exists across the dorsal-ventral axis as well between hippocampal subfields (Igarashi et al. 2014; Strange et al. 2014). The CA1 and Subiculum (Sub) serve as the major output regions of the hippocampus but differ in their cytoarchitecture, intrinsic properties, efferents, and afferents. Both regions contain an easily identifiable layer of pyramidal neurons with interneurons, 21 types identified in CA1 but as yet unknown number in Sub, found in other layers (Klausberger and Somogyi 2008). The CA1 contains neurons that exhibit much greater collateralization (Naber and Witter 1998), allowing for diverse targeting and circuit participation by individual neurons (Arszovszki, Borhegyi, and Klausberger 2014; Ciocchi et al. 2015). The Sub displays a simpler structure, lacking the stratum oriens and radiatum (O'Mara et al. 2001; Witter et al. 1989). Subsequently, given the paucity of knowledge, some authors have speculated that the CA1 and Sub differ in their intrinsic organization, as the Sub may exhibit 'matrix-like' organization consisting of columnar modules as well as the more classical, CA1 laminae (Gigg 2006; Harris et al. 2001; O'Mara et al. 2001; Witter 2006). In the vHC, both regions display looser packing density of pyramidal cells as compared to the dHC, with the vSub showing the greatest widening of the pyramidal layer (Harris et al. 2001).

While both the vCA1 and vSub contain a large number of pyramidal cells that function in both intrinsic and extrinsic networks, these cells differ in their intrinsic properties. The vCA1 pyramidal cells are distinguished, by the presence of the neurochemical calbindin, into a superficial and deep sublayer. This organization is thought to support radial axis differences in

efferent and afferent connectivity, theta oscillations, and synaptic transmission (Blatow et al. 2003; Dumas et al. 2004; Senior et al. 2008; Slomianka et al. 2011). Conversely, the vSub contains a greater number of pyramidal cells that respond to brief depolarizations with high-frequency clusters of 2-3 action potentials (bursts; Staff et al. 2000). The prevalence, physiological properties, and functional connectivity of bursting cells are not yet well understood (Cooper 2002; Gigg, Finch, and O'Mara 2000; Harris and Stewart 2001; Jarsky et al. 2008; Mattia, Hwa, and Avoli 1993; Taube 1993), but they may contribute to differential circuits (Gigg 2006; Graves et al. 2012; Kim and Spruston 2012; Moore, Cooper, and Spruston 2009). Furthermore, bursting activity has been demonstrated to be important for neuronal signaling, plasticity, and behavior (Cooper et al. 2003; Cooper, Chung, and Spruston 2005; Lisman 1997; Williams and Stuart 1999). Accordingly, such phenotypic variation between pyramidal cells in vCA1 and vSub may contribute to distinct subfield output by projections through the regulation of intra-regional circuits (Jarsky et al. 2008; Menendez de la Prida 2006).

The vCA1 and vSub are reciprocally connected with each other as well as with the entorhinal cortex (EC) and amygdala (Agster and Burwell 2013; Cenquizca and Swanson 2007; Room and Groenewegen 1986). Interestingly, the vCA1 and vSub are connected in a pattern of nested loops: proximal CA1 with distal Sub and distal CA1 with proximal Sub (Amaral, Dolorfo, and Alvarez- Royo 1991). Furthermore, both subfields send projections to the lateral septum (LS), bed nucleus of the stria terminalis (BNST), mPFC, and olfactory areas (Canteras and Swanson 1992; Risold and Swanson 1996; Van Groen and Wyss 1990). However, the vSub connects with a greater diversity of regions, receiving input from the locus coeruleus, paramedian reticular nucleus (PMN), raphe nucleus, and ventral tegmental area (VTA), and projecting to nucleus accumbens (NAcc), hypothalamus, mammillary bodies, and nucleus

reuniens (Canteras and Swanson 1992; Greene and Totterdell 1997; Lopes da Silva et al. 1990; Oleskevich, Descarries, and Lacaille 1989; O'Mara 2005; Tang et al. 2016). Since the HC is heterogeneous along several dimensions, its subregions likely make distinct contributions to circuit function. Yet within the vHC, the functional domain which subserves emotional and motivational behaviors (Bannerman et al. 2004), the unique functional roles of vCA1 and vSub in the vHC-mPFC circuit have thus far been minimally investigated.

The PFC, which is defined by its receiving input from the mediodorsal thalamus (Preuss 1995; Uylings and van Eden 1990), is where the projections of the vHC-mPFC circuit terminate. It can be further subdivided into medial, lateral, and ventral subregions (Heidbreder and Groenewegen 2003; Hoover and Vertes 2007). Based on cytoarchitecture, afferents, and efferents, the rodent mPFC can distinguished into dorsal or prelimbic (PL) and ventral or infralimbic (IL) components (Heidbreder and Groenewegen 2003; Little and Carter 2012). Both mPFC subregions are agranular, lacking layer IV (Uylings, Groenewegen, and Kolb 2003), and do not display columnar arrangement of layers V and VI (Van De Werd et al. 2010). Nissl staining allows the PL to be distinguished by a relatively tightly packed cell layer II as well as more visible layers III and V (Little and Carter 2012), while the IL has more homogenous cell layers (Van De Werd et al. 2010).

The mPFC displays differences in intrinsic properties across layers and subregions. PL and IL neurons within layer II/III (L2/3) are more hyperpolarized and less excitable than those in L5. However, IL neurons, particularly those within L2/3, are more excitable, with a lower spike threshold and higher input resistance than PL neurons (Kaczorowski, Davis, and Moyer 2012; Song, Ehlers, and Moyer 2015; Song and Moyer 2018). More superficial cortical layers, L1 and L2/3, are usually involved in processing long range inputs while deeper layers, L5 and L6, are

more likely to serve as origins of long range projections (Bouwmeester, Smits, and Van Ree 2002; Sesack et al. 1989), with several exceptions (Cenquizca and Swanson 2007; Canto, Wouterlood, and Witter 2008). Overall, such mPFC organization allows for appropriate differential integration of input and supports projection specific activity.

The PL and IL both receive input from many regions, such as vHC, thalamic nuclei, basolateral amygdala (BLA), and VTA, with the IL receiving unique projections from olfactory areas (Luskin and Price 1983) and hypothalamus (Vertes 2004). Both regions send projections to the LS, BNST, and VTA (Vertes 2004). The PL uniquely contacts the insular cortex, NAcc, and BLA (Mcdonald, Mascagni, and Guo 1996; Vertes 2004), while the IL projects to dorsomedial hypothalamus (DMH), basomedial amygdala (BMA; Adhikari et al. 2015), central nucleus of amygdala, medial preoptic area (MPO; Mcdonald, Mascagni, and Guo 1996), as well as the PL (Saffari et al. 2016). The rodent mPFC appears to subserve similar functions to the primate PFC (Euston, Gruber, and McNaughton 2012; Kesner and Churchwell 2011; Vertes 2006), as the PL is involved in cognitive functions, corresponding to the dorsolateral PFC, and the IL plays a more prominent role in autonomic or emotional processing, corresponding to the orbitomedial PFC (Churchwell et al. 2010; Condé et al. 1995; Hoover and Vertes 2007; Uylings and van Eden 1990). Therefore, the PL and IL are comparatively well placed to subserve different functions, yet the majority of rodent studies examining the mPFC thus far have focused on just the dorsal subdivision or PL.

Tracing studies of vHC-mPFC circuit have produced mixed findings about its anatomical segregation and distribution (Cenquizca and Swanson 2007; Condé et al. 1995; Jay, Glowinski, and Thierry 1989; Swanson 1981; Verwer et al. 1997). For instance, qualitative assessment of the rat vHC suggests that cells projecting to the IL are relatively more dense than those targeting

the PL (Hoover and Vertes 2007). Most recently, Wang and colleagues (2016) utilized the retrograde tracer CTB in rats to demonstrate a greater number of vHC cells projecting to the IL than PL, with minimal overlap in these two populations. Conversely, using FluoroGold in mice, Tripathi and colleagues (2016) found that the PL receives projections from a greater number of vHC cells. Furthermore, the relative contribution and pattern of vCA1 and vSub projections to the mPFC subregions is as yet unknown. However, when assessing the rat vSub, cells projecting to the PL or IL were found within proximal vSub, with those to the IL especially clustered around the CA1/Sub border (Witter 2006). Therefore, the anatomy of the mouse vHC-mPFC circuit remains inadequately described and prevents comparison to the richer literature in rat models, namely assessing physiological and functional consequences of region interactions.

Interactions between Hippocampus and Medial Prefrontal Cortex

Interaction between the HC and mPFC plays a critical role in a variety of cognitive functions, including decision making, emotional processing, and working and contextual memory (Benchenane, Tiesinga, and Battaglia 2011; Colgin 2011; Harris and Gordon 2015). The rodent vHC and mPFC are connected directly, as noted above, and indirectly through interactions with dHC (Rajasethupathy et al. 2015), basolateral amygdala (BLA; Likhtik et al. 2014), nucleus reuniens (NR; Cassel et al. 2013; Vertes 2006), and lateral EC (LEC; E. I. Moser, Witter, and Moser 2010).

Anatomical connectivity between the vHC and mPFC has been confirmed with physiological manipulations, such that stimulation of vHC induces excitatory synaptic responses within the mPFC (Jay et al. 1992; Thierry et al. 2000) as well as a more complex feedforward response (Dégenètais et al. 2003; Tierney et al. 2004), suggesting excitatory innervation of both pyramidal and interneurons. Thus, vHC activity directly exerts a synaptic influence as well as

activates local cortical networks within the mPFC. In addition, the vHC-mPFC circuit exhibits activity-dependent synaptic plasticity, indicative of interregional information transfer (Izaki et al. 2003; Jay, Burette, and Laroche 1995; Laroche, Jay, and Thierry 1990; Parent et al. 2010; Romcy-Pereira and Pavlides 2004). These modifications of synaptic connectivity, which differentially support formation and consolidation of memories, are regulated by dopamine and other neurotransmitter transmission (Gurden, Takita, and Jay 2000; Ohashi et al. 2003). Moreover, long-term potentiation (LTP) and other physiological adaptations resulting from vHC input differ based on anatomical origin (Izaki et al. 2003), further supporting a high degree of circuit specialization. Thus, given the significant diversity within regions it is of interest to probe the physiological mechanisms underlying functional specialization across the vHC-mPFC circuit.

Functional Roles of the vHC-mPFC Circuit

As mentioned, the vHC-mPFC circuit is critically important in cognitive and emotional processing. It is therefore vital to understand the individual roles of the vHC and the mPFC in diverse behavioral paradigms in rodents. Previous studies have demonstrated that the rodent vHC plays a central role in emotional processing of vague and uncertain threats. The open field test (OFT) and elevated plus maze (EPM) rely on rodents' internal conflict between avoidance of exposed spaces and investigation of novelty for potential food or mates (Grupe and Nitschke 2013). Lesions, pharmacological inactivation, and alternative manipulations of the vHC have been found to reduce anxiety-like behavior, as measured by increased time spent in the center of the OFT or visits to open arms of the EPM (Fournier and Duman 2013; Kjelstrup et al. 2002; Mueller, Dolgas, and Herman 2004).

The mPFC has been implicated in diverse innate anxiety-like behaviors (Adhikari, Topiwala, and Gordon 2011; Deacon, Penny, and Rawlins 2003; Lacroix et al. 2000). In

particular, lesions and pharmacological inactivation of the mPFC lead to increased visits to EPM open arms and conspecific interaction (Shah and Treit 2003, 2004; Shah, Sjovold, and Treit 2004). Nevertheless, some studies have found that PL or IL lesions lead to less time spent in the OFT center and EPM open arms, indicative of increased anxiety-like behavior (Jinks and McGregor 1997). Furthermore, excitation of the PL either fails to alter (Warthen et al. 2016) or produces anxiety-like behaviors (Suzuki et al. 2016), while IL activation has no behavioral effect (Adhikari et al. 2015; Suzuki et al. 2016).

Importantly, not only do the vHC and mPFC make independent contributions to anxiety-like behavior, but their interaction also appears to be relevant. Optogenetic inhibition of the vHC-mPFC projection in mice with Arch-mediated terminal inhibition increases time spent and number of visits to open arms (Padilla-Coreano et al. 2016), suggesting that communication between vHC and mPFC is necessary for expression of anxiety-like behavior.

Whereas it is known that the vHC-mPFC projection is involved in anxiety-like behavior in mice, it is not yet clear how the mPFC subregions are connected to the vHC. Accordingly, we are interested in determining the pattern of vHC projections to the PL and IL, especially as the functional contribution of vHC inputs to the PL and IL subregions remain unclear. For instance, the vHC is known to house discrete populations of cells that promote or suppress anxiety-like behavior depending on projection target (PL or LS, respectively; Parfitt et al. 2017). Indeed, while the PL and IL appear to play subtly different roles in anxiety-like behavior (Jinks and McGregor 1997; Suzuki et al. 2016), past studies of function have tended to look at the role of just the PL or did not distinguish the mPFC subregions.

Research on the neural circuitry underlying social memory is sparse, but several previous studies have pointed toward the involvement of both mPFC and hippocampus in social memory.

Indeed, assessing social behavior may be an additional way to assess emotional processing and anxiety-like behavior. Specifically, social interactions decrease in unfamiliar environments and under bright lighting, suggestive of their utility as a proxy of anxiety-like behavior (File and Hyde 1978; Shah and Treit 2003). Mounting evidence exists for a dedicated neuronal network subserving social memory (Brennan and Kendrick 2006; Dulac and Torello 2003), which has a unique time course, lasting longer than working memory but shorter than long term memory.

Lesions of the ventral hippocampus in adulthood cause impairment in social recognition memory tested 30 min after interaction (Kogan, Frankland, and Silva 2000). Neonatal lesions of the vHC, typically utilized as a model of schizophrenia, lead to reductions in social interactions and social memory deficits in adulthood (Becker and Grecksch 2000). Assessment of cFos expression following stimuli presentation is often utilized as an indirect method of identifying particular brain regions involved because this marker indicates recent neuronal activity. While the brain regions found to be activated, and contain elevated cFos, following social interaction vary between studies, the vSub has been implicated by Kim and colleagues (2015). More recently, the vCA1 has been shown to be necessary for social memory: photoinhibition of this subregion during encoding or retrieval disrupted recall. Further, activity of vCA1 projections to the NAcc shell (vCA1-NAcc circuit) was demonstrated to be necessary but, importantly, vCA1 input to the mPFC (vCA1-mPFC circuit) was not assessed (Okuyama et al. 2016).

Lesions of the mPFC lead to reduced social interactions and memory (Murray et al. 2015). Moreover, cFos expression in mPFC is associated with social interaction (Kim et al. 2015), social recognition (Borelli et al. 2009), and predicts social memory retrieval (Lüscher Dias et al. 2016). The role of mPFC subregions in social memory has yet to be delineated, but optogenetic stimulation of the PL does not alter social recognition (Covington et al. 2010).

It is unknown whether the functional interaction of the vHC and mPFC is required for social memory formation, yet several lines of inquiry have suggested that the pathway plays a role. Photoinhibition of vHC terminals within mPFC during encoding has been demonstrated to result in working memory deficits in spatial tasks (Spellman et al. 2015). Both regions also receive input from the BLA, which has been shown to regulate social interactions through both the BLA-mPFC and BLA-vHC pathways (Felix-Ortiz and Tye 2014; Felix-Ortiz et al. 2016). In addition, the dorsal CA2, which was recently shown to be necessary for social memory (Hitti and Siegelbaum 2014; Kohara et al. 2014; Stevenson and Caldwell 2014), preferentially projects to the distal vCA1 and proximal vSub (Okuyama et al. 2016), suggesting distal vCA1 and proximal vSub as well as projections are particularly well placed to also play a role in social memory. Lastly, analysis of CREB expression implicate vHC and mPFC as part of a functionally connected network of brain regions supporting social recognition (Tanimizu et al. 2017). However, whether the vHC-mPFC circuit is necessary for encoding of social memory remains unclear. In particular, the functional contribution of vHC inputs to the IL remains especially unclear. Equally elusive is the role of this vHC-IL pathway in other aspects of emotional processing, namely that involved in fear conditioning.

Fear conditioning paradigms have long been used as a measure for assessing emotional processing and associative learning. Such paradigms traditionally involve pairing a neutral conditioned stimulus (CS), such as a tone, with an unconditioned stimulus (US), such as a shock, to yield a conditioned response (CR), such as freezing, when presenting the CS alone. Although the context in which conditioning occurred may elicit a CR, fear conditioning is not context-specific because presenting the CS will elicit a CR in any context. Extinction training (i.e., presenting the CS in the absence of the US) makes the memory for the CS context-specific or

more contextually bound. Presenting the CS in the context in which extinction occurred, known as *retrieval*, will yield less of a CR than if the CS is presented in a novel or initial conditioning context, known as *renewal*. Extinction therefore creates a new CS-noUS memory, with retrieval of CS meaning set by context, and may even modulate original CS-US memory (Bouton and King 1983; Harris et al. 2000; Maren, Phan, and Liberzon 2013).

The vHC is necessary for the encoding of initial conditioning context and CS (Chen, Foilb, and Christianson 2016; Maren 1999; Richmond et al. 1999; Rudy and Matus-Amat 2005) as well as extinction retrieval (Hobin, Ji, and Maren 2006; Orsini et al. 2011). In addition, the vSub is well placed to respond to aversive stimuli because it contains cells responsive to footshocks and is connected to the HPA axis (Lipski and Grace 2013 a,b). While the role of the vHC in encoding of contextually specific extinction has not been investigated, limited evidence from dHC manipulations suggest the structure is critical; inactivation may slow extinction acquisition and disrupt subsequent retrieval (Corcoran et al. 2005) or it may make extinction context-independent and reduce freezing in both retrieval and renewal (Zelikowsky et al. 2013). The role of the vHC in establishing context-dependency of extinction remains to be investigated.

Within the mPFC, IL activity mediates extinction, with early lesion studies demonstrating effects on extinction retrieval but not acquisition (Quirk et al. 2000). However, more temporally precise methods have suggested that the IL may play a role in acquisition, such that stimulation of IL during extinction training leads to enhanced extinction retrieval and reduced freezing to CS the next day (Adhikari et al. 2015; Do-Monte et al. 2015; Milad and Quirk 2002; Thompson et al. 2010; Vidal-Gonzalez et al. 2006). Conversely, inhibition of the IL during extinction training impairs extinction retrieval but does not change within session responding (Do-Monte, Quiñones-Laracuente, and Quirk 2015; Laurent and Westbrook 2009). Effects of IL modulation

on fear expression appear only after extinction, as inhibition or excitation of IL does not alter freezing after conditioning (Kim et al. 2016). The importance of IL activity during extinction training is likely due to facilitation of extinction encoding in target regions (Adhikari et al. 2015; Bloodgood et al. 2017; Bukalo et al. 2015; Cheriyan et al. 2016; Song, Ehlers, and Moyer 2015). Activity in IL during extinction is mediated by inputs from structures such as the amygdala (Burgos-Robles et al. 2017; Senn et al. 2014). Importantly, the role of vHC input during the encoding of extinction has not been well examined.

Mounting evidence suggests that the vHC-IL pathway is involved in extinction. It has been suggested that NMDA receptor mediated excitation of IL neurons by the vHC is weakened following fear conditioning but extinction strengthens these synapses (Soler-Cedeño et al. 2016 a, b). Enhanced BDNF expression in the vHC that drives release of BDNF in the IL and enhanced firing of IL neurons following extinction may mediate NMDA receptor changes (Rosas-Vidal et al. 2014). Subsequently, renewal activates vHC projections to IL or PL as well as double projecting cells (Wang, Jin, and Maren 2016). Moreover, vHC and vHC-IL projections are necessary for fear renewal, as DREADD mediated inhibition prior to testing disrupts fear renewal (Marek et al. 2018). Thus, although the vHC-IL pathway is involved in extinction retrieval and renewal, the time course of network activity that supports this functional role has yet to be investigated.

Accordingly, anxiety-like behavior, social memory, and fear extinction are amenable to the investigation of cognitive and emotional processing in mice in ways that could be comparable to humans. In mice, subregions of the vHC and mPFC have been found to play unique roles in each of these behaviors (Kim et al. 2015; Okuyama et al. 2016; Padilla-Coreano et al. 2016; Wang, Jin, and Maren 2016). However, interactions between these subregions have

not been investigated and previous studies have not determined whether distinct populations of vHC cells project to the mPFC to constitute unique functional circuits.

The aim of this study is to determine anatomical connectivity of the vHC-mPFC circuit in more detail and investigate the interactions between its component subregions in behavior. Given the current state of knowledge, as summarized above, several hypotheses and their rationale will be presented to allow for furthering of this field.

Hypotheses and Rationale

We hypothesize that the unique functional roles of mouse PL and IL are supported by anatomical segregation of inputs originating within the vHC subregions of vCA1 and vSub. Moreover, the vHC-IL circuit as molecularly defined in Neurotensin-Cre mice ($Nts^{vHC\text{-}IL}$ circuit) may be necessary for anxiety-like behavior, social memory, and fear extinction. To test this hypothesis we will utilize a variety of modern circuit mapping tools combined with targeting of genetically defined cell populations.

As highlighted previously, the circuit in the mouse remains coarsely described and may differ significantly from the rat. These inconsistent results could be due to species differences, as novel methods have revealed subtle differences in mPFC cytoarchitecture (Van De Werd et al. 2010) and connectivity in other regions (Adhikari et al. 2015), or method limitations, as injections targeting connections that display prominent differences across axes can suffer from sampling bias due to lack of coverage of the entire area (Oh et al. 2014). Furthermore, no study in mice has assessed whether populations of vHC cells targeting the PL or IL overlap. Lastly, some proposals suggest the vHC-mPFC circuit is excitatory (Jay et al. 1992; Jay, Burette, and Laroche 1995; Parent et al. 2010; Thierry et al. 2000) but prior studies have not selectively targeted vHC GABAergic cells to determine whether they project to the mPFC. Here we will use anterograde and retrograde injection approaches to define the vHC-mPFC circuit with greater anatomical specificity in the mouse model. Being better informed about anatomical organization will allow us to more precisely probe specific subparts of this pathway.

Next, we will isolate and investigate unique vHC-mPFC circuits by utilizing Neurotensin-Cre mice. While no reliable marker to distinguish the vCA1 and vSub has thus far been found (Fanselow and Dong 2010; Ishihara and Fukuda 2016; Thompson et al. 2008), the

neuropeptide Neurotensin appears to be largely restricted to the subiculum according to the Allen Brain Institute gene expression database (Harris et al. 2014). The mutant mouse line with Cre expression under the Neurotensin promoter thus allows for greater targeting specificity but must be further characterized. Additionally, given the wide-ranging influence of bursting properties, it is of interest to determine whether molecularly defined Nts vHC cells constitute a unique population of cells with spiking or bursting propensity. Consequently, we will assess the spatial distribution, mPFC projection patterns, cell identity, and electrophysiological properties of vHC Neurotensin cells.

An investigation of Neurotensin vHC cells will allow us to determine the functional role of a unique circuit composed of a spatially restricted population of vHC cells projecting to the IL. Whereas it is known that the vHC and mPFC each play a role in cognitive and emotional processing, it is vital to specifically probe the under-investigated IL given the divergent role it plays in a variety of behaviors compared to PL. Specifically, we will assess the role of the $Nts^{vHC\text{-}IL}$ circuit in anxiety-like behavior, social memory, and fear extinction learning by utilizing optogenetic inhibition. We aim to determine whether inhibition of vHC terminals within the IL will reduce innate anxiety-like behavior, as assessed by OFT and EPM, analogous to that seen with inhibition within the PL (Padilla-Coreano et al. 2016). Furthermore, the vHC-mPFC circuit has been implied to play a role in social memory based on past research (Lüscher Dias et al. 2016; Okuyama et al. 2016; Tanimizu et al. 2017), but its causal role and time course have yet to be assessed. Hence, we will test whether inhibition of vHC terminals within the IL during encoding of social interaction leads to social recognition deficits. Likewise, no prior studies have assessed the role of the vHC-IL pathway during encoding of extinction and the subsequent effects on retrieval and renewal. It is hypothesized that inhibition of vHC terminals within the IL

during encoding will not alter within session extinction learning and behavior but will impair extinction retrieval without disrupting renewal. These assessments will inform our understanding of the role of a specific subpart of the vHC-mPFC circuit and enhance understanding of how vHC inputs are segregated within the mPFC. Indeed, we will shed light on how functional roles may diverge across circuits, allowing for specialized circuits within, what was previously assumed to be, homogenous pathways.

Materials & Methods

Subjects

All experiments were performed according to protocols and guidelines approved by the McGill University Animal Care Committee and the Canadian Council on Animal Care. All animals were housed in a 12 hr (8 AM – 8 PM) light/dark cycle with food and water ad libitum. Neurotensin-Cre (Nts::Cre) knock-in mice (The Jackson Laboratory, stock #017525) were kindly provided by Dr. Martin Myers; homozygotes and heterozygotes were bred within the lab. CamKII-α-Cre (CKII::Cre) transgenic mice (The Jackson Laboratory, stock #005359) were bred as homozygotes within the lab. VGAT-ires-Cre (VGAT-Cre) knock-in mice (The Jackson Laboratory, stock # 016962) were bred as homozygotes within the lab.

Cholera Toxin B (CTB)

Cholera Toxin Subunit B (CTB) conjugated with AlexaFluor-488 or AlexaFluor-647 (Molecular Probes) was made into 1% PBS solutions as directed by supplier and aliquoted.

Adeno-associated virus (AAV)

AAVdj-EF1α-flex-ArchT-GFP, AAVdj-EF1α-DIO-eNpHR3.0-eYFP, and AAVdj-EF1α-flex-eYFP, was acquired from Vollum Viral Core, Oregon Health & Science University (E Washburn). AAV2/9-CBA-Flex-Arch-GFP.WPRE.SV40 was acquired from University of Pennsylvania Vector Core. rAAV2-retro-EF1α-DIO-ArchT-eYFP was acquired from Janelia Research Campus, Howard Hughes Medical Institute (J Ting).

Surgical Procedures

CTB & AAV Injections

Mice were anaesthetized with isoflurane (5% induction, 1.5-2% maintenance) and maintained at 35 °C. Carprofen and 0.9% saline were injected subcutaneously at the beginning of

the surgery. The scalp was shaved and scrubbed with betadine before an incision was made. Following skull leveling, a dental drill was utilized to create burr holes at sites defined by the Paxinos and Watson and the Allen Brain Atlases, and then experimentally confirmed. CTB or viruses were infused with pulled glass sharp micropipettes mounted on an automated infusion pump system (Nanoject III, Drummond Scientific Company) at rate of 1-2 nL/sec. The pipette was kept in place after the injection for at least 10 minutes prior to retraction. The scalp was then sutured and covered with Polysporin. Mice recovered with a heating pad and were monitored for ambulation following surgery and provided with oral carprofen gel in their home cages.

CKII-Cre mice for the CTB or viral experiments were injected between P90 and P180 and were subsequently singly or group housed. 50 nL CTB-A488 or CTB-A647 was unilaterally targeted to the PL (AP 2.15ML +/- 0.25 DV -2) or IL (AP 1.7 ML +/- 0.25 DV -2.75). A subset of animals received injections in both PL and IL on the same side, utilizing a different fluorophore for each site. For viral injections, 100 nL of AAVdj-ArchT-GFP was bilaterally targeted to vHC (AP -3.3; ML +/- 3.75; DV -3.85).

VGAT-Cre mice for the viral experiments were injected between P90 and P180 and were subsequently singly or group housed. 200 nL (per side) of AAVdj-ArchT-GFP was bilaterally targeted to vHC (AP -3.35; ML +/- 3.75; DV -3.85).

Nts-Cre mice for the behavioral experiments were injected between P90 and P150 and were subsequently singly housed. 400 nL (per side) of AAVdj-eNpHR3.0 was bilaterally targeted to vHC (AP -3.6; ML +/- 3.65; DV -3.8). For tracing experiments, 100 nL of rAAV2-retro or AAV2/9 was unilaterally targeted to IL (AP 1.7; ML +/- 0.25; DV -2.75).

Nts-Cre mice for the ex-vivo electrophysiological experiments were injected between P60 and P150 and were subsequently singly or group housed. 400 nL of AAVdj-eNpHR3.0 was bilaterally targeted to vHC (AP -3.6; ML +/- 3.65; DV -3.8).

Optic Fiber Implant

A subset of mice underwent a second surgery after a 2-week recovery period from viral injections. Following the creation of burr holes, optic fibers (Thorlabs) connected to a ferrule (Precision Fiber Products) were lowered to target the top of the IL (AP 1.8, ML +/- 0.9 with 10° angle, DV -2.25 from dura). The optic fibers were tested for efficiency (calibrated power of the laser was ~20 mW when measured at the tip of the optic fiber) and implanted bilaterally. Optic implants were secured to the skull with Metabond and dental cement (Patterson Dental) with additional support provided by screws placed into the skull. Black nail polish was applied to the entire implant to reduce the amount of light emanating from the implant and disrupting the mice.

Ex Vivo Electrophysiology

Electrophysiological recordings were performed following a minimum of 3-week recovery from the viral injection to allow for maximal viral transfection. Mice were anesthetized with ketamine/xylazine rodent cocktail prior to intracardial perfusion with cold NMDG recovery solution (4°C) and subsequent decapitation in ice cold NMDG solution (93 mM NMDG, 93mM HCl, 2.5 mM KCl, 1.2 mM NaH2PO4. 30 NaHCO3, 20 mM HEPES, 25 mM Glucose, 5 mM sodium ascorbate, 2 mM Thiourea, 3 mM sodium pyruvate, 10 mM MgSO4.7H2O, 0.5 mM CaCl2.2H2O, continuously oxygenated with 95% O2/5% CO2; pH 7.3). Brains were mounted dorsal side down, and 350 uM horizontal sections were sliced with a Leica vibratome. Slices were transferred to 4°C NMDG recovery solution for 10-12 minutes prior to being stored for at least an hour in oxygenated, room temperature (RT) ACSF (in mM: 125 NaCl, 26 NaHCO3, 25

glucose, 2.5 KCl, 2 MgCl2,1.25 NaH2PO4, 2 CaCl2, pH 7.35), continuously oxygenated with 95% O2/5% CO2. Slices were recorded in a bath of aCSF heated to 30°C. Patch clamp electrodes were pulled from glass capillary tubes (electrode resistance=3 to 7 Mohm) and filled with intracellular solution containing (in mM): 144 K-gluconate, 10 HEPES, 3 MgCl2, 2 Na2ATP, 0.3 GTP, 0.2 EGTA, adjusted to pH 7.2 with KOH for whole cell current-clamp recordings.

Neurotensin positive cells (identified by fluorescence after AAVdj-YFP transfection) and a similar number of unlabeled (presumably Neurotensin negative cells) located in the vSub were assessed utilizing an upright microscope with a 40x immersion objective (Olympus Canada), X-cite Series 120Q fluorescence system, MultiClamp 700B amplifier, DigiData 1440A digitizer, and pClamp10 software, and analyzed with Clampfit10 Software.

Recordings were kept for analysis only if spikes overshot 0 mV and access resistance was <30 MΩ. Membrane resistance (Rm) and access resistance (Ra) were measured in voltage clamp (vc) using pClamp10 software. Resting membrane potential (Vr) was assessed over a 1 minute recording with no holding current. To assess spike properties, cells were held at a holding potential of -70 mV, and a series of 600 ms depolarizing current steps was applied. The step which elicited the first spike was used to assess an after-hyperpolarization (AHP) amplitude and time, and the 300 pA injection step was used to assess spike amplitude and half width. AHP for bursting cells was measured using the last spike of the first burst. To assess sag, a series of hyperpolarizing current steps was applied at a holding potential of -70 mV. The step which hyperpolarized the cell to -120 mV was used to calculate sag amplitude, measured as the difference between peak and steady state hyperpolarization, and to determine the presence of a rebound spike.

Patched cells were assessed for several properties, including resting membrane properties, responses to depolarizing and hyperpolarizing current steps, and spike properties. Responses to depolarizing current steps were used to distinguish cells into bursting and spiking. Standard t-test was done to test for significant differences of basic properties between NT positive and NT negative cells. These results were also compared to findings within the dSub. Ex-vivo experiments were generously performed by Ingrid Inema in the Williams lab.

Behavioral Apparatuses

The apparatus utilized for the EPM is in a plus-shaped (+) configuration composed of two closed arms (29 x 5 cm) across from each other which are perpendicular to two open arms (29 x 5 cm) with a center platform (9 x 9 cm). The closed arms are enclosed by high (11 cm) walls while the open arms are not enclosed. The entire apparatus is 50 cm above the floor and is built from black painted wood with a gray floor.

The apparatus utilized for OFT is a square (45 x 45 cm) box with tall (50 cm) sides. It is placed on a table for experimental procedures and is composed of opaque gray polymer.

The social recognition paradigm utilized the OFT box with a circular metal pencil holder (radius of 7.5 cm and 15 cm height) to hold the stranger mouse.

The Coulbourn Habitest Operant Cage was utilized for fear conditioning and extinction. Context A is rectangular (30 x 25 cm) with alternating metal and plastic walls (28 cm height) and metal rod floor. A distinctive olfactory cue is provided by cleaning with 79% water:20% ethanol:1% vanilla extract solution between subjects. Context B is circular (diameter of 24 cm) with alternating black and white plastic walls (25 cm height) and grey plastic floor. A distinctive olfactory cue is provided by cleaning with Peroxigard solution between subjects. Graphic State 4 software is utilized for programing and delivery of stimuli and photoinhibition.

Behavioral Procedures

Following 1 week of recovery and another week of tether habituation, animals were tested in behavioral paradigms. To maximize the use of animals, the same cohort of animals was used and tests were performed in the order presented below, starting with the least stressful test followed by increasingly stressful ones. Inhibition was achieved utilizing green (532 nm) laser (Doric Laser Diode Fiber Light Source: 4-Channel). Behavior was recorded with webcam and stored with Cheetah Software (Neuralynx).

Open field test (OFT)

Mice were placed in open field. The laser was turned on during the entire 5 minute duration of the OFT. Behavior was analyzed using TopScan (CleverSys Inc) and OptiMouse software for the number of entries and duration of exploration of the center vs. periphery, distance travelled, and path tracing. The video was subsequently manually reviewed because the tethers sometimes led to detection errors.

Elevated Plus Maze (EPM)

Mice were placed in EPM under 150 lux illumination. The laser was turned on during the entire 5-minute duration of the test. Behavior was analyzed using TopScan software (CleverSys Inc) for number of entries into and duration of exploration of open vs. closed arms, distance travelled, and path tracing. Video was subsequently manually reviewed because the tethers sometimes led to detection errors. Head dips were manually scored.

Social Interaction Test ('direct interaction')

The subject mouse was placed into the open field previously used in the OFT with an empty cup in center for 10 minutes (habituation). A naïve stranger mouse was then placed under the cup for 5 minutes (Trial 1, familiarization), allowing for sniffing but no aggressive behavior.

The laser was turned on each time the subject mouse's nose was within 3.5 cm of the cup (interaction zone). The subject mouse was then returned to home cage. After an inter-trial interval (ITI) of 30 minutes, the subject mouse was placed back into the open field for 5 minutes (Trial 2, discrimination) where under the cup was either the same mouse as in Trial 1 ('familiar') or completely new stranger mouse ('novel'). Subject mice were connected to the laser via tethers throughout habituation, familiarization, and discrimination periods but photoinhibition would only occur during familiarization. Behavior was analyzed using TopScan software (CleverSys Inc) for duration of exploration within the interaction zone (nose had to be in zone), distance travelled, and path tracing. Video was subsequently manually reviewed because tethers sometimes led to detection errors. The recognition index was determined for each mouse to account for individual variability in baseline sociability. Formula for Recognition Index (RI) = Duration of nose around cup (Trial 2) ÷ Duration of nose around cup (Trial 1 + 2).

The social recognition test protocol is adapted from Thor & Holloway (1982). It was chosen instead of the three chamber test (Dantzer et al. 1987) because of tethers interfering with movement and instead of non-conditioned social discrimination tests utilizing juveniles without separation by cups (Engelmann, Hädicke, and Noack 2011) to reduce potential for behavior that could be damaging to the implants. This method is also conducive to accurate detection of social interaction for triggering photoinhibition (Okuyama et al. 2016),

An ITI of 30 minutes was chosen because it is the most commonly used, and it has been previously shown that social recognition memory dissipates between 1–2 h for individually housed mice and rats (Bluthé, Gheusi, and Dantzer 1993; Sekiguchi, Wolterink, and van Ree 1991; Thor and Holloway 1982).

Fear conditioning and fear extinction

Following the conclusion of the other behavioral paradigms, mice underwent cued fear conditioning. On day 1, mice received cued fear conditioning in context A without photoinhibition (laser OFF). Following 120 sec habituation to context, mice were conditioned with three tone (CS; 30 sec, 80 dB, 2.5kHz) – footshock (US; 0.5 mA, 2 sec) pairings with 60-120 sec ITIs (pseudo-randomized). On day 2, twenty-four hours after the conditioning session, mice underwent fear extinction training in novel context B. Extinction consisted of 120 sec habituation to context followed by 40 tone-only (30 sec, 80 dB, 2.5kHz, 15 sec ITI) presentations, with photoinhibition (laser ON) during each tone presentation. On day 3, mice were tested for renewal in context A. Renewal consisted of 120 sec habituation to context followed by 5 tone-only (30 sec, 80 dB, 2.5kHz, 10 sec ITI) presentations, without photoinhibition (laser OFF). Subject mice were connected to the laser via tethers throughout (conditioning, extinction, and renewal), but photoinhibition would only occur during extinction training. Behavior was manually assessed by quantifying observed freezing behavior, defined as absence of movement except for breathing, lasting longer than 1 sec. In addition, freezing to CS was used to calculate the rate of learning during extinction session as well as recall the following day.

Immunohistochemistry

Mice were euthanized with an overdose of a ketamine/xylitol mixture and transcardially perfused with ice-cold saline-Heparin 0.1% followed by 4% paraformaldehyde (PFA) in 1X PBS (pH 7.4). Brains were post-fixed in 4% paraformaldehyde overnight at 4°C then placed in 15% sucrose solution at 4°C until they sank. Brains were then embedded in OCT and frozen before

being sliced into 25 uM coronal or horizontal sections using a cryostat set at -21°C. Sections were directly mounted on positively charged slides and 1 series of 4 was processed.

CTB: Following section mounting, slides were sealed and coverslipped using Fluoromount-DAPI.

AAV: Slide-mounted sections were permeabilized and blocked utilizing PGT (1X PBS, 0.45% Cold Water Fish Skin Gelatin, and 0.25% Triton). Slides were incubated overnight at 4°C with primary antibody diluted in PGT: anti-GFP Goat IgG Polyclonal (Novus Biologicals) at [1:5k], anti-GFP Rabbit (Life Technologies) at [1:1k], anti-ZnT3 Rabbit (Synaptic Systems) at [1:500]. The next day, slides were washed 3 times with PGT. Slides were then incubated 1.5 h at RT with secondary antibody diluted in PGT: Donkey anti-Gt A488 secondary antibody (Mol Probes) at [1:1k], Donkey anti-Rb A488 secondary antibody (Mol Probes) at [1:1k], Donkey anti-Rb A647 secondary antibody (Thermofisher) at [1:1k]. Following PBS wash, slides were sealed and coverslipped using Fluoromount-DAPI.

Fluorescence In-Situ Hybridization (FISH)

Mice were anesthetized with 5% isoflurane prior to being decapitated, with subsequently extracted brains being flash frozen on dry ice. Brains were sliced into 10 uM coronal or horizontal sections, under RNase-free conditions using a cryostat set at -21°C, and directly mounted to slides. Custom probes for Nts, CamKII, and Cre were generated in-house utilizing PCR gel extraction prior to DIG or Fluorescein RNA labeling and subsequent purification on Amersham G-50 micro-columns. Slides were thawed in PBS before being fixed in 4% PFA for 10 min followed by PBS washes, 10 min acetylation, PBS washes, and incubation in a humid chamber for 30 min at RT with Hybe solution. Slides were then incubated overnight at 60°C in hybridization oven with probe-Hybe solution mixture covered with nescofilm. The following

day, slides underwent stringency washes with SSC and then MABT prior to 30 min incubation at RT in blocking buffer (20% maleic acid buffer, 20% FBS, and 20% blocking reagent). Subsequently, slides were incubated 1h at RT with anti-Fluorescein-POD at [1:2.5k] diluted in blocking buffer before MABT and PBS-T washes. Next, slides were incubated 10 min at RT with TSA-PLUS BIOTIN (Perkin Elmer) at [1:100] diluted in amplification buffer (kit supplied) before PBS-T washes. Lastly, slides were incubated 10 min at RT with Neutravidin-Oregon Green (Invitrogen) at [1:500] before being washed with PBS-T and left overnight at RT. The following day, slides underwent sequential washes with Glycine buffer, PBS-T, H2O2, PBS-T, and MABT prior to 20 min incubation at RT in blocking buffer. Subsequently, slides were incubated 1h at RT with anti-DIG-POD at [1:2.5k] diluted in blocking buffer before MABT and PBS-T washes. Next, slides were incubated 10 min at RT with TSA-PLUS-CY3 (Perkin Elmer) at [1:100] diluted in amplification buffer (kit supplied) before PBS-T washes. Following Hoescht staining for 5 min and washes with PBS-T and then PBS, slides were sealed and coverslipped using Fluoromount.

Microscopy

The slides were visualized with an Olympus VS120 Slide Scanner. Overview images were obtained with 4X objective. Sections utilized for quantification were obtained with 20X objective.

Select slides were imaged with an Olympus FV1200 confocal microscope.

Image Analysis

Overlays and ROIs were adapted from Allen Brain Institute to guide histological assessment. CTB injection centers were verified to only be within target regions of PL or IL. AAV injections and spread were verified to be within target regions with minimal spread to

adjacent structures such as EC (animals with more than a few transfected somas were excluded from analysis).

CTB: Cell Counting = Coronal sections of the hippocampus (-3.2 to -4.2 posterior to bregma) were quantified at 200 nM intervals (minimum of 4 sections per animal) using ImageJ to count somas. Horizontal sections of the hippocampus (-2.5 to -4.5 ventral to bregma) were quantified at 400 nm intervals (minimum of 4 sections per animal). Single and/or double-labeled somas for each fluorophore were manually counted using ImageJ under blind conditions. Soma counts were analyzed as raw counts or as percentage of total counted within HC.

AAV: Ridge analysis = Density of anterogradely labeled vHC axon projections was detected using a ridge detection method adapted from Zhang et al. (2016). Fluorescent images of mPFC were analyzed at different scales and ROI density (% area covered) was measured with ImageJ. This method depends on the length but not thickness of the axon, eliminating the problem of out of focus axons taking up more space. *Fig 21* demonstrates this method.

FISH: For quantification of vHC cells co-expressing Nts mRNA and Cre or CKII mRNA, single and/or double-labeled cells for each fluorophore were manually tagged using ImageJ under blind conditions. FISH labeling was compared to location of nuclei labeling to determine spatial distribution and co-expression.

Only mice with histologically confirmed optic fiber placement as well as proper construct expression in the vHC were used in the present study.

Data Analysis

Statistical analysis was performed using Prism 6. All data are presented as mean ± standard error of the mean (SEM). $P < 0.05$ was considered statistically significant.

Results

Anatomical Experiments

vHC neurons innervate the IL to a greater extent than PL

CTB-labeled somas across a large portion of the vHC were quantified following single injections of the retrograde tracer CTB into either the PL or IL to determine differences in extent of mPFC subregion innervation in mice. Fluorescently conjugated CTB-A488 injections were spatially restricted to either the PL or IL (*Fig 1*), with injection centers showing variation in AP level and layers targeted (*Fig 2*). Quantification of labeled somas throughout the vHC demonstrated a greater number (~3X) of vHC cells projecting to the IL (*Fig 3*) than the PL.

PL vs. IL projecting vHC cells show anatomical segregation

Double-labeled CTB somas were quantified across a large portion of the vHC following injections of CTB conjugated with distinct fluorophores into the PL and IL to determine whether vHC inputs are anatomically segregated in mice. Fluorescently conjugated CTB-A647 injections were spatially restricted to the PL and CTB-A488 to the IL (*Fig 4*), or vice versa, with minimal overlap of injection sites. Horizontal HC sections were utilized to distinguish the vCA1 and vSub (unable to do so with coronal sections).

Double-labeled somas were found throughout the vCA1 and vSub (*Fig 5*) but made up a small portion (7%) of the total number of fluorescently labeled somas (*Fig 5d*). A greater number of vHC projections to the mPFC were found to originate within the CA1 than the Sub, $M=0.3719$, $F(1, 36) = 195.2$, $p < 0.001$. This effect remained significant for PL and IL projections as well as double projections (*Fig 5c*).

vHC-mPFC pathway does not contain GABAergic cells

No labeled projections were observed within the mPFC (*Fig 6*) following injections of Cre-dependent AAVdj-ArchT-GFP into the vHC of VGAT-Cre mice. For confirmation, no fluorescently labeled somas were observed throughout the entire AP extent of the HC after injections of Cre-dependent and partially retrograde AAV2/9-Arch-GFP into the mPFC of VGAT-Cre mice.

Greater vHC innervation of IL is present across AP levels

Given confirmation that the vHC-mPFC projection is excitatory, Cre-dependent AAVdj-ArchT-GFP was injected into the vHC of CamKII-Cre mice to take advantage of the increased specificity of a viral approach. Anterograde vHC injections of AAV yielded projection patterns within mPFC that visually coincided with CTB results, with a greater amount of projections seen within the IL vs. PL (*Fig 6*). The density of projections within the PL and IL was quantified with the ridge detection method to verify the visual observation. Greater IL (~2X) than PL innervation by vHC was confirmed across several AP levels (*Figs 4c, 4d*).

Cre is selectively expressed in Nts cells

Fluorescent in-situ hybridization (FISH) was performed using custom Nts and Cre probes to detect expression in vHC of Nts-Cre mice. Sections were assessed for double labeling to determine overlap in individual neurons as a measure of appropriately targeted Cre recombinase expression. Preliminary results demonstrate that Cre is expressed only in Nts expressing cells (*Fig 5a*).

Nts vHC cells are excitatory

FISH was performed using custom Nts and CamKII probes to detect expression in vHC of Nts-Cre mice. Sections were assessed for double labeling to determine co-expression in

individual neurons as a measure of cell identity. Preliminary results demonstrate that Nts-containing vHC neurons comprise a subpopulation of excitatory cells (*Fig 5b*).

mPFC projecting Nts cells are spatially restricted to distal vCA1 and proximal vSub

Following injections of Cre-dependent AAVdj-ArchT-GFP into the vHC to characterize anatomical distribution of Nts-positive cells, I found substantial transfection on the distal vCA1 and proximal vSub border with minimal transfection of proximal vCA1 (*Fig 6c*). In addition, preliminary analysis demonstrates that the proportion of transfected Nts vHC cells increases from distal vCA1 to proximal vSub (*Fig 7*). Given the wide distribution of mPFC projecting cells within the vHC and the limited extent of Nts expressing cells, it is important to assess the overlap between these two populations. Consequently, either AAV2/9-Arch-GFP or AAV2retro-ArchT-YFP was injected into the mPFC to characterize the spatial distribution of mPFC projecting Nts vHC cells. I determined that mPFC projecting Nts cells originate in distal vCA1 and proximal vSub, with no distal vSub contributions (*Fig 6e, 6f*).

Nts vHC cells have a unique pattern of mPFC innervation

I compared the pattern of mPFC innervation in Nts-Cre and CKII-Cre mice following injections of AAVdj-ArchT-GFP into the vHC. Compared to CamKII, Nts vHC cells showed an even greater propensity of increased IL innervation (*Fig 6h*).

Given the unique topography of targeted cells in distal vCA1 and proximal vSub, and the resultant mPFC innervation pattern, as well as the uninvestigated function of Neurotensin in vHC projections, the molecularly defined pathway we are investigating will henceforth be referred to as the $Nts^{vHC\text{-}IL}$circuit.

Nts vHC cells do not demonstrate a unique propensity for spiking or bursting

Given the wide-ranging influence of bursting properties, it is of interest to determine whether molecularly defined Nts vHC cells constitute a unique population of cells with spiking or bursting propensity. In order to test this hypothesis, Cre-dependent AAVdj-YFP was injected into the vHC of Nts mice before electrophysiological properties of both labeled and unlabeled vSub neurons were characterized with ex-vivo patch clamping. The vSub was chosen for analysis due to a greater proportion of bursting cells (vs. vCA1) as well as greater overall number of Nts expressing cells. Preliminary results demonstrated that the population of vSub Nts cells is not significantly different from the surrounding general population in bursting propensity or other electrophysiological properties assessed (*Fig 9*, *Table 1*), similar to results seen in dSub Nts neurons (*Table 2*).

Optogenetic Experiments Manipulating Nts$^{vHC\text{-}IL}$circuit

Histological Assessment

For the analysis presented here, animals were excluded largely on the basis of histological assessment (n=20: YFP=8, NpHR=12), as they had to have sufficient viral expression in vHC and accurate fiber placements in the top half of the IL, or due to bald mutation associated with smaller size (n=3: YFP=1, NpHR=2). Other reasons included issues with tethers during individual experiments, infection, or death prior to behavioral experiments. In addition, animals were subsequently excluded selectively from some individual behavioral experiments. For social interaction test, results were excluded if animals explored the stranger mouse less than 75 seconds during the initial familiarization in trial 1 or if the stranger mice (in novel condition) were from different litters but identical parents (n=3; YFP=1, NpHR=2). For

fear extinction, animals were excluded due to the recording not being saved properly (n=4: YFP=2, NpHR=2).

Inhibition of Nts^{vHC-IL} circuit during OFT did not alter anxiety-like behavior

Data were obtained from n=10 (YFP=6, NpHR=4) mice in which the Nts^{vHC-IL} circuit was optogenetically inhibited for the entire 5 minute duration of the OFT. Analysis of behavior revealed no effects of optogenetic inhibition on number of entries into center or duration of exploration of center vs. periphery (Figure 16)

Inhibition of Nts^{vHC-IL} circuit during EPM did not alter anxiety-like behavior

Data were obtained from n=10 (YFP=6, NpHR=4) mice in which the Nts^{vHC-IL} circuit was optogenetically inhibited for the entire 5 minute duration of the EPM. Analysis of behavior revealed no effects of optogenetic inhibition on number of head dips, entries into the open arms, or duration of exploration of the open arms (Figure 17)

Inhibition of Nts^{vHC-IL} circuit during social interaction did not alter social memory

Data were obtained from (n=5 for familiar, YFP=3, NpHR=2; n=3 for novel, YFP=2, NpHR=1) mice in which the Nts^{vHC-IL} circuit was optogenetically inhibited each time the subject mouse's nose was within the interaction zone during familiarization in trial 1. Results were excluded if animals explored the stranger mouse less than 75 seconds during initial familiarization in trial 1 (n=5 for familiar, YFP=3, NpHR=2; n=4 for novel, YFP=3, NpHR=1). Analysis of behavior revealed no effects of optogenetic inhibition on duration of exploration during discrimination or recognition index (Figure 18). However, control (YFP) animals also failed to distinguish novel or familiar conspecifics as revealed by the recognition index, indicating potential lack of robust social recognition memory.

Inhibition of $Nts^{vHC\text{-}IL}$ circuit during cue presentation in extinction had unclear effects

Data were obtained from (n=4: YFP=3, NpHR=1) mice in which the $Nts^{vHC\text{-}IL}$ circuit was optogenetically inhibited each with each cue presentation during extinction training on Day 2. Analysis of behavior revealed optogenetic inhibition may have increased freezing across cue presentation during extinction in one animal (Figure 19). The effects of NpHR on renewal and cue presentation on Day 3 was not assessed due to lack of animals. All animals demonstrated some level of freezing by the end of conditioning.

Discussion

The objective of these studies was to investigate the pattern of distribution of vHC projections to the mPFC subregions, PL and IL, in greater detail within the mouse. Furthermore, we aimed to assess the role of a subset of vHC projections to the IL in various behaviors.

Anatomical findings

vHC neurons innervate the IL to a greater extent than PL

In one of the key experiments to determine projection pattern within the vHC-mPFC circuit, we injected retrograde CTB into the PL or IL and quantified somas within the vHC. Moreover, we confirmed these results with injections of anterograde AAV into the vHC and quantification of fiber density within the PL and IL. Previous studies of ventral hippocampal input to the mPFC have suggested that rats and mice differ in their pattern of distribution, with greater innervation of IL in rats and greater innervation of PL in mice (Tripathi et al. 2016; Wang, Jin, and Maren 2016). However, our results demonstrating greater innervation of IL (2-3X, depending on method utilized) in mice suggest that those previous results may have been due to study designs that failed to assess the entire extent of these regions, particularly as it is known that such projections may exhibit very precise spatial input and output targeting (Kim and Cho 2017; Tannenholz, Jimenez, and Kheirbek 2014).

Furthermore, our novel finding that the mouse PL and IL are innervated largely by separate populations of vHC neurons (only 6% overlap of CTB labeling), is in line with what has been found in rats (Wang, Jin, and Maren 2016). Likewise, we have demonstrated for the first time in rodents that the vCA1 provides significantly more input to both the IL and PL than the vSub. Such a separation of inputs to these regions provides strong support for distinguishing these regions when assessing the role of the vHC-mPFC circuit. As discussed previously, a large

number of studies have either looked at the mPFC as a whole or only assessed the PL (Padilla-Coreano et al. 2016; Parfitt et al. 2017). Future studies should further investigate the pattern and functional role of differential vHC input to the PL and IL.

Similarly, the individual contribution of vCA1 and vSub to the mPFC has never been assessed previously, although these regions are known to vary across several dimensions of structure and function (Bannerman et al. 2004; Strange et al. 2014). Indeed, our results in NT mice suggests that the vSub may show a different balance of PL vs. IL innervation. Future studies should attempt to evaluate this unique subregion marker further to assess differences in spatial distribution of mPFC innervation based on origin in vHC. Additionally, the functional significance of this distribution pattern is of interest to assess.

Lastly, while previous studies have suggested that the vHC-mPFC circuit is excitatory, they have not utilized the combination of viruses and Cre-expressing mouse strains that has enabled investigations of a variety of circuits (Callaway 2005; Kohara et al. 2014; Zingg et al. 2017). Hence, we took advantage of such an innovative intersectional approach in VGAT-Cre animals to demonstrate a lack of GABAergic projections within the vHC-mPFC pathway.

We propose that as the vHC-mPFC circuit is anatomically comparable across mice and rats, it may also play a similar role in behavior in both species. This resemblance would allow for increased translation of findings across species, allowing for improved knowledge as studies from rats could be integrated with those from mice.

Anatomical control measures and limitations

Although our methods contain several improvements over previous studies, several concerns still require addressing.

- Limited by placement of injection centers

While neurons within the vHC are known to project to a significant portion of the mPFC, a retrograde CTB approach allows us to only able to label neurons that project to the targeted area; that is, the portion of neurons labeled in the vHC will depend on the injection center location and size. Specifically, CTB injections were of small volume (50 nL) to minimize injection spread to the adjoining PL or IL region. Similarly, double CTB injections were targeted toward more anterior PL and more posterior IL, thereby increasing distance between injections in the same hemisphere to reduce overlap. The same coordinates were utilized for both double and single injections but the criteria for exclusion in double were more stringent. Thus, our single injections included injection centers across a wide range of AP levels (PL=1.6-2.2; IL=1.3-1.9). Granted, each injection was not indicative of the entire structure, neither affecting the entire PL or IL, nor the entire 5 layer cytoarchitecture. Nevertheless, as results were summed and included injections at various levels, results should represent the entire structure. Furthermore, we utilized injections of anterograde AAV into the vHC to confirm our results. These injections affected a large area within the vHC and gave results consistent with that seen with CTB, albeit with less extreme differences in PL vs. IL innervation.

- Lack of GABAergic projections

Both anterograde and retrograde AAV approaches in VGAT-Cre animals yielded lack of fluorescent labelling. While our results corroborate with previous findings, negative results cannot exclude the possibility that the methods used here failed to identify or transfect a unique population of GABAergic cells within the vHC-mPFC pathway.

- Utilizing CKII vs wild type strain

In contrast to previous studies assessing anatomy (Tripathi et al. 2016), our anatomical tracing studies, utilizing both CTB and anterograde AAV, were performed in CKII-Cre (HO) mice. Although it is possible that our results may not be translatable to other mice, anatomical organization is not expected to differ between strains. It is also reasonable to assume that projection patterns within transgenic Cre recombinase expressing mouse strains will be similar to that seen in wild-type experimental mice (Julie A. Harris et al. 2014). Particularly as such mice are ubiquitous in neuroscience research, and CKII-Cre mice have a C57BL/6 (B6) background, the one most commonly found in mice used as wild-type controls. For comparison and to strengthen our results, additional injections could be replicated in wild type mice.

- Cell identity and physiological properties of PL vs. IL projecting cells

Our comparison was focused on the purely anatomical differences to distinguish distribution of cells, vCA1 vs. vSub, projecting to the PL, IL, or both. Yet, other factors could contribute to the role a circuit plays. The PL and IL are known to show different physiological properties (Kim and Cho 2017; van Aerde, Heistek, and Mansvelder 2008), but it is unclear whether these differences are inherent within their structure and organization or are due to input contributions from significantly different origins (Izaki et al. 2003). Accordingly, it would be of interest to assess the cell identity and physiological properties of PL vs. IL projecting vHC cells. Likewise, projections originating in vCA1 and vSub could be compared. A particularly interesting candidate is calbindin, a molecule proposed to distinguish superficial and deep pyramidal cells within the CA1 (Slomianka et al. 2011). Additionally, cells along this superficial-deep axis vary in their physiological properties and efferents (Masurkar et al. 2017).

In conclusion, future studies of the vHC-mPFC pathway should investigate the properties that contribute to functional variation within the circuit.

- Determination of NT differences

Our initial assessment of Neurotensin-positive cells included immunohistological verification of their excitatory identify via overlap with CKII. Moreover, we determined that NT cells do not appear to display in-vitro physiological differences from the surrounding vSub (and dSub) population. Nevertheless, it remains unclear whether the IL projecting vSub cells display a distinct physiological profile to support their unique functional roles. Likewise, the types of cells and neuronal compartments targeted by NT cells are unknown. Lastly, it is unclear whether NT cells are unique in the input they receive, contributing to differential circuit contributions. For instance, it has been demonstrated that the proximal Sub contains a large amount of NPY-expressing interneurons, which are very efficient at reducing synaptic excitation (Cembrowski et al. 2018; Ho, Beck-Sickinger, and Colmers 2000). It would be of interest to determine whether NPY cells preferentially target NT cells, particularly those with PFC projections. Indeed, as we assessed the role of a subset of vHC projections to the IL in several behaviors in a Neurotensin-Cre mouse line, increased understanding of the properties of the manipulated $Nts^{vHC\text{-}IL}$circuit would enhance extrapolation of findings to wild type mice as well as other species.

Behavior

<u>Inhibition of $Nts^{vHC\text{-}IL}$ circuit does not alter anxiety-like behavior or social memory</u>

Our results demonstrating a lack of behavioral effects following optogenetic inhibition of NT vHC terminals within the IL were somewhat surprising but could be due to several factors. One important consideration is the small number of animals that remained for analysis following histological exclusions. Furthermore, an highly anxiogenic strain, retrograde EC expression,

efficiency of NpHR, and wrong behavioral tasks may also have contributed. Nevertheless, it is also possible that our results reveal important details about this circuit, including excitation/inhibition (E/I) balance and NT release. Moreover, they suggest that the PL and IL may play unique roles in the regulation of behavior, particularly when guided by affective information. Finally, utilizing NT-Cre mice may allow the probing of a unique neuropeptide circuit with a role in a diverse range of behaviors, analogous to what has been seen with glucagon-like peptide-1 signaling in feeding behavior associated with the vHC-mpFC circuit (Hsu et al. 2017). Hence, our study provides a unique perspective on the functional role of the vHC-mPFC circuit, highlighting the need for more nuanced investigations.

Behavioral control measures and limitations

- Disruption of E/I balance or integration within the PL and IL

It has previously been suggested than an appropriate E/I balance supports appropriate behavior, with disruptions seen in conditions such as autism and schizophrenia (Selten, van Bokhoven, and Nadif Kasri 2018; Yizhar, Fenno, Prigge, et al. 2011). In particular, the IL is known to inhibit the PL (Saffari et al. 2016), contributing to the opposing roles the two regions play in behavior. Thus, our manipulation of reducing vHC input to the IL at select times may have altered the mixed encoding that the mPFC has been suggested to engage in (Grunfeld and Likhtik 2018). This possibility is particularly important because as the vHC synapses onto both pyramidal and interneurons (Carr and Sesack 1996; Gabbott, Headlam, and Busby 2002; Tierney et al. 2004), the effect would not be a simple inhibition or excitation effect. Lastly, while it has been shown that PV neurons within the PL generate low theta (Hartwich, Pollak, and Klausberger 2009), allowing for synchrony between mPFC and BLA or vHC (Gabbott, Headlam, and Busby 2002; Likhtik et al. 2014), such a pattern of theta production has not been

found within the IL. Therefore, input from the vHC to the IL may not be as critical for the output related synchrony of these regions, limiting the behaviors impacted by optogenetic inhibition of input. Consequently, our study may reveal something critical regarding the role of vHC input, specifically from the distal vCA1 and proximal vSub, on integration of information by the mPFC.

It has been suggested that mPFC subregions may play opposing roles when confronted with threatening stimuli, such that the PL leads to motor inhibition (freezing) while IL leads to excitation (movement) (Grunfeld and Likhtik 2018; Halladay and Blair 2017). Likewise, given evidence that the IL may function as a feed forward inhibitory structure, serving as a 'brake' for fear expression (Giustino and Maren 2015; Riga et al. 2014), it is possible that inhibition of vHC input to the IL may have allowed other structures, namely BLA and PL, to exert their influence. This network activity may have been altered through disrupted E/I balance within mPFC or due to long range projections by the IL to periaqueductal gray (PAG) or BLA (Bloodgood et al. 2017; Ferreira et al. 2015). While the majority of the behaviors we assessed were innate and not particularly negatively valenced, it is likely that these two regions play unique roles in a wide variety of behaviors and in response to a range of stimuli.

If our experiments left vHC-PL signaling intact, especially given the separate populations of vHC cells targeting PL vs. IL, then our findings suggest a more nuanced role for PL vs. IL in behavior. While vHC input to regions such as LHA or NAc may drive approach and avoidance behavior directly (Jimenez et al. 2018), the input to the mPFC may support higher order integration and slower modulation of behavior via outputs to downstream target regions. Additional experiments should probe the effects of inhibition on E/I balance within the mPFC subregions and utilize complex behavioral paradigms that test for conflict between these two

regions. Finally, as E/I balance disruption in mPFC has been associated with social deficits (Yizhar, Fenno, Prigge, et al. 2011), studies need to assess inhibition effects on social interaction time not just memory.

- Efficiency of NpHR inhibition

While efficiency of NpHR inhibition has been assessed previously, it is important to verify that our inhibition is sufficient to induce physiologically relevant changes. One key control experiment would involve assessment of NpHR inhibition with patch clamping or field recordings in the mPFC. Similarly, while we utilized a non-optimal wavelength of light (532 nm), previous studies and in-vitro testing from our lab has demonstrated the efficacy of this wavelength with NpHR (Baratta et al. 2012). Lastly, given the presence of fibers with NpHR within the PL and several surrounding regions, we may not have achieved our goal of isolating the IL specifically. Notwithstanding the ongoing debate regarding the extent of light dispersion in tissue (Shin et al. 2016; Yizhar, Fenno, Davidson, et al. 2011), our stringent implant targeting criteria allowed us to eliminate questionable cases and only retain animals with IL inhibition.

- Effects of NpHR inhibition on NT release

Given our use of a Cre mouse line with expression controlled by a neuropeptide promoter, it is important to assess whether neuropeptide, specifically NT, release is altered by optogenetic inhibition. Indeed, the presence or role of NT release by vHC projections in the IL has never been described and such signaling should be investigated in future studies of this circuit. For example, NT may regulate and even enhance glutamate transmission in certain brain areas (Antonelli et al. 2007; Ferraro et al. 2011; Kempadoo et al. 2013). Conversely, NT release in the PFC, most likely by dopamine axons from VTA (Studler et al. 1988), has been shown to increase GABA and activate PV-expressing GABAergic interneurons (Audinat, Hermel, and

Crépel 1989; Petrie et al. 2005). Lastly, peptidergic signaling often occurs alongside faster glutamatergic or GABAergic neurotransmitter signaling by individuals neurons (van den Pol, Wuarin, and Dudek 1990), contributing to the complex role they play in circuits (Schöne and Burdakov 2012). Still, while it remains unclear whether both peptide signaling and neurotransmitter release is altered with photoinhibition, recent evidence suggests an opposite effect on behavioral output as that seen with photostimulation (Han et al. 2015; McHenry et al. 2017).

- Retrograde EC transfection

Transfection of cell bodies within the EC was observed in a significant portion of NT animals injected with AAVdj-NpHR. This EC transfection may have been due to AAV serotype or promoters. While retrograde transfection has been previously observed with utilizing the AAVdj serotype, the impact of the effect is unclear. While portions of the transfected EC have been shown to project and inhibit the IL (Insausti, Herrero, and Witter 1997; Valenti and Grace 2009), our retrograde injections within the IL demonstrated that the EC-IL pathway is less robust than the vHC-IL pathway. Furthermore, it is unknown whether the EC contains cells with collaterals to both vHC and IL, with the likelihood that the transfected cells are such biprojecting cells being rather low. Consequently, the potential confounding effects of inhibition of EC projections within the IL are deemed to be rather low.

- Highly anxiogenic strain

Lack of behavioral effects with optogenetic inhibition during tests for anxiety-related behavior as well as social memory may have been due to the highly anxiogenic nature of the NT-Cre strain, as observed in our lab. Some results were suggestive of our manipulations increasing anxiety but this is impossible to conclude due to our floor effect. Interestingly, we may have

been unable to show an effect of inhibition because recent evidence has suggested that heightened vCA1 activity is important for avoidance behavior in anxiogenic environments. However, this activity (or its inhibition) does not alter locomotor activity or open arm visitations (Jimenez et al. 2018). Thus, as our mice were avoidant of visiting the open arms in the first place, the number of visits may not have been enough to demonstrate a change in length of time exploring the open arms each visit (or exploring the center of OFT when they entered). Likewise, as anxiogenic strains may exhibit altered social behavior, assessment of social memory may be confounded by reduction in interaction time and quality. Accordingly, it is difficult to conclude whether our manipulations affect anxiety-related behavior or social memory due to both control and experimental mice displaying limited exploration of OFT center and EPM open arms as well as anomalous social memory as revealed by the recognition index. Future studies should assess baseline anxiogenic strain without single housing and surgery as well as attempt to further reduce baseline anxiety-related behavior and determine effects on other measures of innate anxiety and social interaction.

- Optic fiber implant issues

Due to the anterior placement of optogenetic fiber implants, animals had a propensity to hit objects when running as well as get the fibers and tethers stuck on corners and other obstacles. This manipulation may have made the EPM especially anxiogenic because sometimes animals would not be able to leave the open arm when they wished and would almost fall off the maze entirely when trying to dislodge the tethers, leading to increased avoidance of open arms. Similarly, animals had a difficult time turning within the closed arms, needing to maneuver in such a way that their implant didn't hit the opposing wall. Despite being habituated to having the implant and wearing the optogenetic tethers, animals had little experience navigating obstacles.

Thus, 5 minutes may not have been enough to assess exploration of EPM as this interval may have been habituation to navigation in such close quarters

To avoid these problems, the last batch (#3) of animals was run utilizing the larger rat EPM and for 10 minutes. This altered paradigm led to a dramatic increase in exploration in both groups as animals could freely turn in the closed arms, leading to faster entry and exit. Likewise, the tethers did not get stuck on corners when exiting the open arms. Moreover, almost all animals had a full open arm entry by the end of the 10 minute time interval, although some did not enter the arm until some time had elapsed. Unfortunately, due to the size of batch #3 following histology exclusions, we cannot conclude group differences between YFP and NpHR. Nevertheless, this modified EPM test may be more appropriate for testing anxiety-like behaviors in these experimental animals. Additionally, animals could be habituated to running a maze, or some other task that requires navigating obstacles, before initiation of behavioral testing.

Summary and Conclusions

To summarize, the present findings provide novel insight into the precise anatomical organization, as well as functional contribution, of the vHC-mPFC circuit in mice. Taken together, experiments defining the mouse vHC-mPFC circuit with greater specificity demonstrated similarity to what has been found in the rat: namely, segregation of input to PL and IL, with the latter receiving greater innervation. In addition, it was shown for the first time that the mPFC receives a greater amount of projections from the vCA1 than the vSub. Lastly, novel AAV approaches were utilized to demonstrate the lack of VGAT GABAergic long range projections as well as confirm greater IL innervation by the vHC. Such findings suggest the presence of distinct circuits within the vHC-mPFC pathway and encourage alternative methods of restricting manipulations to assess functioning.

Consequently, our results manipulating a unique portion of the pathway, namely the $Nts^{vHC\text{-}IL}$circuit, through optogenetic inhibition are suggestive of a more nuanced role in behavior. Although we failed to find any significant differences in anxiety-like behavior, social memory, or fear extinction, our null results may reveal previously unknown complexity in the role played by vHC-mPFC circuit. Accordingly, future studies should investigate some of the issues brought to the forefront, particularly E/I balance and NT release. Collectively, these data suggest that the vHC-mPFC pathway contains multiple unexplored subcircuits that likely make distinct contributions to information integration and subsequent responses. Such findings help shed light on the anatomical substrates of complex behaviors. Moreover, they further our understanding of circuits that may become disrupted in diverse neuropsychiatric disorders.

References

Adhikari, Avishek, Talia N. Lerner, Joel Finkelstein, Sally Pak, Joshua H. Jennings, Thomas J. Davidson, Emily Ferenczi, et al. 2015. "Basomedial Amygdala Mediates Top-down Control of Anxiety and Fear." *Nature* 527 (7577): 179–85.

Adhikari, Avishek, Mihir A. Topiwala, and Joshua A. Gordon. 2011. "Single Units in the Medial Prefrontal Cortex with Anxiety-Related Firing Patterns Are Preferentially Influenced by Ventral Hippocampal Activity." *Neuron* 71 (5): 898–910.

Aerde, Karlijn I. van, Tim S. Heistek, and Huibert D. Mansvelder. 2008. "Prelimbic and Infralimbic Prefrontal Cortex Interact during Fast Network Oscillations." *PloS One* 3 (7): e2725.

Agster, Kara L., and Rebecca D. Burwell. 2013. "Hippocampal and Subicular Efferents and Afferents of the Perirhinal, Postrhinal, and Entorhinal Cortices of the Rat." *Behavioural Brain Research* 254 (October): 50–64.

Amaral, D. G., C. Dolorfo, and P. Alvarez- Royo. 1991. "Organization of CA1 Projections to the Subiculum: A PHA- L Analysis in the Rat." *Hippocampus*. Wiley Online Library. http://onlinelibrary.wiley.com/doi/10.1002/hipo.450010410/full.

Antonelli, T., K. Fuxe, M. C. Tomasini, E. Mazzoni, L. F. Agnati, S. Tanganelli, and L. Ferraro. 2007. "Neurotensin Receptor Mechanisms and Its Modulation of Glutamate Transmission in the Brain: Relevance for Neurodegenerative Diseases and Their Treatment." *Progress in Neurobiology* 83 (2): 92–109.

Arszovszki, Antónia, Zsolt Borhegyi, and Thomas Klausberger. 2014. "Three Axonal Projection Routes of Individual Pyramidal Cells in the Ventral CA1 Hippocampus." *Frontiers in Neuroanatomy* 8 (June): 53.

Audinat, E., J. M. Hermel, and F. Crépel. 1989. "Neurotensin-Induced Excitation of Neurons of the Rat's Frontal Cortex Studied Intracellularly in Vitro." *Experimental Brain Research. Experimentelle Hirnforschung. Experimentation Cerebrale* 78 (2): 358–68.

Bannerman, D. M., J. N. P. Rawlins, S. B. McHugh, R. M. J. Deacon, B. K. Yee, T. Bast, W-N Zhang, H. H. J. Pothuizen, and J. Feldon. 2004. "Regional Dissociations within the Hippocampus—memory and Anxiety." *Neuroscience and Biobehavioral Reviews* 28 (3): 273–83.

Baratta, Michael V., Shinya Nakamura, Peter Dobelis, Matthew B. Pomrenze, Samuel D. Dolzani, and Donald C. Cooper. 2012. "Optogenetic Control of Genetically-Targeted Pyramidal Neuron Activity in Prefrontal Cortex." *arXiv [q-bio.NC]*. arXiv. http://arxiv.org/abs/1204.0710.

Becker, A., and G. Grecksch. 2000. "Social Memory Is Impaired in Neonatally Ibotenic Acid Lesioned Rats." *Behavioural Brain Research* 109 (1): 137–40.

Benchenane, Karim, Paul H. Tiesinga, and Francesco P. Battaglia. 2011. "Oscillations in the Prefrontal Cortex: A Gateway to Memory and Attention." *Current Opinion in Neurobiology* 21 (3): 475–85.

Blatow, Maria, Antonio Caputi, Nail Burnashev, Hannah Monyer, and Andrei Rozov. 2003. "Ca2+ Buffer Saturation Underlies Paired Pulse Facilitation in Calbindin-D28k-Containing Terminals." *Neuron* 38 (1): 79–88.

Bloodgood, Daniel W., Jonathan A. Sugam, Andrew Holmes, and Thomas L. Kash. 2017. "Fear Extinction Requires Infralimbic Cortex Projections to the Basolateral Amygdala." *bioRxiv*. https://doi.org/10.1101/172791.

Bluthé, R. M., G. Gheusi, and R. Dantzer. 1993. "Gonadal Steroids Influence the Involvement of

Arginine Vasopressin in Social Recognition in Mice." *Psychoneuroendocrinology* 18 (4): 323–35.
Borelli, K. G., D. C. Blanchard, L. K. Javier, E. B. Defensor, M. L. Brandão, and R. J. Blanchard. 2009. "Neural Correlates of Scent Marking Behavior in C57BL/6J Mice: Detection and Recognition of a Social Stimulus." *Neuroscience* 162 (4): 914–23.
Bouton, M. E., and D. A. King. 1983. "Contextual Control of the Extinction of Conditioned Fear: Tests for the Associative Value of the Context." *Journal of Experimental Psychology. Animal Behavior Processes* 9 (3): 248–65.
Bouwmeester, Hans, Kim Smits, and Jan M. Van Ree. 2002. "Neonatal Development of Projections to the Basolateral Amygdala from Prefrontal and Thalamic Structures in Rat." *The Journal of Comparative Neurology* 450 (3): 241–55.
Braga, Raphael J., Mauro V. Mendlowicz, Rogério P. Marrocos, and Ivan L. Figueira. 2005. "Anxiety Disorders in Outpatients with Schizophrenia: Prevalence and Impact on the Subjective Quality of Life." *Journal of Psychiatric Research* 39 (4): 409–14.
Brennan, Peter A., and Keith M. Kendrick. 2006. "Mammalian Social Odours: Attraction and Individual Recognition." *Philosophical Transactions of the Royal Society of London. Series B, Biological Sciences* 361 (1476): 2061–78.
Bukalo, Olena, Courtney R. Pinard, Shana Silverstein, Christina Brehm, Nolan D. Hartley, Nigel Whittle, Giovanni Colacicco, et al. 2015. "Prefrontal Inputs to the Amygdala Instruct Fear Extinction Memory Formation." *Science Advances* 1 (6). https://doi.org/10.1126/sciadv.1500251.
Burgos-Robles, Anthony, Eyal Y. Kimchi, Ehsan M. Izadmehr, Mary Jane Porzenheim, William A. Ramos-Guasp, Edward H. Nieh, Ada C. Felix-Ortiz, et al. 2017. "Amygdala Inputs to Prefrontal Cortex Guide Behavior amid Conflicting Cues of Reward and Punishment." *Nature Neuroscience* 20 (6): 824–35.
Callaway, Edward M. 2005. "A Molecular and Genetic Arsenal for Systems Neuroscience." *Trends in Neurosciences* 28 (4): 196–201.
Canteras, N. S., and L. W. Swanson. 1992. "Projections of the Ventral Subiculum to the Amygdala, Septum, and Hypothalamus: A PHAL Anterograde Tract-Tracing Study in the Rat." *The Journal of Comparative Neurology* 324 (2): 180–94.
Canto, Cathrin B., Floris G. Wouterlood, and Menno P. Witter. 2008. "What Does the Anatomical Organization of the Entorhinal Cortex Tell Us?" *Neural Plasticity* 2008: 381243.
Carr, D. B., and S. R. Sesack. 1996. "Hippocampal Afferents to the Rat Prefrontal Cortex: Synaptic Targets and Relation to Dopamine Terminals." *The Journal of Comparative Neurology* 369 (1): 1–15.
Cassel, Jean-Christophe, Anne Pereira de Vasconcelos, Michaël Loureiro, Thibault Cholvin, John C. Dalrymple-Alford, and Robert P. Vertes. 2013. "The Reuniens and Rhomboid Nuclei: Neuroanatomy, Electrophysiological Characteristics and Behavioral Implications." *Progress in Neurobiology* 111 (December): 34–52.
Cembrowski, Mark S., Matthew G. Phillips, Salvatore F. DiLisio, Brenda C. Shields, Johan Winnubst, Jayaram Chandrashekar, Erhan Bas, and Nelson Spruston. 2018. "Dissociable Structural and Functional Hippocampal Outputs via Distinct Subiculum Cell Classes." *Cell*, April. https://doi.org/10.1016/j.cell.2018.03.031.
Cenquizca, Lee A., and Larry W. Swanson. 2007. "Spatial Organization of Direct Hippocampal Field CA1 Axonal Projections to the Rest of the Cerebral Cortex." *Brain Research Reviews*

56 (1): 1–26.
Chen, Veronica M., Allison R. Foilb, and John P. Christianson. 2016. “Inactivation of Ventral Hippocampus Interfered with Cued-Fear Acquisition but Did Not Influence Later Recall or Discrimination.” *Behavioural Brain Research* 296 (January): 249–53.
Cheriyan, John, Mahesh K. Kaushik, Ashley N. Ferreira, and Patrick L. Sheets. 2016. “Specific Targeting of the Basolateral Amygdala to Projectionally Defined Pyramidal Neurons in Prelimbic and Infralimbic Cortex.” *eNeuro* 3 (2). https://doi.org/10.1523/ENEURO.0002-16.2016.
Churchwell, John C., Andrea M. Morris, Nicholas D. Musso, and Raymond P. Kesner. 2010. “Prefrontal and Hippocampal Contributions to Encoding and Retrieval of Spatial Memory.” *Neurobiology of Learning and Memory* 93 (3): 415–21.
Ciocchi, S., J. Passecker, H. Malagon-Vina, N. Mikus, and T. Klausberger. 2015. “Brain Computation. Selective Information Routing by Ventral Hippocampal CA1 Projection Neurons.” *Science* 348 (6234): 560–63.
Colgin, Laura Lee. 2011. “Oscillations and Hippocampal-Prefrontal Synchrony.” *Current Opinion in Neurobiology* 21 (3): 467–74.
Condé, F., E. Maire-Lepoivre, E. Audinat, and F. Crépel. 1995. “Afferent Connections of the Medial Frontal Cortex of the Rat. II. Cortical and Subcortical Afferents.” *The Journal of Comparative Neurology* 352 (4): 567–93.
Cooper, Donald C. 2002. “The Significance of Action Potential Bursting in the Brain Reward Circuit.” *Neurochemistry International* 41 (5): 333–40.
Cooper, Donald C., Sungkwon Chung, and Nelson Spruston. 2005. “Output-Mode Transitions Are Controlled by Prolonged Inactivation of Sodium Channels in Pyramidal Neurons of Subiculum.” *PLoS Biology* 3 (6): e175.
Cooper, Donald C., Shannon J. Moore, Nathan P. Staff, and Nelson Spruston. 2003. “Psychostimulant-Induced Plasticity of Intrinsic Neuronal Excitability in Ventral Subiculum.” *The Journal of Neuroscience: The Official Journal of the Society for Neuroscience* 23 (30): 9937–46.
Corcoran, Kevin A., Timothy J. Desmond, Kirk A. Frey, and Stephen Maren. 2005. “Hippocampal Inactivation Disrupts the Acquisition and Contextual Encoding of Fear Extinction.” *The Journal of Neuroscience: The Official Journal of the Society for Neuroscience* 25 (39): 8978–87.
Covington, Herbert E., 3rd, Mary Kay Lobo, Ian Maze, Vincent Vialou, James M. Hyman, Samir Zaman, Quincey LaPlant, et al. 2010. “Antidepressant Effect of Optogenetic Stimulation of the Medial Prefrontal Cortex.” *The Journal of Neuroscience: The Official Journal of the Society for Neuroscience* 30 (48): 16082–90.
Croxson, Paula L., Heidi Johansen-Berg, Timothy E. J. Behrens, Matthew D. Robson, Mark A. Pinsk, Charles G. Gross, Wolfgang Richter, Marlene C. Richter, Sabine Kastner, and Matthew F. S. Rushworth. 2005. “Quantitative Investigation of Connections of the Prefrontal Cortex in the Human and Macaque Using Probabilistic Diffusion Tractography.” *The Journal of Neuroscience: The Official Journal of the Society for Neuroscience* 25 (39): 8854–66.
Dantzer, R., R. M. Bluthe, G. F. Koob, and M. Le Moal. 1987. “Modulation of Social Memory in Male Rats by Neurohypophyseal Peptides.” *Psychopharmacology* 91 (3): 363–68.
Deacon, Robert M. J., Catherine Penny, and J. Nicholas P. Rawlins. 2003. “Effects of Medial Prefrontal Cortex Cytotoxic Lesions in Mice.” *Behavioural Brain Research* 139 (1-2): 139–

55.
Dégenètais, Eric, Anne-Marie Thierry, Jacques Glowinski, and Yves Gioanni. 2003. “Synaptic Influence of Hippocampus on Pyramidal Cells of the Rat Prefrontal Cortex: An in Vivo Intracellular Recording Study.” *Cerebral Cortex* 13 (7): 782–92.
Do-Monte, Fabricio H., Gabriela Manzano-Nieves, Kelvin Quiñones-Laracuente, Liorimar Ramos-Medina, and Gregory J. Quirk. 2015. “Revisiting the Role of Infralimbic Cortex in Fear Extinction with Optogenetics.” *The Journal of Neuroscience: The Official Journal of the Society for Neuroscience* 35 (8): 3607–15.
Do-Monte, Fabricio H., Kelvin Quiñones-Laracuente, and Gregory J. Quirk. 2015. “A Temporal Shift in the Circuits Mediating Retrieval of Fear Memory.” *Nature* 519 (7544): 460–63.
Dulac, Catherine, and A. Thomas Torello. 2003. “Molecular Detection of Pheromone Signals in Mammals: From Genes to Behaviour.” *Nature Reviews. Neuroscience* 4 (7): 551–62.
Dumas, T. C., E. C. Powers, P. E. Tarapore, and R. M. Sapolsky. 2004. “Overexpression of Calbindin D(28k) in Dentate Gyrus Granule Cells Alters Mossy Fiber Presynaptic Function and Impairs Hippocampal-Dependent Memory.” *Hippocampus* 14 (6): 701–9.
Engelmann, Mario, Jana Hädicke, and Julia Noack. 2011. “Testing Declarative Memory in Laboratory Rats and Mice Using the Nonconditioned Social Discrimination Procedure.” *Nature Protocols* 6 (8): 1152–62.
Euston, David R., Aaron J. Gruber, and Bruce L. McNaughton. 2012. “The Role of Medial Prefrontal Cortex in Memory and Decision Making.” *Neuron* 76 (6): 1057–70.
Fanselow, Michael S., and Hong-Wei Dong. 2010. “Are the Dorsal and Ventral Hippocampus Functionally Distinct Structures?” *Neuron* 65 (1): 7–19.
Felix-Ortiz, A. C., A. Burgos-Robles, N. D. Bhagat, C. A. Leppla, and K. M. Tye. 2016. “Bidirectional Modulation of Anxiety-Related and Social Behaviors by Amygdala Projections to the Medial Prefrontal Cortex.” *Neuroscience* 321 (May): 197–209.
Felix-Ortiz, Ada C., and Kay M. Tye. 2014. “Amygdala Inputs to the Ventral Hippocampus Bidirectionally Modulate Social Behavior.” *The Journal of Neuroscience: The Official Journal of the Society for Neuroscience* 34 (2): 586–95.
Ferraro, Luca, Sarah Beggiato, Maria Cristina Tomasini, Kjell Fuxe, Sergio Tanganelli, and Tiziana Antonelli. 2011. “Neurotensin Regulates Cortical Glutamate Transmission by Modulating N-Methyl-D-Aspartate Receptor Functional Activity: An in Vivo Microdialysis Study.” *Journal of Neuroscience Research* 89 (10): 1618–26.
Ferreira, Ashley N., Hanna Yousuf, Sarah Dalton, and Patrick L. Sheets. 2015. “Highly Differentiated Cellular and Circuit Properties of Infralimbic Pyramidal Neurons Projecting to the Periaqueductal Gray and Amygdala.” *Frontiers in Cellular Neuroscience* 9 (April): 161.
File, S. E., and J. R. Hyde. 1978. “Can Social Interaction Be Used to Measure Anxiety?” *British Journal of Pharmacology* 62 (1): 19–24.
Fournier, Neil M., and Ronald S. Duman. 2013. “Illuminating Hippocampal Control of Fear Memory and Anxiety.” *Neuron* 77 (5): 803–6.
Gabbott, Paul, Anthony Headlam, and Sarah Busby. 2002. “M Orphological Evidence That CA1 Hippocampal Afferents Monosynaptically Innervate PV-Containing Neurons and NADPH-Diaphorase Reactive Cells in the Medial Prefrontal Cortex (Areas 25 / 32) of the Rat.” *Brain Research* 946: 314–22.
Gall, Christine. 1990. “Comparative Anatomy of the Hippocampus.” In *Cerebral Cortex*, 167–213.

Gigg, J., D. M. Finch, and S. M. O'Mara. 2000. "Responses of Rat Subicular Neurons to Convergent Stimulation of Lateral Entorhinal Cortex and CA1 in Vivo." *Brain Research* 884 (1--2): 35–50.
Gigg, John. 2006. "Constraints on Hippocampal Processing Imposed by the Connectivity between CA1, Subiculum and Subicular Targets." *Behavioural Brain Research* 174 (2): 265–71.
Giustino, Thomas F., and Stephen Maren. 2015. "The Role of the Medial Prefrontal Cortex in the Conditioning and Extinction of Fear." *Frontiers in Behavioral Neuroscience* 9 (November): 298.
Godsil, Bill P., Janos P. Kiss, Michael Spedding, and Thérèse M. Jay. 2013. "The Hippocampal–prefrontal Pathway: The Weak Link in Psychiatric Disorders?" *European Neuropsychopharmacology: The Journal of the European College of Neuropsychopharmacology* 23 (10). Elsevier: 1165–81.
Goode, T. D., J. Jin, R. Holehonnur, J. E. Ploski, and S. Maren. 2015. "Combinatorial DREADD Silencing of Ventral Hippocampal Neurons Projecting to Infralimbic Cortex Prevents Fear Renewal." presented at the Society for Neuroscience, Washington, DC.
Graves, Austin R., Shannon J. Moore, Erik B. Bloss, Brett D. Mensh, William L. Kath, and Nelson Spruston. 2012. "Hippocampal Pyramidal Neurons Comprise Two Distinct Cell Types That Are Countermodulated by Metabotropic Receptors." *Neuron* 76 (4): 776–89.
Greene, J. R., and S. Totterdell. 1997. "Morphology and Distribution of Electrophysiologically Defined Classes of Pyramidal and Nonpyramidal Neurons in Rat Ventral Subiculum in Vitro." *The Journal of Comparative Neurology* 380 (3): 395–408.
Grunfeld, Itamar S., and Ekaterina Likhtik. 2018. "Mixed Selectivity Encoding and Action Selection in the Prefrontal Cortex during Threat Assessment." *Current Opinion in Neurobiology* 49 (February): 108–15.
Grupe, Dan W., and Jack B. Nitschke. 2013. "Uncertainty and Anticipation in Anxiety: An Integrated Neurobiological and Psychological Perspective." *Nature Reviews. Neuroscience* 14 (7): 488–501.
Gurden, H., M. Takita, and T. M. Jay. 2000. "Essential Role of D1 but Not D2 Receptors in the NMDA Receptor-Dependent Long-Term Potentiation at Hippocampal-Prefrontal Cortex Synapses in Vivo." *The Journal of Neuroscience: The Official Journal of the Society for Neuroscience* 20 (22): RC106.
Halladay, Lindsay R., and Hugh T. Blair. 2017. "Prefrontal Infralimbic Cortex Mediates Competition between Excitation and Inhibition of Body Movements during Pavlovian Fear Conditioning." *Journal of Neuroscience Research* 95 (3): 853–62.
Han, Sung, Matthew T. Soleiman, Marta E. Soden, Larry S. Zweifel, and Richard D. Palmiter. 2015. "Elucidating an Affective Pain Circuit That Creates a Threat Memory." *Cell* 162 (2): 363–74.
Harris, Alexander Z., and Joshua A. Gordon. 2015. "Long-Range Neural Synchrony in Behavior." *Annual Review of Neuroscience* 38 (July): 171–94.
Harris, E., and M. Stewart. 2001. "Propagation of Synchronous Epileptiform Events from Subiculum Backward into Area CA1 of Rat Brain Slices." *Brain Research* 895 (1-2): 41–49.
Harris, E., M. P. Witter, G. Weinstein, and M. Stewart. 2001. "Intrinsic Connectivity of the Rat Subiculum: I. Dendritic Morphology and Patterns of Axonal Arborization by Pyramidal Neurons." *The Journal of Comparative Neurology* 435 (4): 490–505.

Harris, J. A., M. L. Jones, G. K. Bailey, and R. F. Westbrook. 2000. "Contextual Control over Conditioned Responding in an Extinction Paradigm." *Journal of Experimental Psychology. Animal Behavior Processes* 26 (2): 174–85.
Harris, Julie A., Karla E. Hirokawa, Staci A. Sorensen, Hong Gu, Maya Mills, Lydia L. Ng, Phillip Bohn, et al. 2014. "Anatomical Characterization of Cre Driver Mice for Neural Circuit Mapping and Manipulation." *Frontiers in Neural Circuits* 8 (July): 76.
Hartwich, Katja, Thomas Pollak, and Thomas Klausberger. 2009. "Distinct Firing Patterns of Identified Basket and Dendrite-Targeting Interneurons in the Prefrontal Cortex during Hippocampal Theta and Local Spindle Oscillations." *The Journal of Neuroscience: The Official Journal of the Society for Neuroscience* 29 (30): 9563–74.
Heidbreder, Christian A., and Henk J. Groenewegen. 2003. "The Medial Prefrontal Cortex in the Rat: Evidence for a Dorso-Ventral Distinction Based upon Functional and Anatomical Characteristics." *Neuroscience and Biobehavioral Reviews* 27 (6): 555–79.
Hitti, Frederick L., and Steven A. Siegelbaum. 2014. "The Hippocampal CA2 Region Is Essential for Social Memory." *Nature* 508 (7494): 88–92.
Hobin, Jennifer A., Jinzhao Ji, and Stephen Maren. 2006. "Ventral Hippocampal Muscimol Disrupts Context-Specific Fear Memory Retrieval after Extinction in Rats." *Hippocampus* 16 (2): 174–82.
Ho, M. W., A. G. Beck-Sickinger, and W. F. Colmers. 2000. "Neuropeptide Y(5) Receptors Reduce Synaptic Excitation in Proximal Subiculum, but Not Epileptiform Activity in Rat Hippocampal Slices." *Journal of Neurophysiology* 83 (2): 723–34.
Hoover, Walter B., and Robert P. Vertes. 2007. "Anatomical Analysis of Afferent Projections to the Medial Prefrontal Cortex in the Rat." *Brain Structure & Function* 212 (2): 149–79.
Hsu, T. M., E. E. Noble, C. M. Liu, A. M. Cortella, V. R. Konanur, A. N. Suarez, D. J. Reiner, J. D. Hahn, M. R. Hayes, and S. E. Kanoski. 2017. "A Hippocampus to Prefrontal Cortex Neural Pathway Inhibits Food Motivation through Glucagon-like Peptide-1 Signaling." *Molecular Psychiatry*, May. https://doi.org/10.1038/mp.2017.91.
Igarashi, Kei M., Hiroshi T. Ito, Edvard I. Moser, and May-Britt Moser. 2014. "Functional Diversity along the Transverse Axis of Hippocampal Area CA1." *FEBS Letters* 588 (15): 2470–76.
Insausti, R., M. T. Herrero, and M. P. Witter. 1997. "Entorhinal Cortex of the Rat: Cytoarchitectonic Subdivisions and the Origin and Distribution of Cortical Efferents." *Hippocampus* 7 (2): 146–83.
Insel, Thomas R. 2014. "The NIMH Research Domain Criteria (RDoC) Project: Precision Medicine for Psychiatry." *The American Journal of Psychiatry* 171 (4): 395–97.
Ishihara, Yoshihisa, and Takaichi Fukuda. 2016. "Immunohistochemical Investigation of the Internal Structure of the Mouse Subiculum." *Neuroscience* 337 (November): 242–66.
Izaki, Yoshinori, Masatoshi Takita, Masahiko Nomura, and Tatsuo Akema. 2003. "Differences between Paired-Pulse Facilitation and Long-Term Potentiation in the Dorsal and Ventral Hippocampal CA1-Prefrontal Pathways of Rats." *Brain Research* 992 (1): 142–45.
Jarsky, Tim, Rina Mady, Benjamin Kennedy, and Nelson Spruston. 2008. "Distribution of Bursting Neurons in the CA1 Region and the Subiculum of the Rat Hippocampus." *The Journal of Comparative Neurology* 506 (4): 535–47.
Jay, Thérèse M., Anne-Marie Thierry, Leif Wiklund, and Jacques Glowinski. 1992. "Excitatory Amino Acid Pathway from the Hippocampus to the Prefrontal Cortex. Contribution of AMPA Receptors in Hippocampo-Prefrontal Cortex Transmission." *The European Journal*

of Neuroscience 4 (12): 1285–95.
Jay, T. M., F. Burette, and S. Laroche. 1995. "NMDA Receptor-Dependent Long-Term Potentiation in the Hippocampal Afferent Fibre System to the Prefrontal Cortex in the Rat." *The European Journal of Neuroscience* 7 (2): 247–50.
Jay, T. M., J. Glowinski, and A. M. Thierry. 1989. "Selectivity of the Hippocampal Projection to the Prelimbic Area of the Prefrontal Cortex in the Rat." *Brain Research* 505 (2): 337–40.
Jimenez, Jessica C., Katy Su, Alexander R. Goldberg, Victor M. Luna, Jeremy S. Biane, Gokhan Ordek, Pengcheng Zhou, et al. 2018. "Anxiety Cells in a Hippocampal-Hypothalamic Circuit." *Neuron* 97 (3): 670–83.e6.
Jinks, A. L., and I. S. McGregor. 1997. "Modulation of Anxiety-Related Behaviours Following Lesions of the Prelimbic or Infralimbic Cortex in the Rat." *Brain Research* 772 (1-2): 181–90.
Kaczorowski, Catherine C., Scott J. Davis, and James R. Moyer Jr. 2012. "Aging Redistributes Medial Prefrontal Neuronal Excitability and Impedes Extinction of Trace Fear Conditioning." *Neurobiology of Aging* 33 (8): 1744–57.
Kalisch, Raffael, Elian Korenfeld, Klaas E. Stephan, Nikolaus Weiskopf, Ben Seymour, and Raymond J. Dolan. 2006. "Context-Dependent Human Extinction Memory Is Mediated by a Ventromedial Prefrontal and Hippocampal Network." *The Journal of Neuroscience: The Official Journal of the Society for Neuroscience* 26 (37): 9503–11.
Kempadoo, Kimberly A., Clara Tourino, Saemi L. Cho, Francesco Magnani, Gina-Marie Leinninger, Garret D. Stuber, Feng Zhang, et al. 2013. "Hypothalamic Neurotensin Projections Promote Reward by Enhancing Glutamate Transmission in the VTA." *The Journal of Neuroscience: The Official Journal of the Society for Neuroscience* 33 (18): 7618–26.
Kesner, Raymond P., and John C. Churchwell. 2011. "An Analysis of Rat Prefrontal Cortex in Mediating Executive Function." *Neurobiology of Learning and Memory* 96 (3): 417–31.
Kim, Hyung-Su, Hye-Yeon Cho, George J. Augustine, and Jin-Hee Han. 2016. "Selective Control of Fear Expression by Optogenetic Manipulation of Infralimbic Cortex after Extinction." *Neuropsychopharmacology: Official Publication of the American College of Neuropsychopharmacology* 41 (5): 1261–73.
Kim, Woong Bin, and Jun-Hyeong Cho. 2017. "Synaptic Targeting of Double-Projecting Ventral CA1 Hippocampal Neurons to the Medial Prefrontal Cortex and Basal Amygdala." *The Journal of Neuroscience: The Official Journal of the Society for Neuroscience* 37 (19): 4868–82.
Kim, Yongsoo, Kannan Umadevi Venkataraju, Kith Pradhan, Carolin Mende, Julian Taranda, Srinivas C. Turaga, Ignacio Arganda-Carreras, et al. 2015. "Mapping Social Behavior-Induced Brain Activation at Cellular Resolution in the Mouse." *Cell Reports* 10 (2): 292–305.
Kim, Yujin, and Nelson Spruston. 2012. "Target-Specific Output Patterns Are Predicted by the Distribution of Regular-Spiking and Bursting Pyramidal Neurons in the Subiculum." *Hippocampus* 22 (4): 693–706.
Kjelstrup, Kirsten G., Frode A. Tuvnes, Hill-Aina Steffenach, Robert Murison, Edvard I. Moser, and May-Britt Moser. 2002. "Reduced Fear Expression after Lesions of the Ventral Hippocampus." *Proceedings of the National Academy of Sciences of the United States of America* 99 (16): 10825–30.
Klausberger, Thomas, and Peter Somogyi. 2008. "Neuronal Diversity and Temporal Dynamics:

The Unity of Hippocampal Circuit Operations." *Science* 321 (5885): 53–57.
Kogan, J. H., P. W. Frankland, and A. J. Silva. 2000. "Long-Term Memory Underlying Hippocampus-Dependent Social Recognition in Mice." *Hippocampus* 10 (1): 47–56.
Kohara, Keigo, Michele Pignatelli, Alexander J. Rivest, Hae-Yoon Jung, Takashi Kitamura, Junghyup Suh, Dominic Frank, et al. 2014. "Cell Type-Specific Genetic and Optogenetic Tools Reveal Hippocampal CA2 Circuits." *Nature Neuroscience* 17 (2): 269–79.
Lacroix, L., S. Spinelli, C. A. Heidbreder, and J. Feldon. 2000. "Differential Role of the Medial and Lateral Prefrontal Cortices in Fear and Anxiety." *Behavioral Neuroscience* 114 (6): 1119–30.
Laroche, S., T. M. Jay, and A. M. Thierry. 1990. "Long-Term Potentiation in the Prefrontal Cortex Following Stimulation of the Hippocampal CA1/subicular Region." *Neuroscience Letters* 114 (2): 184–90.
Laurent, Vincent, and R. Frederick Westbrook. 2009. "Inactivation of the Infralimbic but Not the Prelimbic Cortex Impairs Consolidation and Retrieval of Fear Extinction." *Learning & Memory* 16 (9): 520–29.
Liberzon, Israel, and Chandra Sekhar Sripada. 2008. "The Functional Neuroanatomy of PTSD: A Critical Review." *Progress in Brain Research* 167: 151–69.
Likhtik, Ekaterina, Joseph M. Stujenske, Mihir A. Topiwala, Alexander Z. Harris, and Joshua A. Gordon. 2014. "Prefrontal Entrainment of Amygdala Activity Signals Safety in Learned Fear and Innate Anxiety." *Nature Neuroscience* 17 (1): 106–13.
Li, Ming, Cheng Long, and Li Yang. 2015. "Hippocampal-Prefrontal Circuit and Disrupted Functional Connectivity in Psychiatric and Neurodegenerative Disorders." *BioMed Research International* 2015 (April): 810548.
Lipski, Witold J., and Anthony A. Grace. 2013a. "Activation and Inhibition of Neurons in the Hippocampal Ventral Subiculum by Norepinephrine and Locus Coeruleus Stimulation." *Neuropsychopharmacology: Official Publication of the American College of Neuropsychopharmacology* 38 (2): 285–92.
———. 2013b. "Footshock-Induced Responses in Ventral Subiculum Neurons Are Mediated by Locus Coeruleus Noradrenergic Afferents." *European Neuropsychopharmacology: The Journal of the European College of Neuropsychopharmacology* 23 (10): 1320–28.
Lisman, J. E. 1997. "Bursts as a Unit of Neural Information: Making Unreliable Synapses Reliable." *Trends in Neurosciences* 20 (1): 38–43.
Little, Justin P., and Adam G. Carter. 2012. "Subcellular Synaptic Connectivity of Layer 2 Pyramidal Neurons in the Medial Prefrontal Cortex." *The Journal of Neuroscience: The Official Journal of the Society for Neuroscience* 32 (37): 12808–19.
Lopes da Silva, F. H., M. P. Witter, P. H. Boeijinga, and A. H. Lohman. 1990. "Anatomic Organization and Physiology of the Limbic Cortex." *Physiological Reviews* 70 (2): 453–511.
Lüscher Dias, Thomaz, Hudson Fernandes Golino, Vinícius Elias Moura de Oliveira, Márcio Flávio Dutra Moraes, and Grace Schenatto Pereira. 2016. "C-Fos Expression Predicts Long-Term Social Memory Retrieval in Mice." *Behavioural Brain Research* 313 (October): 260–71.
Luskin, M. B., and J. L. Price. 1983. "The Topographic Organization of Associational Fibers of the Olfactory System in the Rat, Including Centrifugal Fibers to the Olfactory Bulb." *The Journal of Comparative Neurology* 216 (3): 264–91.
Malik, Ruchi, Kelly Ann Dougherty, Komal Parikh, Connor Byrne, and Daniel Johnston. 2016.

"Mapping the Electrophysiological and Morphological Properties of CA1 Pyramidal Neurons along the Longitudinal Hippocampal Axis." *Hippocampus* 26 (3): 341–61.
Maren, S. 1999. "Neurotoxic or Electrolytic Lesions of the Ventral Subiculum Produce Deficits in the Acquisition and Expression of Pavlovian Fear Conditioning in Rats." *Behavioral Neuroscience* 113 (2): 283–90.
Maren, Stephen, K. Luan Phan, and Israel Liberzon. 2013. "The Contextual Brain: Implications for Fear Conditioning, Extinction and Psychopathology." *Nature Reviews. Neuroscience* 14 (6): 417–28.
Masurkar, Arjun V., Kalyan V. Srinivas, David H. Brann, Richard Warren, Daniel C. Lowes, and Steven A. Siegelbaum. 2017. "Medial and Lateral Entorhinal Cortex Differentially Excite Deep versus Superficial CA1 Pyramidal Neurons." *Cell Reports* 18 (1): 148–60.
Mattia, D., G. G. Hwa, and M. Avoli. 1993. "Membrane Properties of Rat Subicular Neurons in Vitro." *Journal of Neurophysiology* 70 (3): 1244–48.
Mcdonald, A. J., F. Mascagni, and L. Guo. 1996. "Projections of the Medial and Lateral Prefrontal Cortices to the Amygdala: A Phaseolus Vulgaris Leucoagglutinin Study in the Rat." *Neuroscience* 71 (1): 55–75.
McHenry, Jenna A., James M. Otis, Mark A. Rossi, J. Elliott Robinson, Oksana Kosyk, Noah W. Miller, Zoe A. McElligott, Evgeny A. Budygin, David R. Rubinow, and Garret D. Stuber. 2017. "Hormonal Gain Control of a Medial Preoptic Area Social Reward Circuit." *Nature Neuroscience* 20 (3): 449–58.
Menendez de la Prida, L. 2006. "Functional Features of the Rat Subicular Microcircuits Studied in Vitro." *Behavioural Brain Research* 174 (2): 198–205.
Meyer-Lindenberg, Andreas S., Rosanna K. Olsen, Philip D. Kohn, Timothy Brown, Michael F. Egan, Daniel R. Weinberger, and Karen Faith Berman. 2005. "Regionally Specific Disturbance of Dorsolateral Prefrontal–Hippocampal Functional Connectivity in Schizophrenia." *Archives of General Psychiatry* 62 (4). American Medical Association: 379–86.
Milad, Mohammed R., and Gregory J. Quirk. 2002. "Neurons in Medial Prefrontal Cortex Signal Memory for Fear Extinction." *Nature* 420 (6911): 70–74.
Moore, Shannon J., Donald C. Cooper, and Nelson Spruston. 2009. "Plasticity of Burst Firing Induced by Synergistic Activation of Metabotropic Glutamate and Acetylcholine Receptors." *Neuron* 61 (2): 287–300.
Moser, Edvard I., Menno P. Witter, and May-Britt Moser. 2010. "Entorhinal Cortex." In *Handbook of Brain Microcircuits*, edited by Gordon Shepherd MD DPhil and Sten Grillner MD, 175–90. Oxford University Press.
Moser, M. B., and E. I. Moser. 1998. "Distributed Encoding and Retrieval of Spatial Memory in the Hippocampus." *The Journal of Neuroscience: The Official Journal of the Society for Neuroscience* 18 (18): 7535–42.
Mueller, Nancy K., C. Mark Dolgas, and James P. Herman. 2004. "Stressor-Selective Role of the Ventral Subiculum in Regulation of Neuroendocrine Stress Responses." *Endocrinology* 145 (8): 3763–68.
Murray, Andrew J., Marta U. Woloszynowska-Fraser, Laura Ansel-Bollepalli, Katy L. H. Cole, Angelica Foggetti, Barry Crouch, Gernot Riedel, and Peer Wulff. 2015. "Parvalbumin-Positive Interneurons of the Prefrontal Cortex Support Working Memory and Cognitive Flexibility." *Scientific Reports* 5 (November): 16778.
Naber, P. A., and M. P. Witter. 1998. "Subicular Efferents Are Organized Mostly as Parallel

Projections: A Double-Labeling, Retrograde-Tracing Study in the Rat." *The Journal of Comparative Neurology* 393 (3): 284–97.
Naber, P. A., M. P. Witter, and F. H. Lopes da Silva. 2000. "Networks of the Hippocampal Memory System of the Rat. The Pivotal Role of the Subiculum." *Annals of the New York Academy of Sciences* 911 (June): 392–403.
Nakazawa, Yuki, Aleksandr Pevzner, Kazumasa Z. Tanaka, and Brian J. Wiltgen. 2016. "Memory Retrieval along the Proximodistal Axis of CA1." *Hippocampus* 26 (9): 1140–48.
Ohashi, Satoshi, Machiko Matsumoto, Hiroko Togashi, Ken-Ichi Ueno, and Mitsuhiro Yoshioka. 2003. "The Serotonergic Modulation of Synaptic Plasticity in the Rat Hippocampo-Medial Prefrontal Cortex Pathway." *Neuroscience Letters* 342 (3): 179–82.
Oh, Seung Wook, Julie A. Harris, Lydia Ng, Brent Winslow, Nicholas Cain, Stefan Mihalas, Quanxin Wang, et al. 2014. "A Mesoscale Connectome of the Mouse Brain." *Nature* 508 (7495): 207–14.
Okuyama, Teruhiro, Takashi Kitamura, Dheeraj S. Roy, Shigeyoshi Itohara, and Susumu Tonegawa. 2016. "Ventral CA1 Neurons Store Social Memory." *Science* 353 (6307): 1536–41.
Oleskevich, S., L. Descarries, and J. C. Lacaille. 1989. "Quantified Distribution of the Noradrenaline Innervation in the Hippocampus of Adult Rat." *The Journal of Neuroscience: The Official Journal of the Society for Neuroscience* 9 (11): 3803–15.
O'Mara, Shane. 2005. "The Subiculum: What It Does, What It Might Do, and What Neuroanatomy Has yet to Tell Us." *Journal of Anatomy* 207 (3): 271–82.
O'Mara, Shane M., Sean Commins, Michael Anderson, and John Gigg. 2001. "The Subiculum: A Review of Form, Physiology and Function." *Progress in Neurobiology* 64 (2): 129–55.
Orsini, Caitlin A., Jee Hyun Kim, Ewelina Knapska, and Stephen Maren. 2011. "Hippocampal and Prefrontal Projections to the Basal Amygdala Mediate Contextual Regulation of Fear after Extinction." *The Journal of Neuroscience: The Official Journal of the Society for Neuroscience* 31 (47): 17269–77.
Padilla-Coreano, Nancy, Scott S. Bolkan, Georgia M. Pierce, Dakota R. Blackman, William D. Hardin, Alvaro L. Garcia-Garcia, Timothy J. Spellman, and Joshua A. Gordon. 2016. "Direct Ventral Hippocampal-Prefrontal Input Is Required for Anxiety-Related Neural Activity and Behavior." *Neuron* 89 (4): 857–66.
Parent, Marc A., Lang Wang, Jianjun Su, Theoden Netoff, and Li-Lian Yuan. 2010. "Identification of the Hippocampal Input to Medial Prefrontal Cortex in Vitro." *Cerebral Cortex* 20 (2): 393–403.
Parfitt, Gustavo Morrone, Robin Nguyen, Jee Yoon Bang, Afif J. Aqrabawi, Matthew M. Tran, D. Kanghoon Seo, Blake A. Richards, and Jun Chul Kim. 2017. "Bidirectional Control of Anxiety-Related Behaviors in Mice: Role of Inputs Arising from the Ventral Hippocampus to the Lateral Septum and Medial Prefrontal Cortex." *Neuropsychopharmacology: Official Publication of the American College of Neuropsychopharmacology* 42 (8): 1715–28.
Perusini, Jennifer N., and Michael S. Fanselow. 2015. "Neurobehavioral Perspectives on the Distinction between Fear and Anxiety." *Learning & Memory* 22 (9): 417–25.
Petrie, Kimberly A., Dennis Schmidt, Michael Bubser, Jim Fadel, Robert E. Carraway, and Ariel Y. Deutch. 2005. "Neurotensin Activates GABAergic Interneurons in the Prefrontal Cortex." *The Journal of Neuroscience: The Official Journal of the Society for Neuroscience* 25 (7): 1629–36.
Pol, A. N. van den, J. P. Wuarin, and F. E. Dudek. 1990. "Glutamate, the Dominant Excitatory

Transmitter in Neuroendocrine Regulation." *Science* 250 (4985): 1276–78.
Preuss, T. M. 1995. "Do Rats Have Prefrontal Cortex? The Rose-Woolsey-Akert Program Reconsidered." *Journal of Cognitive Neuroscience* 7 (1): 1–24.
Quirk, G. J., G. K. Russo, J. L. Barron, and K. Lebron. 2000. "The Role of Ventromedial Prefrontal Cortex in the Recovery of Extinguished Fear." *The Journal of Neuroscience: The Official Journal of the Society for Neuroscience* 20 (16): 6225–31.
Rajasethupathy, Priyamvada, Sethuraman Sankaran, James H. Marshel, Christina K. Kim, Emily Ferenczi, Soo Yeun Lee, Andre Berndt, et al. 2015. "Projections from Neocortex Mediate Top-down Control of Memory Retrieval." *Nature* 526 (7575): 653–59.
Richmond, M. A., B. K. Yee, B. Pouzet, L. Veenman, J. N. Rawlins, J. Feldon, and D. M. Bannerman. 1999. "Dissociating Context and Space within the Hippocampus: Effects of Complete, Dorsal, and Ventral Excitotoxic Hippocampal Lesions on Conditioned Freezing and Spatial Learning." *Behavioral Neuroscience* 113 (6): 1189–1203.
Riga, Danai, Mariana R. Matos, Annet Glas, August B. Smit, Sabine Spijker, and Michel C. Van den Oever. 2014. "Optogenetic Dissection of Medial Prefrontal Cortex Circuitry." *Frontiers in Systems Neuroscience* 8 (December): 230.
Risold, P. Y., and L. W. Swanson. 1996. "Structural Evidence for Functional Domains in the Rat Hippocampus." *Science* 272 (5267): 1484–86.
Romcy-Pereira, Rodrigo, and Constantine Pavlides. 2004. "Distinct Modulatory Effects of Sleep on the Maintenance of Hippocampal and Medial Prefrontal Cortex LTP." *The European Journal of Neuroscience* 20 (12): 3453–62.
Room, P., and H. J. Groenewegen. 1986. "Connections of the Parahippocampal Cortex. I. Cortical Afferents." *The Journal of Comparative Neurology* 251 (4): 415–50.
Rosas-Vidal, Luis E., Fabricio H. Do-Monte, Francisco Sotres-Bayon, and Gregory J. Quirk. 2014. "Hippocampal--Prefrontal BDNF and Memory for Fear Extinction." *Neuropsychopharmacology: Official Publication of the American College of Neuropsychopharmacology* 39 (9): 2161–69.
Rudy, Jerry W., and Patricia Matus-Amat. 2005. "The Ventral Hippocampus Supports a Memory Representation of Context and Contextual Fear Conditioning: Implications for a Unitary Function of the Hippocampus." *Behavioral Neuroscience* 119 (1): 154–63.
Saffari, R., Z. Teng, M. Zhang, M. Kravchenko, C. Hohoff, O. Ambrée, and W. Zhang. 2016. "NPY+-, but Not PV+- GABAergic Neurons Mediated Long-Range Inhibition from Infra- to Prelimbic Cortex." *Translational Psychiatry* 6 (February): e736.
Schöne, Cornelia, and Denis Burdakov. 2012. "Glutamate and GABA as Rapid Effectors of Hypothalamic 'Peptidergic' Neurons." *Frontiers in Behavioral Neuroscience* 6 (November): 81.
Sekiguchi, R., G. Wolterink, and J. M. van Ree. 1991. "Analysis of the Influence of Vasopressin Neuropeptides on Social Recognition of Rats." *European Neuropsychopharmacology: The Journal of the European College of Neuropsychopharmacology* 1 (2): 123–26.
Selten, Martijn, Hans van Bokhoven, and Nael Nadif Kasri. 2018. "Inhibitory Control of the Excitatory/inhibitory Balance in Psychiatric Disorders." *F1000Research* 7 (January): 23.
Senior, Timothy J., John R. Huxter, Kevin Allen, Joseph O'Neill, and Jozsef Csicsvari. 2008. "Gamma Oscillatory Firing Reveals Distinct Populations of Pyramidal Cells in the CA1 Region of the Hippocampus." *The Journal of Neuroscience: The Official Journal of the Society for Neuroscience* 28 (9): 2274–86.
Senn, Verena, Steffen B. E. Wolff, Cyril Herry, François Grenier, Ingrid Ehrlich, Jan

Gründemann, Jonathan P. Fadok, Christian Müller, Johannes J. Letzkus, and Andreas Lüthi. 2014. “Long-Range Connectivity Defines Behavioral Specificity of Amygdala Neurons.” *Neuron* 81 (2): 428–37.

Sesack, S. R., A. Y. Deutch, R. H. Roth, and B. S. Bunney. 1989. “Topographical Organization of the Efferent Projections of the Medial Prefrontal Cortex in the Rat: An Anterograde Tract-Tracing Study with Phaseolus Vulgaris Leucoagglutinin.” *The Journal of Comparative Neurology* 290 (2): 213–42.

Shah, Akeel A., Travis Sjovold, and Dallas Treit. 2004. “Inactivation of the Medial Prefrontal Cortex with the GABAA Receptor Agonist Muscimol Increases Open-Arm Activity in the Elevated plus-Maze and Attenuates Shock-Probe Burying in Rats.” *Brain Research* 1028 (1): 112–15.

Shah, Akeel A., and Dallas Treit. 2003. “Excitotoxic Lesions of the Medial Prefrontal Cortex Attenuate Fear Responses in the Elevated-plus Maze, Social Interaction and Shock Probe Burying Tests.” *Brain Research* 969 (1): 183–94.

———. 2004. “Infusions of Midazolam into the Medial Prefrontal Cortex Produce Anxiolytic Effects in the Elevated plus-Maze and Shock-Probe Burying Tests.” *Brain Research* 996 (1): 31–40.

Shaw, Philip, Argyris Stringaris, Joel Nigg, and Ellen Leibenluft. 2014. “Emotion Dysregulation in Attention Deficit Hyperactivity Disorder.” *The American Journal of Psychiatry* 171 (3): 276–93.

Shin, Younghoon, Minsu Yoo, Hyung-Sun Kim, Sung-Ki Nam, Hyoung-Ihl Kim, Sun-Kyu Lee, Sohee Kim, and Hyuk-Sang Kwon. 2016. “Characterization of Fiber-Optic Light Delivery and Light-Induced Temperature Changes in a Rodent Brain for Precise Optogenetic Neuromodulation.” *Biomedical Optics Express* 7 (11): 4450–71.

Sigurdsson, Torfi, and Sevil Duvarci. 2015. “Hippocampal-Prefrontal Interactions in Cognition, Behavior and Psychiatric Disease.” *Frontiers in Systems Neuroscience* 9: 190.

Simons, Jon S., and Hugo J. Spiers. 2003. “Prefrontal and Medial Temporal Lobe Interactions in Long-Term Memory.” *Nature Reviews. Neuroscience* 4 (8): 637–48.

Slomianka, Lutz, Irmgard Amrein, Irene Knuesel, Jens Christian Sørensen, and David P. Wolfer. 2011. “Hippocampal Pyramidal Cells: The Reemergence of Cortical Lamination.” *Brain Structure & Function* 216 (4): 301–17.

Soler-Cedeño, Omar, Emmanuel Cruz, Marangelie Criado-Marrero, and James T. Porter. 2016. “Contextual Fear Conditioning Depresses Infralimbic Excitability.” *Neurobiology of Learning and Memory* 130 (April): 77–82.

Soler-Cedeño, O., O. Torres-Rodriguez, L. Maldonado-Laboy, A. Hernandez-Lopez, and James T. Porter. 2016. “Fear Conditioning and Extinction Alter Ventral Hippocampus Activation of Nmdar Currents in Infralimbic Neurons.” presented at the Society for Neuroscience, San Diego, CA.

Song, Chenghui, Vanessa L. Ehlers, and James R. Moyer Jr. 2015. “Trace Fear Conditioning Differentially Modulates Intrinsic Excitability of Medial Prefrontal Cortex-Basolateral Complex of Amygdala Projection Neurons in Infralimbic and Prelimbic Cortices.” *The Journal of Neuroscience: The Official Journal of the Society for Neuroscience* 35 (39): 13511–24.

Song, Chenghui, and James R. Moyer Jr. 2018. “Layer- and Subregion-Specific Differences in the Neurophysiological Properties of Rat Medial Prefrontal Cortex Pyramidal Neurons.” *Journal of Neurophysiology* 119 (1): 177–91.

Spellman, Timothy, Mattia Rigotti, Susanne E. Ahmari, Stefano Fusi, Joseph A. Gogos, and Joshua A. Gordon. 2015. "Hippocampal-Prefrontal Input Supports Spatial Encoding in Working Memory." *Nature* 522 (7556): 309–14.
Staff, N. P., H. Y. Jung, T. Thiagarajan, M. Yao, and N. Spruston. 2000. "Resting and Active Properties of Pyramidal Neurons in Subiculum and CA1 of Rat Hippocampus." *Journal of Neurophysiology* 84 (5): 2398–2408.
Steel, Zachary, Claire Marnane, Changiz Iranpour, Tien Chey, John W. Jackson, Vikram Patel, and Derrick Silove. 2014. "The Global Prevalence of Common Mental Disorders: A Systematic Review and Meta-Analysis 1980–2013." *International Journal of Epidemiology* 43 (2). Oxford University Press: 476–93.
Stevenson, Erica L., and Heather K. Caldwell. 2014. "Lesions to the CA2 Region of the Hippocampus Impair Social Memory in Mice." *The European Journal of Neuroscience* 40 (9): 3294–3301.
Strange, Bryan A., Menno P. Witter, Ed S. Lein, and Edvard I. Moser. 2014. "Functional Organization of the Hippocampal Longitudinal Axis." *Nature Reviews. Neuroscience* 15 (10): 655–69.
Studler, J. M., P. Kitabgi, G. Tramu, D. Herve, J. Glowinski, and J. P. Tassin. 1988. "Extensive Co-Localization of Neurotensin with Dopamine in Rat Meso-Cortico-Frontal Dopaminergic Neurons." *Neuropeptides* 11 (3): 95–100.
Suzuki, Satoshi, Akiyoshi Saitoh, Masanori Ohashi, Misa Yamada, Jun-Ichiro Oka, and Mitsuhiko Yamada. 2016. "The Infralimbic and Prelimbic Medial Prefrontal Cortices Have Differential Functions in the Expression of Anxiety-like Behaviors in Mice." *Behavioural Brain Research* 304 (May): 120–24.
Swanson, L. W. 1981. "A Direct Projection from Ammon's Horn to Prefrontal Cortex in the Rat." *Brain Research* 217 (1): 150–54.
Tang, He, Gui-Sheng Wu, Jing Xie, Xiaobin He, Ke Deng, Huadong Wang, Fuqiang Xu, and Huai-Rong Luo. 2016. "Brain-Wide Map of Projections from Mice Ventral Subiculum." *Neuroscience Letters* 629 (August): 171–79.
Tanimizu, Toshiyuki, Justin W. Kenney, Emiko Okano, Kazune Kadoma, Paul W. Frankland, and Satoshi Kida. 2017. "Functional Connectivity of Multiple Brain Regions Required for the Consolidation of Social Recognition Memory." *The Journal of Neuroscience: The Official Journal of the Society for Neuroscience* 37 (15): 4103–16.
Tannenholz, Lindsay, Jessica C. Jimenez, and Mazen A. Kheirbek. 2014. "Local and Regional Heterogeneity Underlying Hippocampal Modulation of Cognition and Mood." *Frontiers in Behavioral Neuroscience* 8 (May): 147.
Taube, J. S. 1993. "Electrophysiological Properties of Neurons in the Rat Subiculum in Vitro." *Experimental Brain Research. Experimentelle Hirnforschung. Experimentation Cerebrale* 96 (2): 304–18.
Thierry, A. M., Y. Gioanni, E. Dégénétais, and J. Glowinski. 2000. "Hippocampo-Prefrontal Cortex Pathway: Anatomical and Electrophysiological Characteristics." *Hippocampus* 10 (4): 411–19.
Thompson, Brittany M., Michael V. Baratta, Joseph C. Biedenkapp, Jerry W. Rudy, Linda R. Watkins, and Steven F. Maier. 2010. "Activation of the Infralimbic Cortex in a Fear Context Enhances Extinction Learning." *Learning & Memory* 17 (11): 591–99.
Thompson, Carol L., Sayan D. Pathak, Andreas Jeromin, Lydia L. Ng, Cameron R. MacPherson, Marty T. Mortrud, Allison Cusick, et al. 2008. "Genomic Anatomy of the Hippocampus."

Neuron 60 (6): 1010–21.
Thor, D. H., and W. R. Holloway. 1982. "Social Memory of the Male Laboratory Rat." *Journal of Comparative and Physiological Psychology* 96 (6): 1000–1006.
Tierney, Patrick L., Eric Dégenètais, Anne-Marie Thierry, Jacques Glowinski, and Yves Gioanni. 2004. "Influence of the Hippocampus on Interneurons of the Rat Prefrontal Cortex." *The European Journal of Neuroscience* 20 (2): 514–24.
Tost, Heike, Edda Bilek, and Andreas Meyer-Lindenberg. 2012. "Brain Connectivity in Psychiatric Imaging Genetics." *NeuroImage* 62 (4): 2250–60.
Tripathi, Anushree, Esther Schenker, Michael Spedding, and Therese M. Jay. 2016. "The Hippocampal to Prefrontal Cortex Circuit in Mice: A Promising Electrophysiological Signature in Models for Psychiatric Disorders." *Brain Structure & Function* 221 (4): 2385–91.
Uylings, Harry B. M., Henk J. Groenewegen, and Bryan Kolb. 2003. "Do Rats Have a Prefrontal Cortex?" *Behavioural Brain Research* 146 (1): 3–17.
Uylings, H. B., and C. G. van Eden. 1990. "Qualitative and Quantitative Comparison of the Prefrontal Cortex in Rat and in Primates, Including Humans." *Progress in Brain Research* 85: 31–62.
Valenti, Ornella, and Anthony A. Grace. 2009. "Entorhinal Cortex Inhibits Medial Prefrontal Cortex and Modulates the Activity States of Electrophysiologically Characterized Pyramidal Neurons in Vivo." *Cerebral Cortex* 19 (3): 658–74.
Van De Werd, H. J. J. M., G. Rajkowska, P. Evers, and Harry B. M. Uylings. 2010. "Cytoarchitectonic and Chemoarchitectonic Characterization of the Prefrontal Cortical Areas in the Mouse." *Brain Structure & Function* 214 (4): 339–53.
Van Groen Am) J. Michael Wyss, Thomas. 1990. "Extrinsic Projections From Area CAI of the Rat Hippocampus: Olfactory, Cortical, Subcortical, and Bilateral Hippocampal Formation Projections." *The Journal of Comparative Neurology* 302: 51–528.
Vertes, Robert P. 2004. "Differential Projections of the Infralimbic and Prelimbic Cortex in the Rat." *Synapse* 51 (1): 32–58.
———. 2006. "Interactions among the Medial Prefrontal Cortex, Hippocampus and Midline Thalamus in Emotional and Cognitive Processing in the Rat." *Neuroscience* 142 (1): 1–20.
Verwer, R. W., R. J. Meijer, H. F. Van Uum, and M. P. Witter. 1997. "Collateral Projections from the Rat Hippocampal Formation to the Lateral and Medial Prefrontal Cortex." *Hippocampus* 7 (4): 397–402.
Vidal-Gonzalez, Ivan, Benjamín Vidal-Gonzalez, Scott L. Rauch, and Gregory J. Quirk. 2006. "Microstimulation Reveals Opposing Influences of Prelimbic and Infralimbic Cortex on the Expression of Conditioned Fear." *Learning & Memory* 13 (6): 728–33.
Wang, Qian, Jingji Jin, and Stephen Maren. 2016. "Renewal of Extinguished Fear Activates Ventral Hippocampal Neurons Projecting to the Prelimbic and Infralimbic Cortices in Rats." *Neurobiology of Learning and Memory* 134 Pt A (October): 38–43.
Warthen, Daniel M., Philip S. Lambeth, Matteo Ottolini, Yingtang Shi, Bryan Scot Barker, Ronald P. Gaykema, Brandon A. Newmyer, et al. 2016. "Activation of Pyramidal Neurons in Mouse Medial Prefrontal Cortex Enhances Food-Seeking Behavior While Reducing Impulsivity in the Absence of an Effect on Food Intake." *Frontiers in Behavioral Neuroscience* 10. Frontiers: 63.
Williams, S. R., and G. J. Stuart. 1999. "Mechanisms and Consequences of Action Potential Burst Firing in Rat Neocortical Pyramidal Neurons." *The Journal of Physiology* 521 Pt 2

(December): 467–82.
Witter, Menno P. 2006. “Connections of the Subiculum of the Rat: Topography in Relation to Columnar and Laminar Organization.” *Behavioural Brain Research* 174 (2): 251–64.
Witter, M. P., H. J. Groenewegen, F. H. Lopes da Silva, and A. H. Lohman. 1989. “Functional Organization of the Extrinsic and Intrinsic Circuitry of the Parahippocampal Region.” *Progress in Neurobiology* 33 (3): 161–253.
Yizhar, Ofer, Lief E. Fenno, Thomas J. Davidson, Murtaza Mogri, and Karl Deisseroth. 2011. “Optogenetics in Neural Systems.” *Neuron* 71 (1): 9–34.
Yizhar, Ofer, Lief E. Fenno, Matthias Prigge, Franziska Schneider, Thomas J. Davidson, Daniel J. O’Shea, Vikaas S. Sohal, et al. 2011. “Neocortical Excitation/inhibition Balance in Information Processing and Social Dysfunction.” *Nature* 477 (7363): 171–78.
Zelikowsky, Moriel, Stephanie Bissiere, Timothy A. Hast, Rebecca Z. Bennett, Andrea Abdipranoto, Bryce Vissel, and Michael S. Fanselow. 2013. “Prefrontal Microcircuit Underlies Contextual Learning after Hippocampal Loss.” *Proceedings of the National Academy of Sciences of the United States of America* 110 (24): 9938–43.
Zhang, Siyu, Min Xu, Wei-Cheng Chang, Chenyan Ma, Johnny Phong Hoang Do, Daniel Jeong, Tiffany Lei, Jiang Lan Fan, and Yang Dan. 2016. “Organization of Long-Range Inputs and Outputs of Frontal Cortex for Top-down Control.” *Nature Neuroscience* 19 (12): 1733–42.
Zingg, Brian, Xiao-Lin Chou, Zheng-Gang Zhang, Lukas Mesik, Feixue Liang, Huizhong Whit Tao, and Li I. Zhang. 2017. “AAV-Mediated Anterograde Transsynaptic Tagging: Mapping Corticocollicular Input-Defined Neural Pathways for Defense Behaviors.” *Neuron* 93 (1): 33–47.

Figures and Tables

Figure 1: CTB-488 was injected in either the PL (n=6) or IL (n=6) for subsequent quantification of retrogradely labeled somas in vHC. (a) 3D representation of regions targeted and assessed (b) experimental set up (c, d) representative coronal PFC slice of PL (c) or IL (d) injection tract/site with white lines indicating region of interest

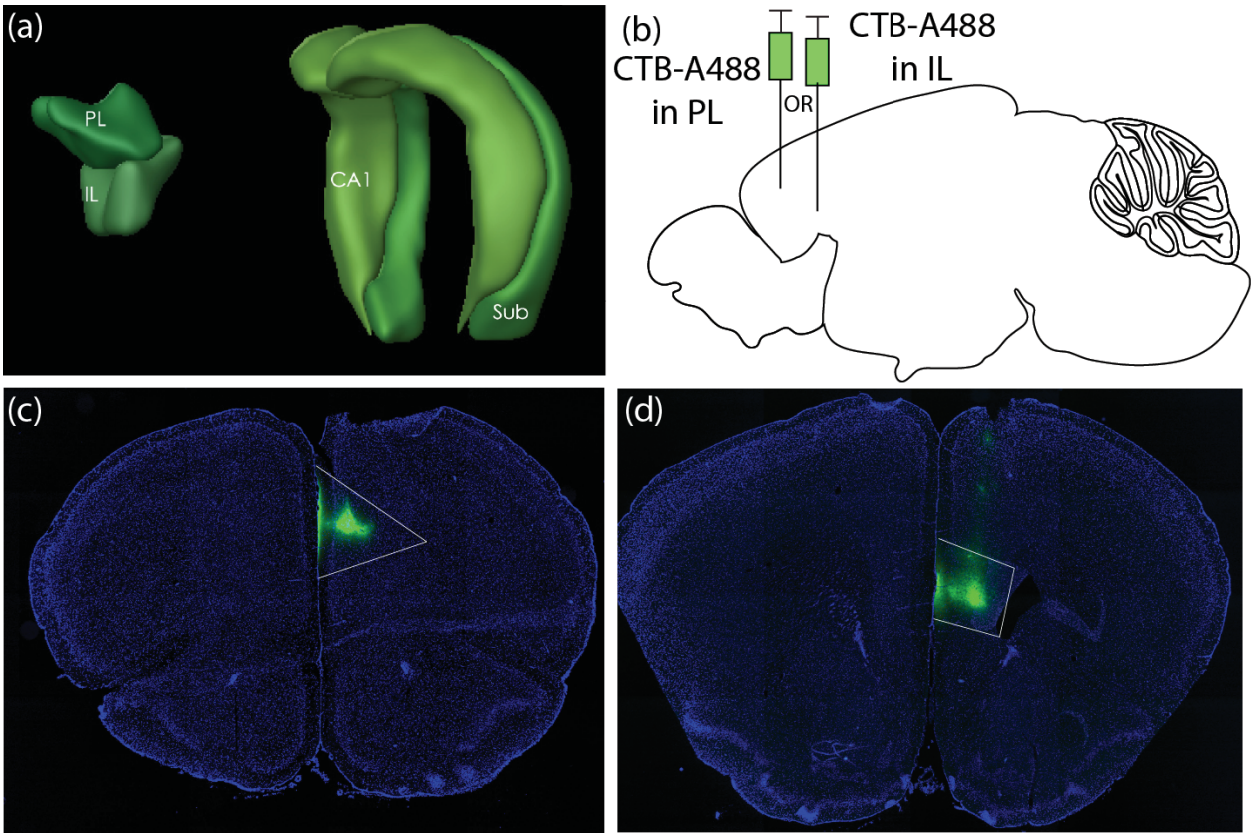

Figure 2: Schematic demonstrating injection centers and approximation of spread in mPFC one week following PL injection of CTB-A488. There is variation in AP level and layers targeted but all injections are in PL. Dot colors represent animal IDs.

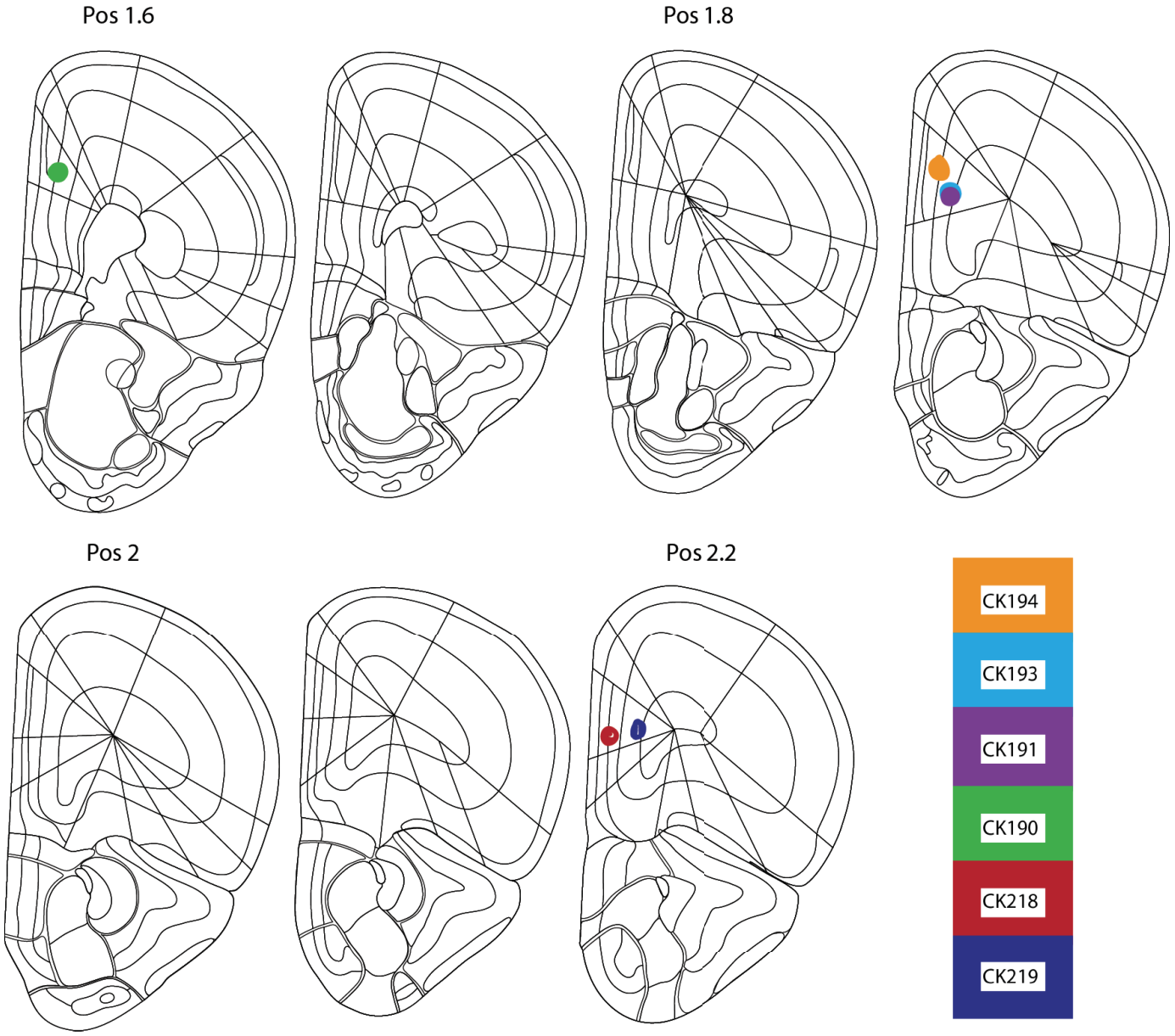

Figure 3: Schematic demonstrating injection centers and approximation of primary spread in mPFC one week following IL injection of CTB-A488. Variability exists in the AP level and layers targeted but all injections are in IL. Dot colors represent animal IDs.

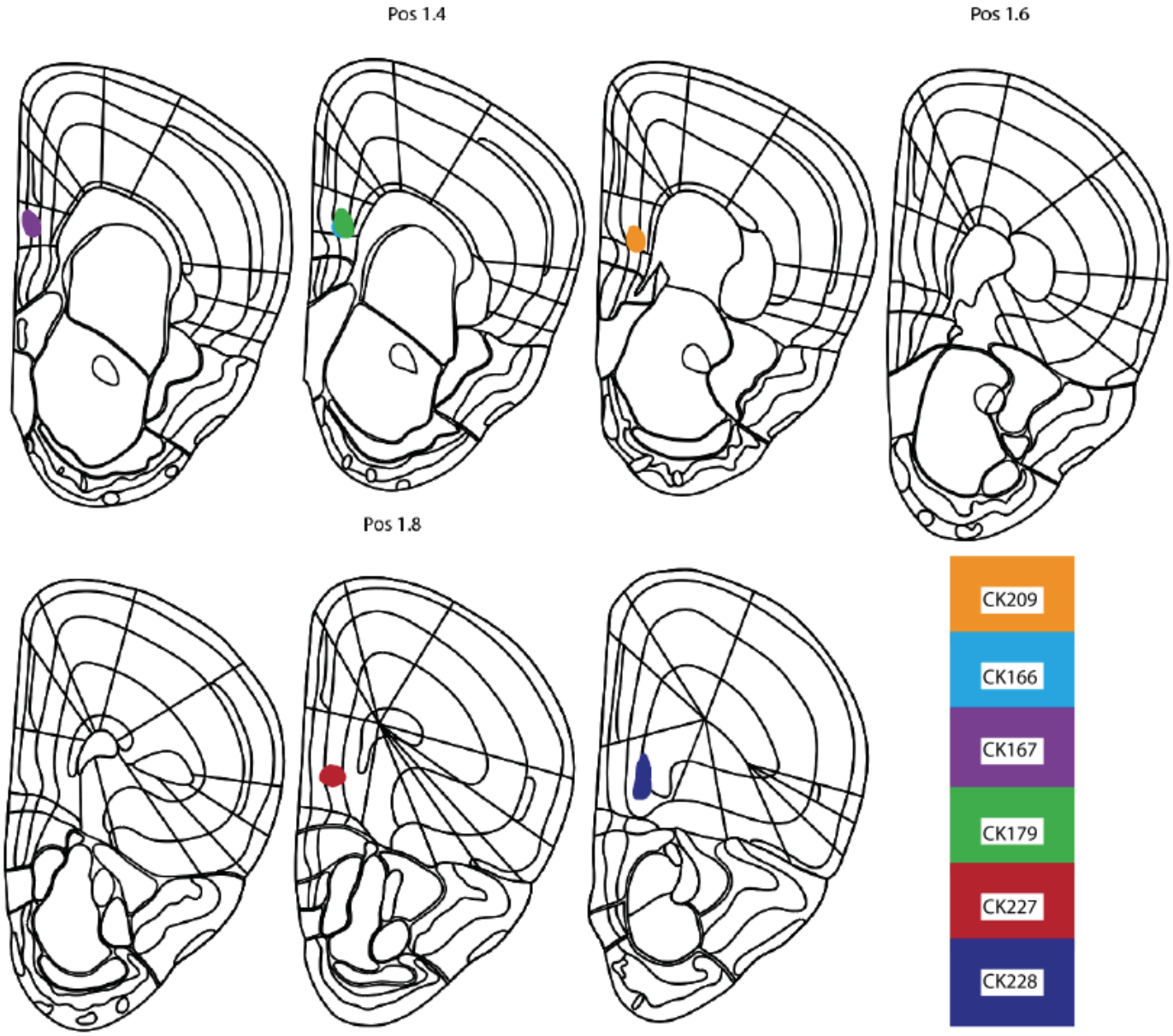

Figure 4: Retrogradely labeled vHC somas were quantified at various AP levels following CTB-488 injection in either the PL (n=6) or IL (n=6), demonstrating greater vHC innervation of IL. (a, b) Representative coronal vHC slice after PL (a) or IL (b) injection. (c) Bar graph depicting raw counts of somas found in HC after CTB injections.

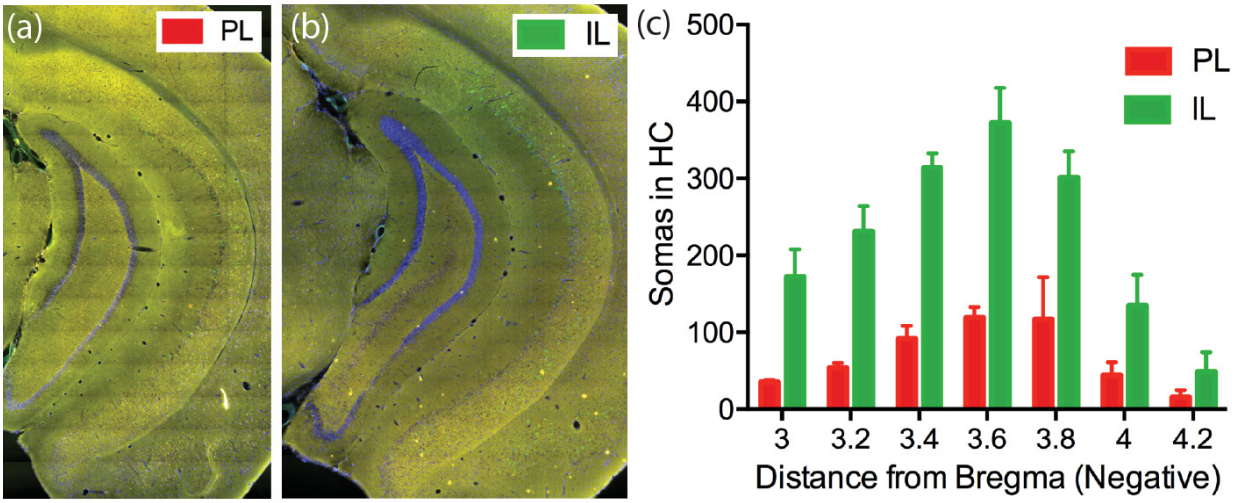

Figure 5: CTB A647 and CTB-488 were unilaterally injected in PL or IL, respectively or vice versa, for subsequent quantification of retrogradely labeled somas in vHC. (a) Experimental set up (b) Representative PFC slice demonstrating minimal overlap of the two CTB injection sites (c, d) Representative coronal PFC slice of PL (c) or IL (d) injection tract/site

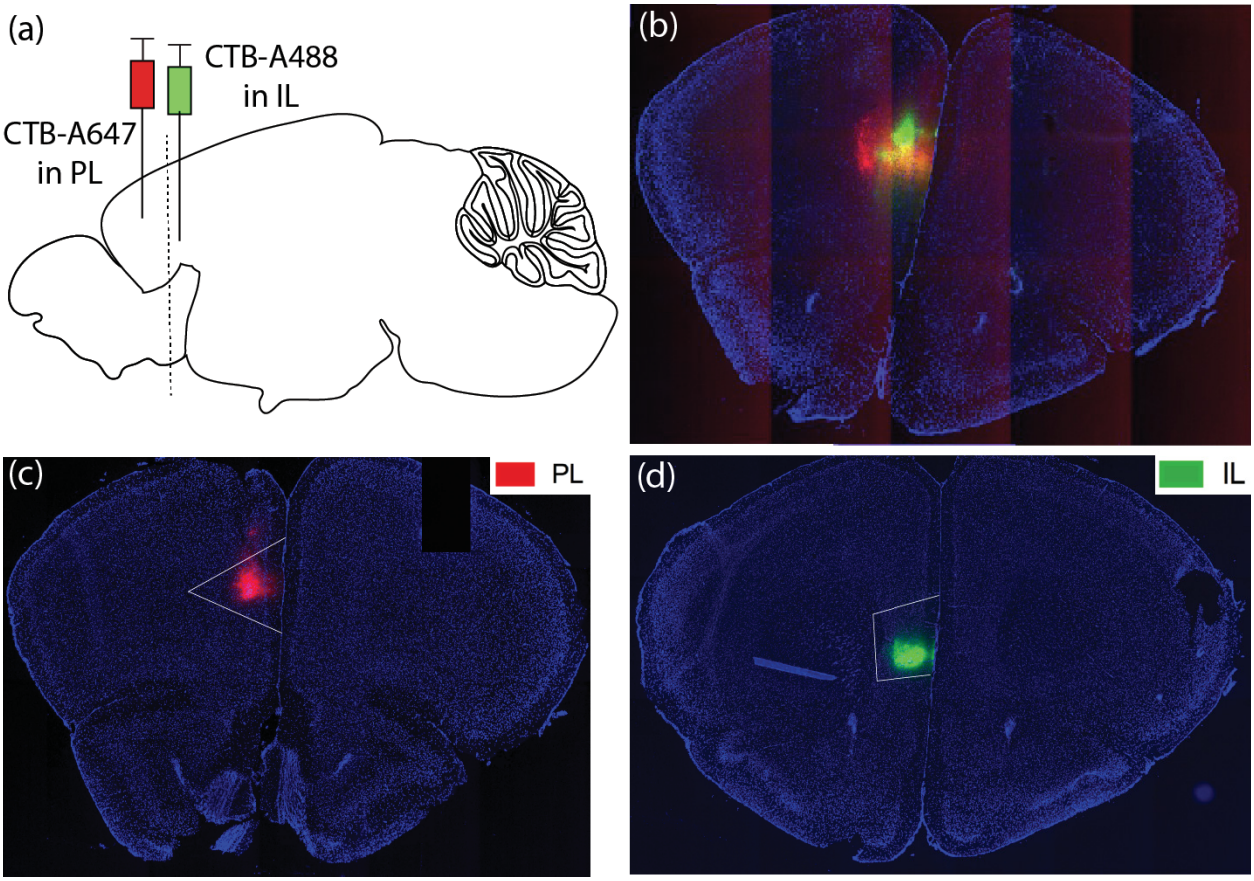

Figure 6: Greater mPFC innervation by vCA1 neurons with minimal overlap between projections to PL vs. IL revealed with unilateral injections of CTB A647 and A488 (a) Representative slice with vCA1 vs. vSub delineation as well as zooms of single vs. double CTB labeling with slide scanner or confocal (b) Diagram of addressed questions regarding single and double mPFC projecting cells within vHC (c) Results of CTB retrograde tracing (n=6 after exclusions), demonstrating significantly greater ($p<0.01$) innervation of PL and IL by CA1 (vs. Sub) (d) Pie chart of approximate distribution of vHC projections within mPFC.

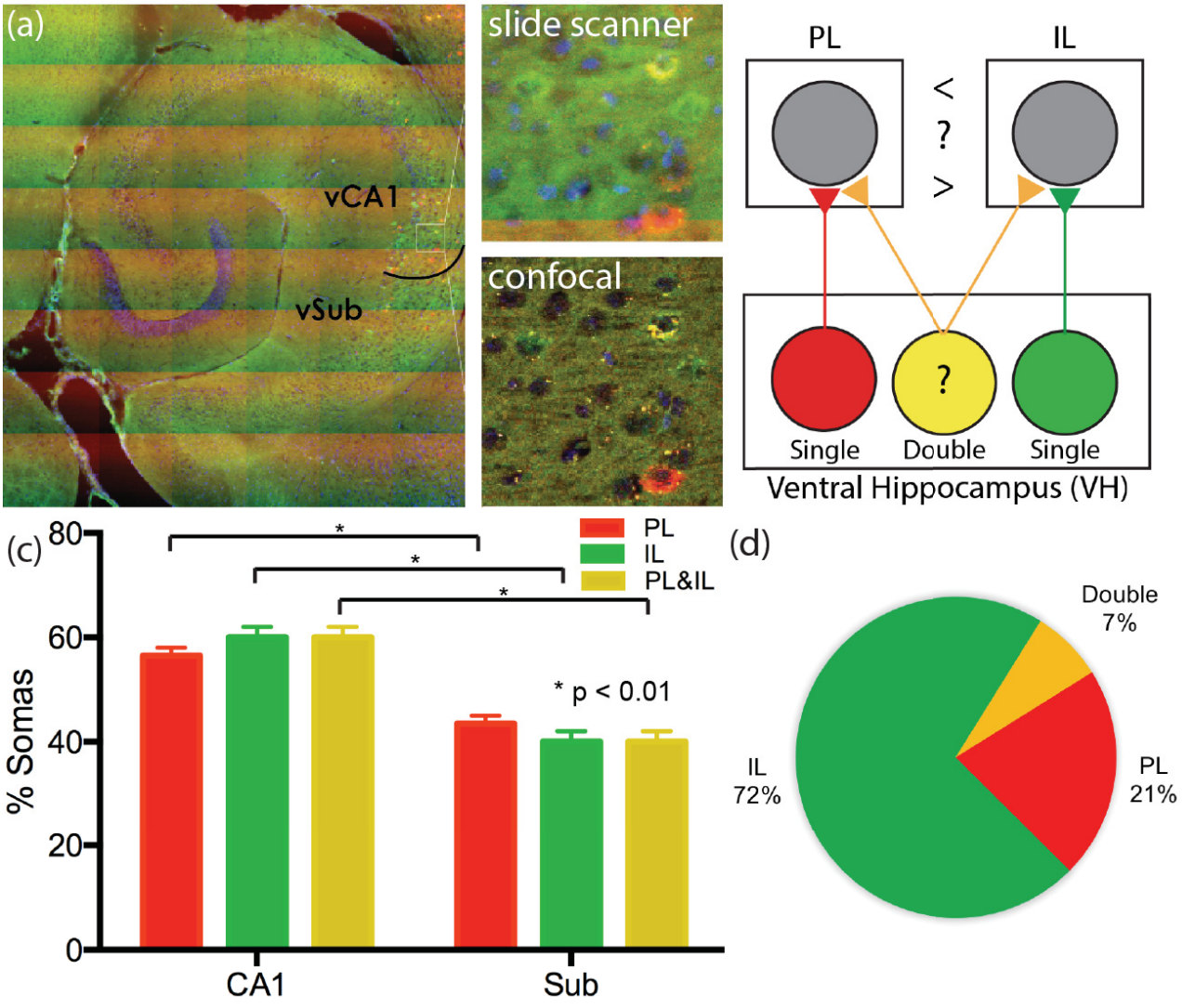

Figure 7: VGAT GABAergic vHC cells do not project to the mPFC. (a) Experimental set up (b) Representative vHC slice demonstrating viral transfection of VGAT cells (c, d) Representative mPFC slice (c), with zoom (d) on PL and IL, demonstrating lack of VGAT projections.

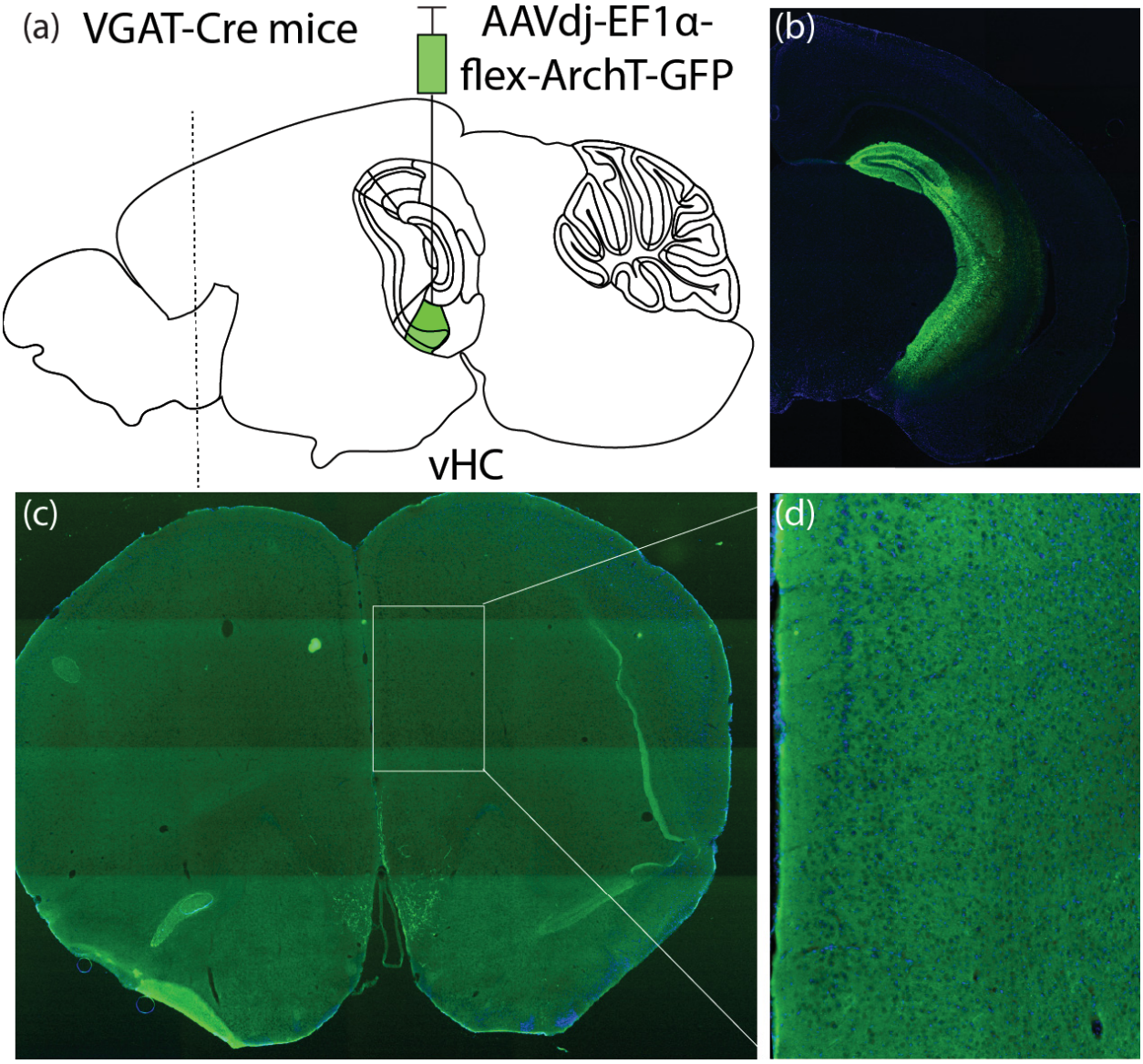

Figure 8: IL receives 2X more vHC projections than PL. (a) Experimental set up (b) Representative vHC slice demonstrating transfection spread and red DiI labeled injection tract (c) Representative mPFC slice (with anatomical overlay) demonstrating greater amount of vHC projections within IL than PL (d) Bar graph of projection density within mPFC (e) Pie chart of proportions of vHC projections within mPFC.

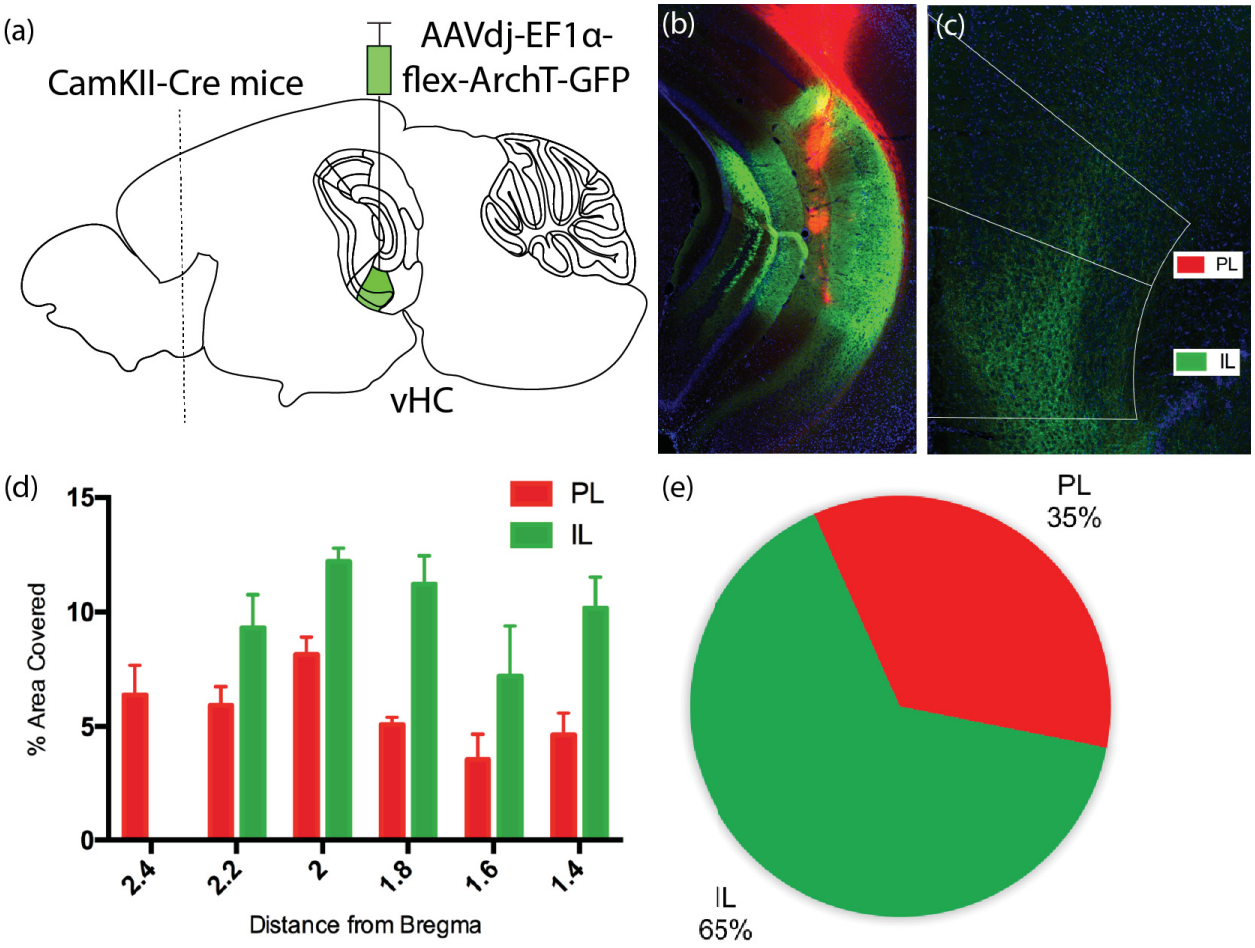

Figure 9: vHC Nts cells selectively express Cre. (a) Representative FISH stained vHC slice with (b, c) zooms at distal CA1 (b) and distal Sub (c), demonstrating greater proportion of both Nts and Cre in distal Sub. Green=Cre & Red=Nts.

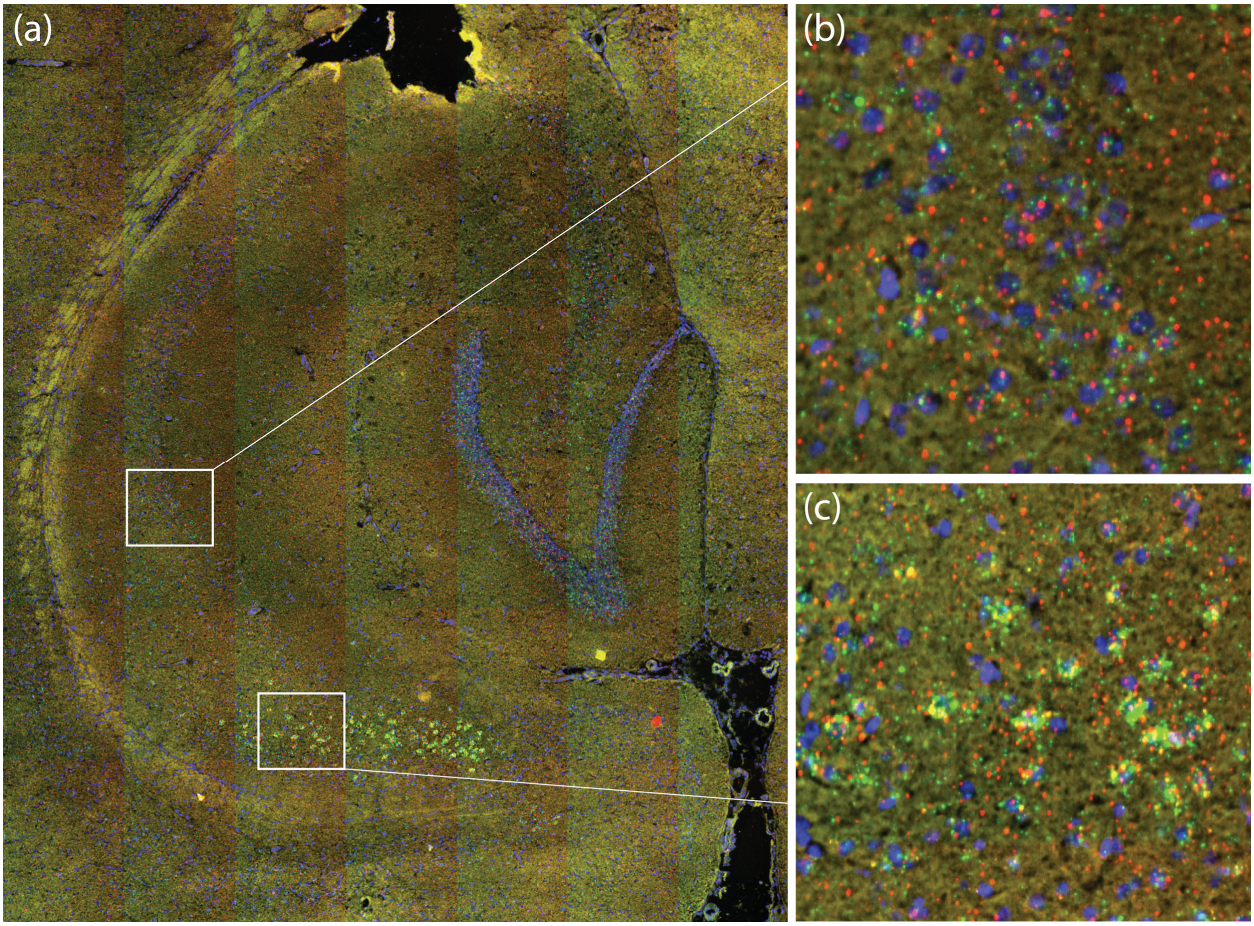

Figure 10: vHC Nts cells constitute a portion of CKII expressing cells. (b) Representative FISH stained vHC slice with (b, c) zooms at distal CA1 (b) and distal Sub (c), demonstrating greater expression of Nts in distal Sub. Green=CKII & Red=Nts.

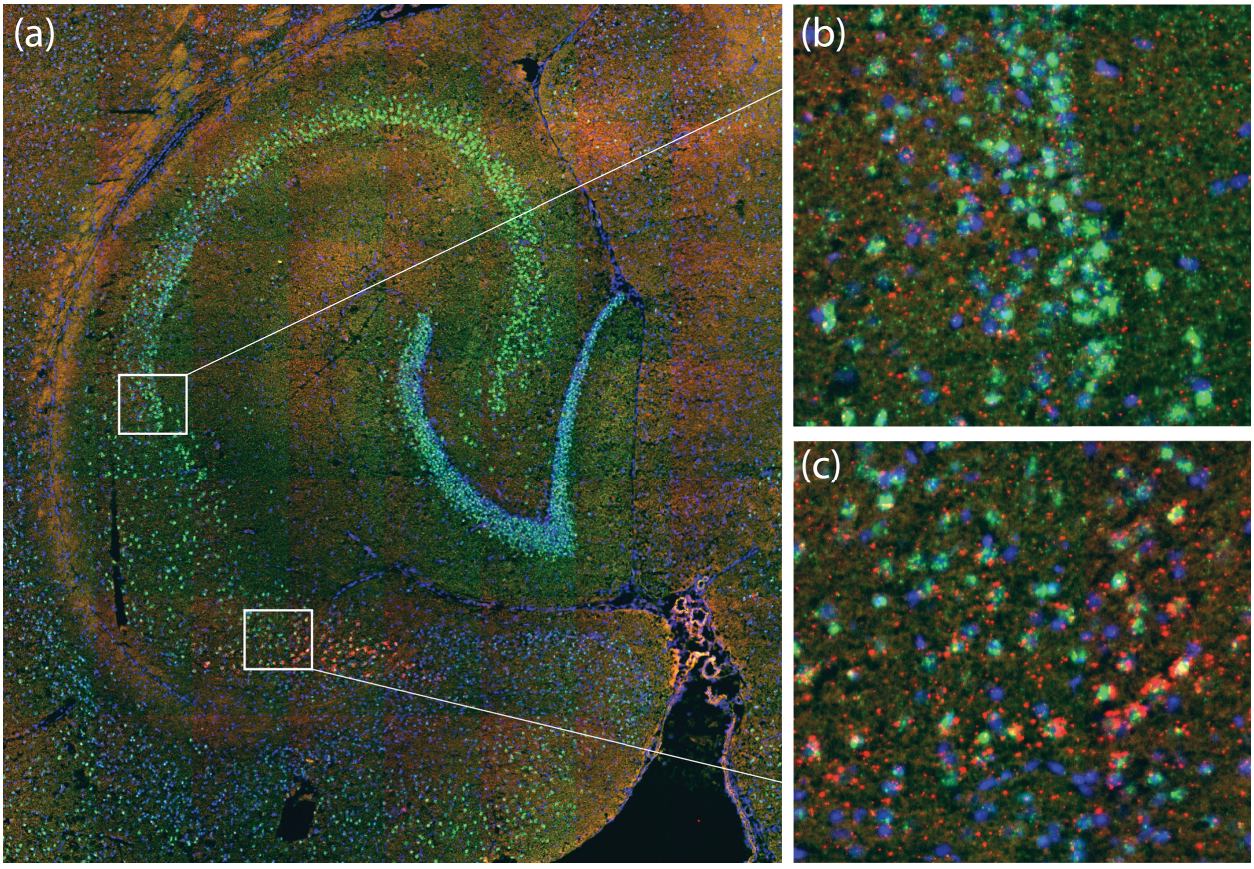

Figure 11: vHC NT cells are restricted to distal vCA1 as well as proximal and distal vSub (a) Experimental set up of vHC injections (b, c) Representative vHC slice (c), with zoom on distal vSub, following injection at vCA1/vSub border (indicated in red with DiI and on anatomical reference, b).

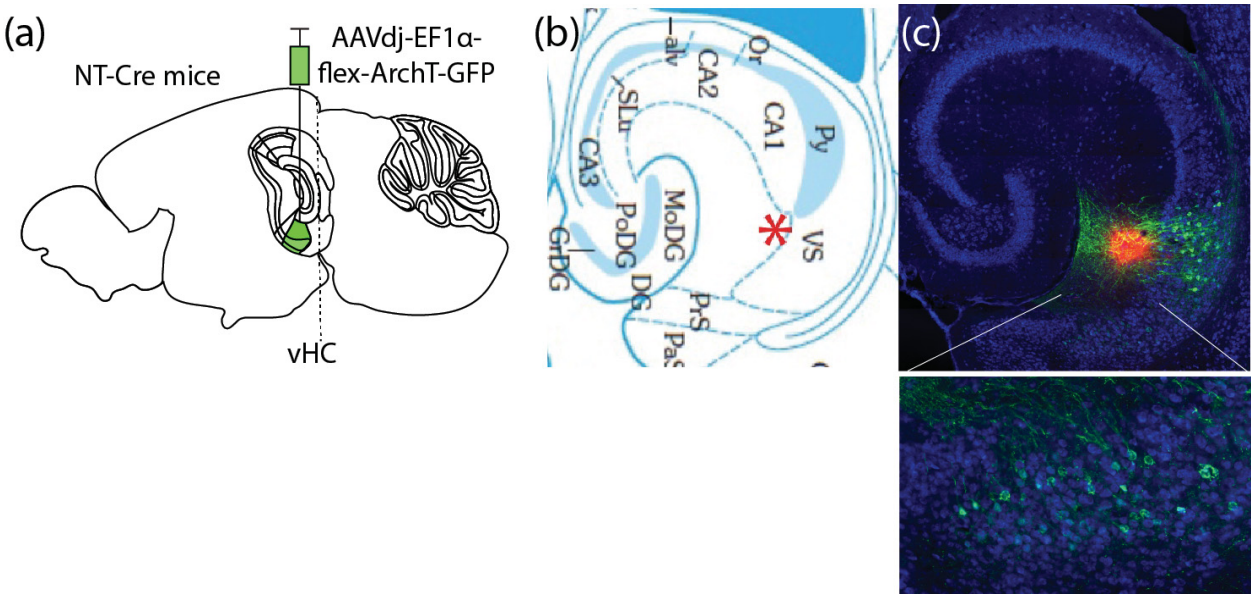

Figure 12: IL projecting vHC NT cells are restricted to distal vCA1 and proximal vSub. (a) Experimental set up for IL injections (b, c) Representative vHC slice utilizing AAV2/9 (b) or AAVretro (c) virus.

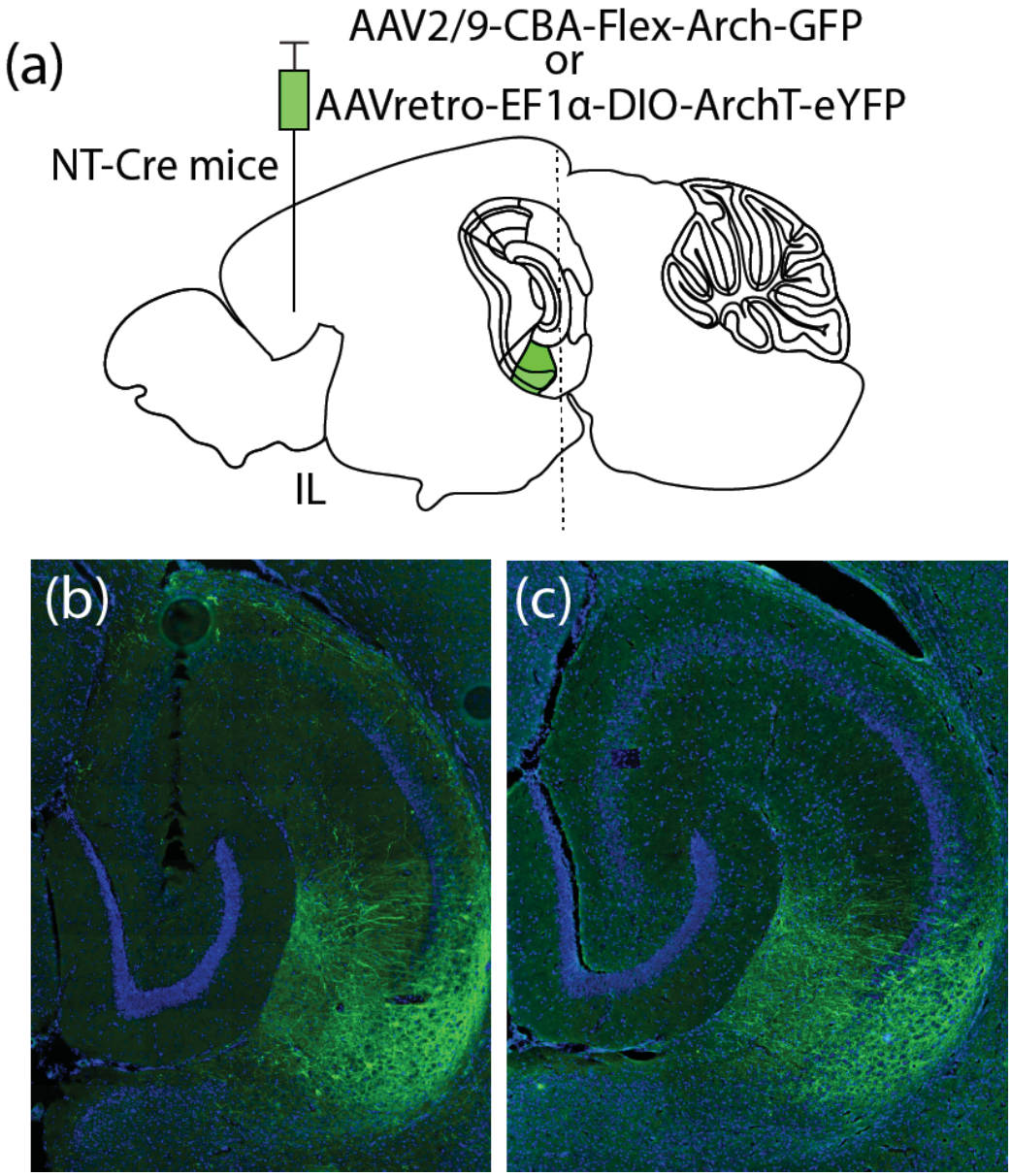

Figure 13: vHC Nts cells show a unique pattern of mPFC innervation. (a) Experimental set up (b) Representative hybrid mPFC slice (white PL & IL overlays) with CKII (left) and NT (right).

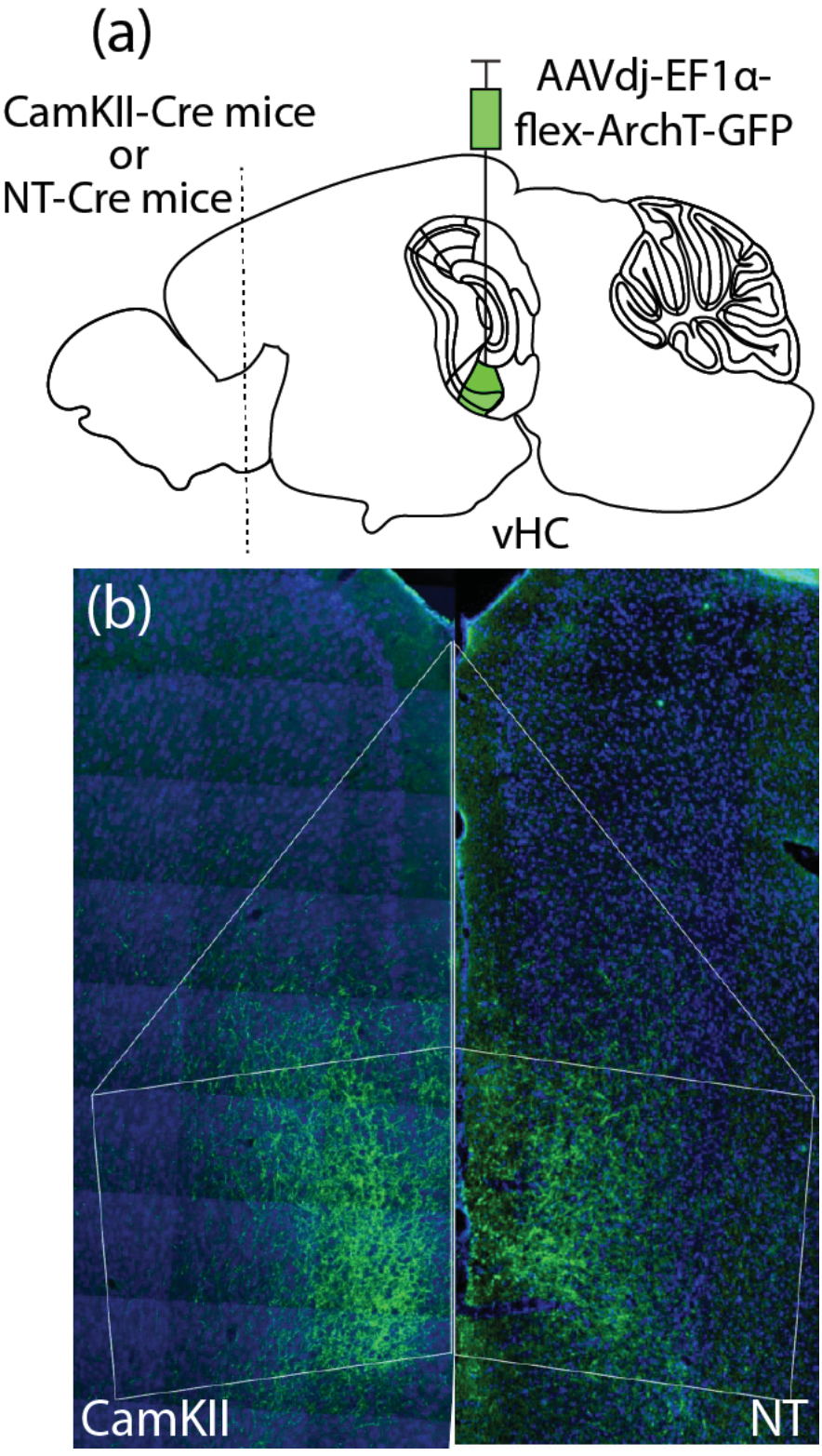

Figure 14: Nts vHC cells increase in proportion from distal vCA1 to distal vSub. (a) Triple labeled immunohistochemistry in representative Nts vHC slice with staining for (b) GFP (green) (c) ZnT3 (red), and (d) DAPI (blue). ZnT3 immunostaining allows for more accurate determination of vCA1/vSub border, indicated by white arrow.

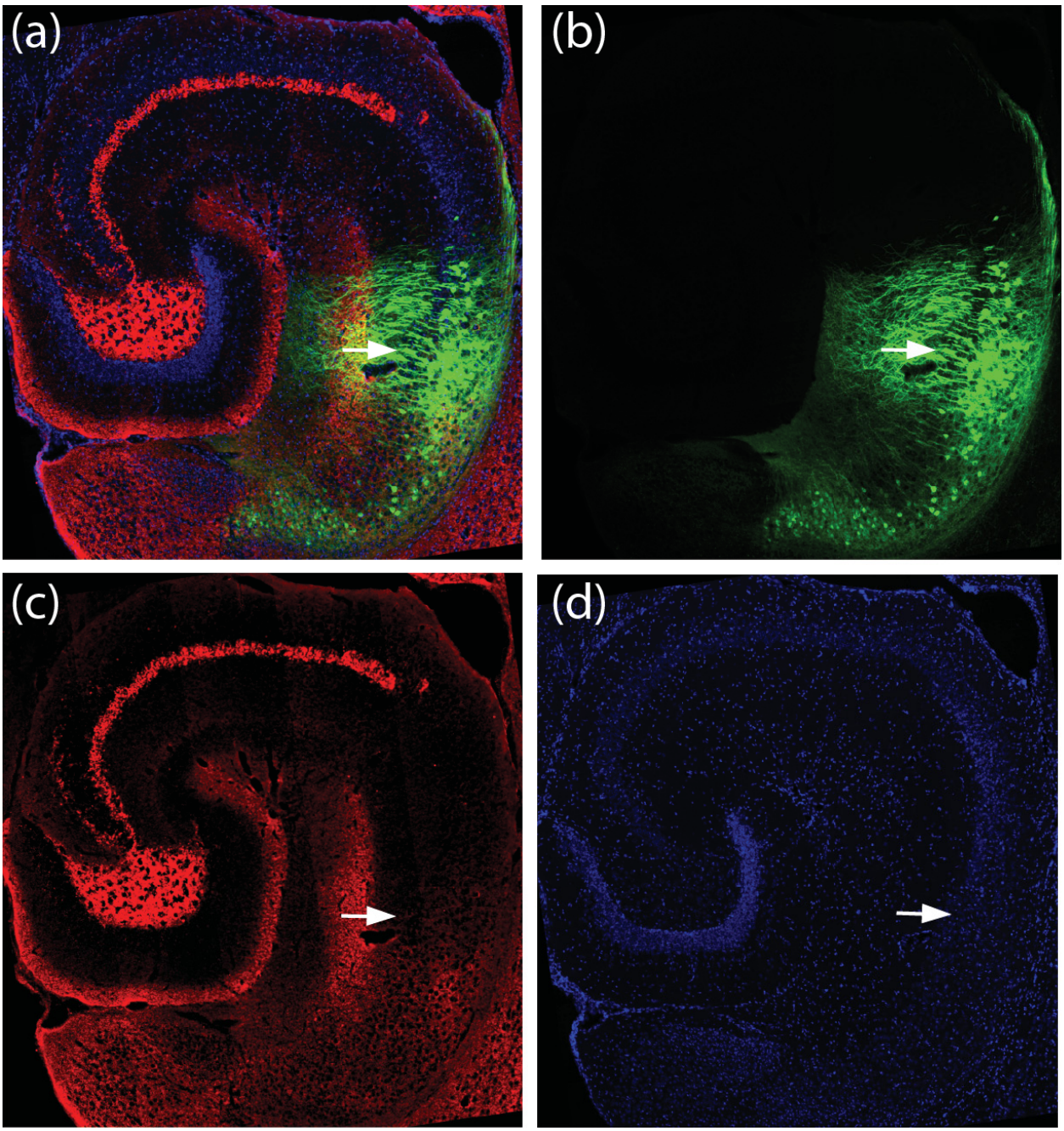

Figure 15: (a) Experimental setup of IL terminal inhibition (b) Anatomical reference of injection target (c, d) Representative vHC transfection slice following YFP (c) and NpHR (d) injections (e) Representative mPFC slice with implant tracts and overlay.

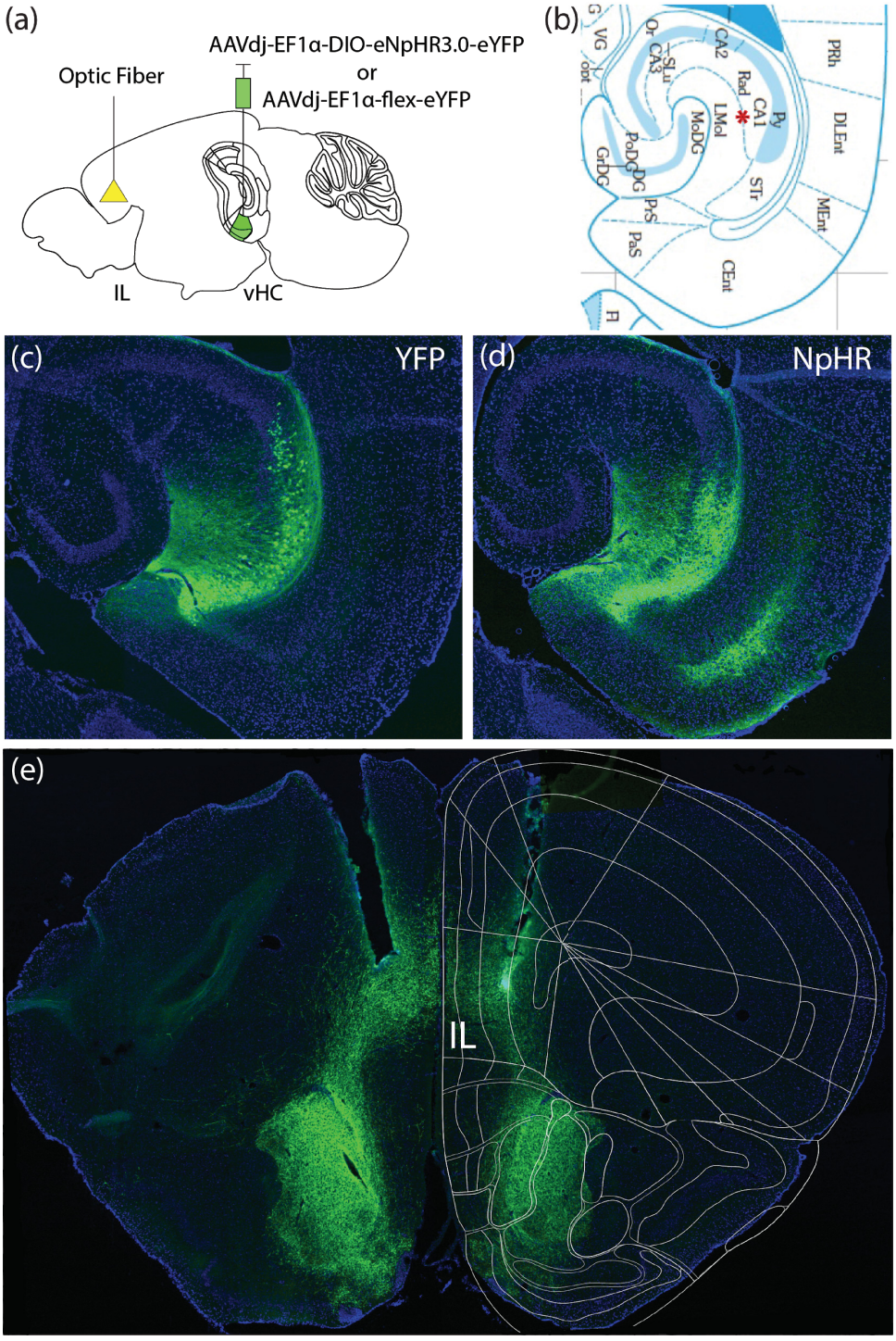

Figure 16: Inhibition of $Nts^{vHC\text{-}IL}$ circuit terminals did not alter anxiety-related behavior in OFT. (a) Diagram of OFT with optogenetic inhibition during 5 min protocol (b) Manipulation did not alter number of entries into center 50% (c) Manipulation did not alter duration of time spent in center; n=6 in YFP & n=4 in NpHR.

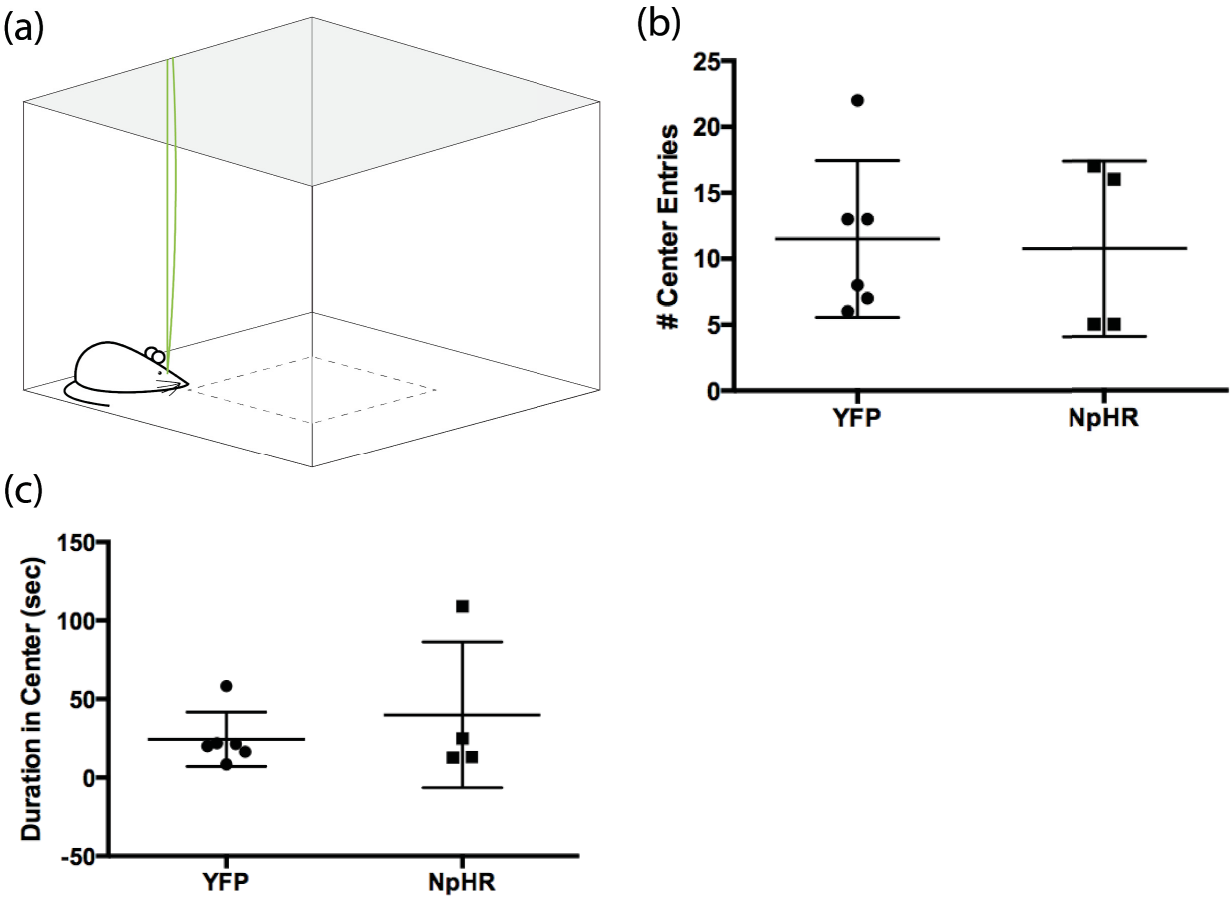

Figure 17: (a) Diagram of EPM with optogenetic inhibition during 5 min protocol (b) Manipulation did not alter number of head dips into center 50% (c) Manipulation did not alter number of open arm entries (d) Manipulation did not alter duration of time spent in open arms; n=6 in YFP & n=4 in NpHR.

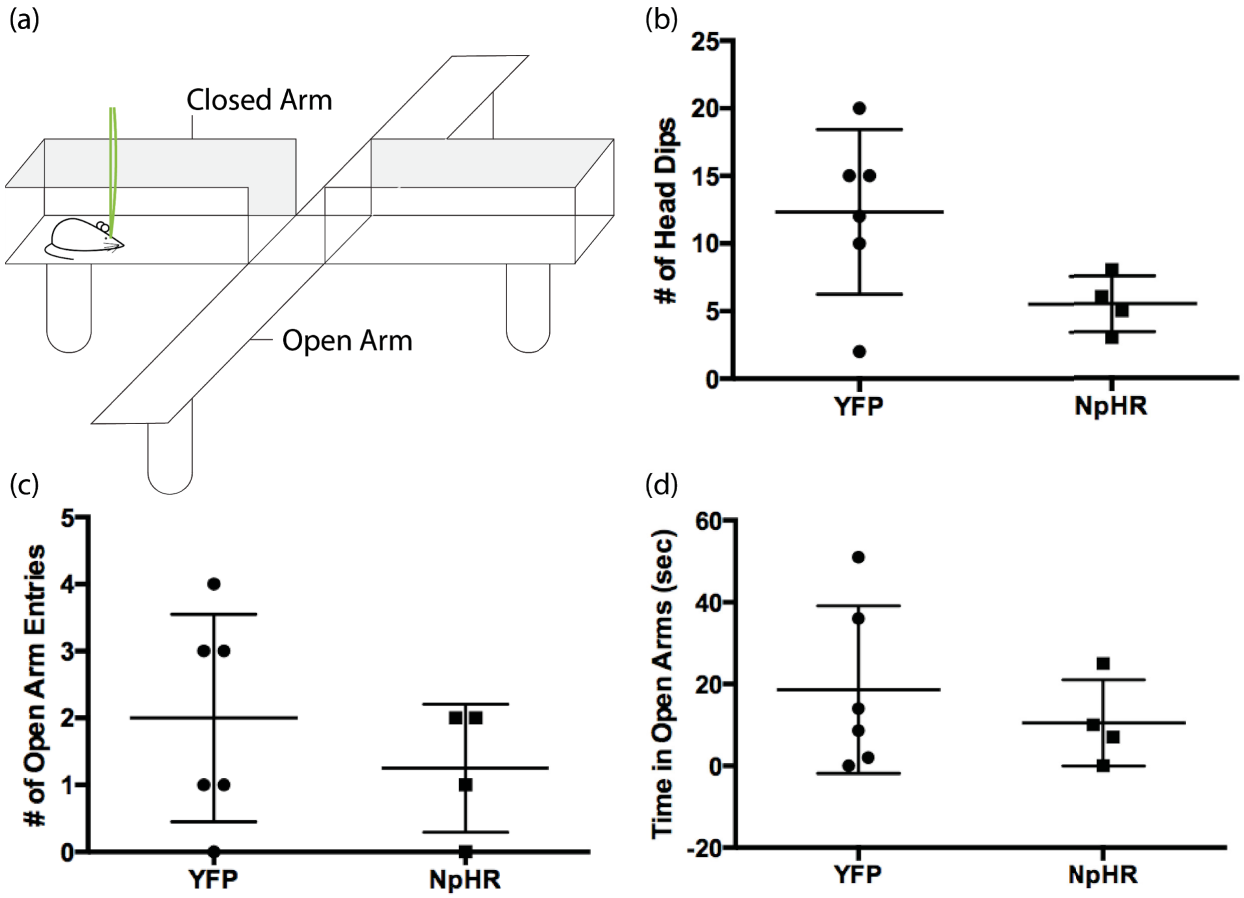

Figure 18: (a) Diagram of social interaction test with optogenetic inhibition during familiarization and when in interaction zone (b) Shows the duration of time that the mouse's nose was within 3.5 cm of the cup, during familiarization/Trial 1 (left side of each pair) and discrimination/Trial 2 (right side of each pair) (c) recognition index for YFP (black) and NpHR (yellow) in NT mice.

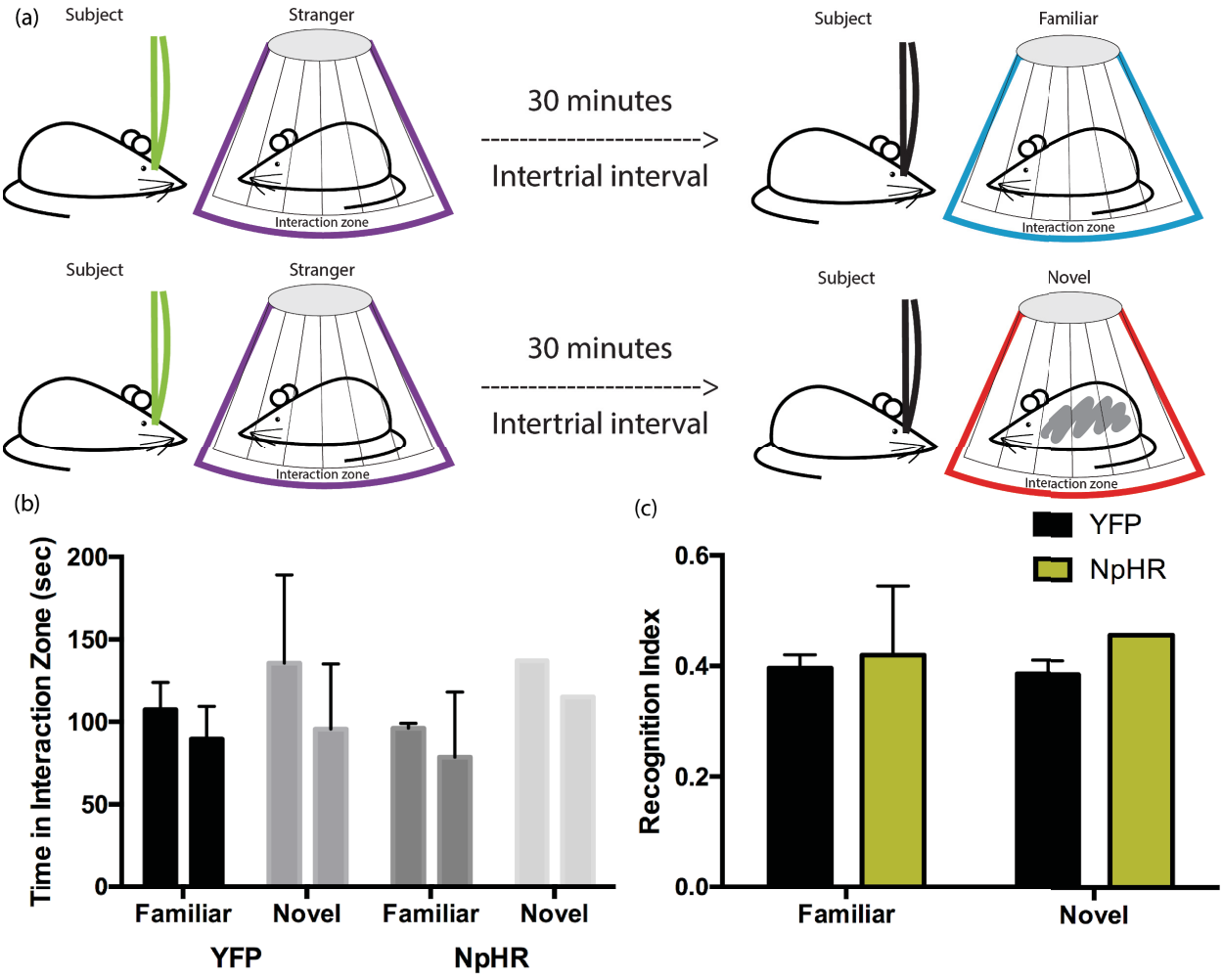

Figure 19: (a) Diagram of fear conditioning, extinction, and renewal with optogenetic inhibition during presentation of tone/CS during extinction (b) Shows the percentage of time spent freezing during pre-conditioning baseline (BL) and after final conditioning trial (c) Shows the mean percentage of time spent freezing during the first and final five-trial blocks following cue presentation during extinction.

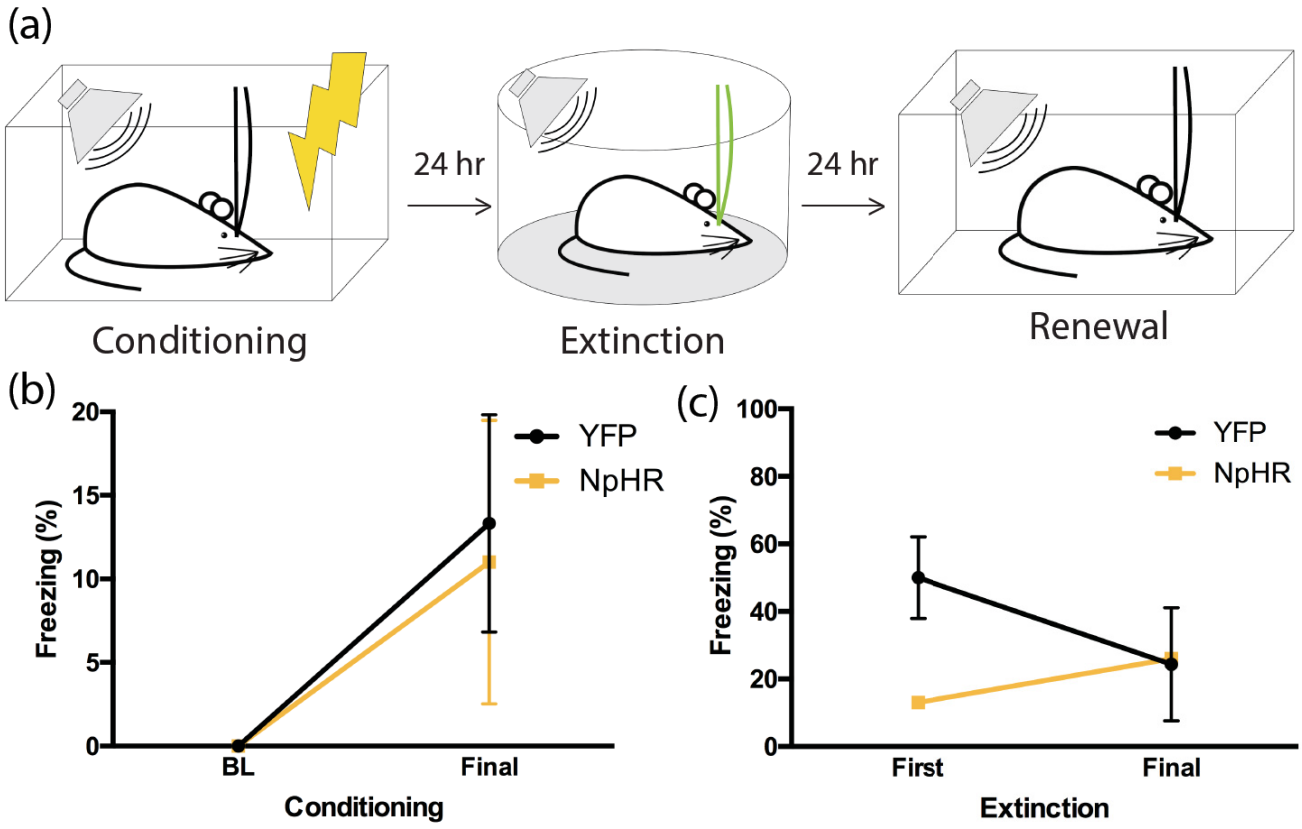

Figure 20: Patch clamp recordings of YFP positive and YFP negative NT vSub cells. (A) Images of patched NT neurons in the vSub. Left: 4x brightfield images of pipette location with anatomical reference. Right: Images of example cells at 40x (left: BF, right: GFP) (B) Example traces of responses to depolarizing and hyperpolarizing currents in cc.

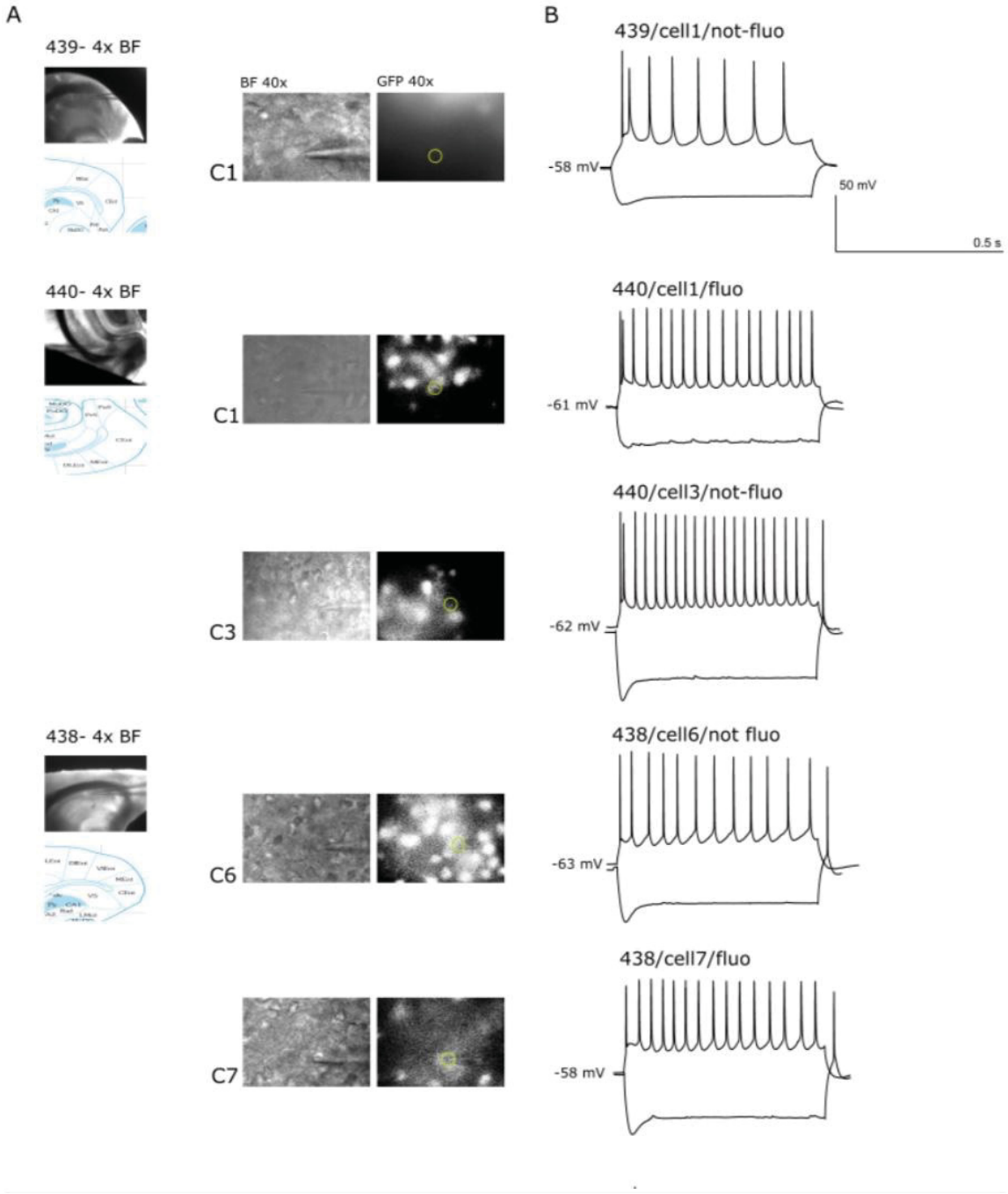

Figure 21: Flowchart of image analysis steps undertaken to determine density of projections in mPFC following AAVdj injection into vCA1. Overlays and regions were taken from Allen Brain Institute.

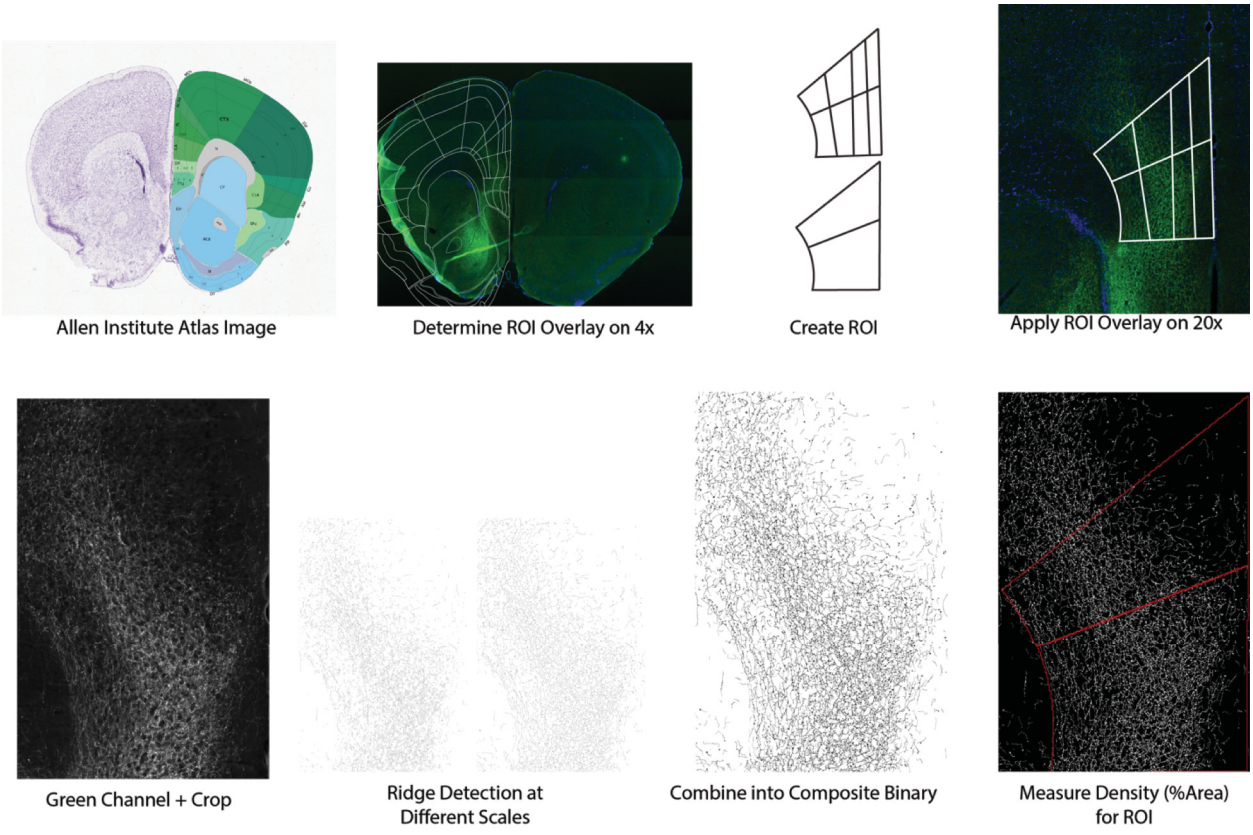

Table 1. Electrophysiological properties of NT positive cells recorded in vSub. ±SEM.

	NT positive n=6	NT negative n=5
V_r	-57.8 ±1.8	-60.8 ±1.7
R_a (MΩ)	22.8±4.4	16.18±2.9
Spike amplitude (mV)	45.99±3	44.18±2.7
Spike half width (ms)	0.85±0.07	0.73±0.04
AHP Amplitude (mV)	3.34 ±0.89	2.89 ±0.75
AHP time (ms)	113 ±16	142 ±19
Sag amplitude (mV)	13.08±2.2	14.94±1.6
Bursting	16.6%	40%
Rebound spike	33.3%	60%

Table 2. Electrophysiological properties of NT positive cells recorded in dSub. ±SEM.

	NT positive n=11	NT negative n=9
V_r	-62.7.8 ±1.4	-60.6 ±2.4
R_a (MΩ)	26.7±2.9	19.6±2.9
Spike amplitude (mV)	43.4±3	40.7±2.6
Spike half width (ms)	0.66 ±0.06	0.58 ±0.04
AHP Amplitude (mV)	5.28 ±0.75	4.45 ±1.74
AHP time (ms)	129±8	122±12
Sag amplitude (mV)	12.46±1.6	7.80 ±1.7
Bursting	81%	66%
Rebound spike	64%	22%